Session 19

OPEN END

THURSDAY: October 23, 1980
CHAIRMAN: M.W. First
Harvard Air Cleaning Laboratory

CARBON TETRACHLORIDE DESORPTION FROM ACTIVATED CARBON
Leonard A. Jonas, E.B. Sansone

LOADING CAPACITY OF VARIOUS FILTERS FOR LITHIUM FIRE GENERATED AEROSOLS
D.W. Jeppson, J.R. Barreca

A UNIQUE APPROACH TO CARBON SAMPLING
D.D. Whitney, J.R. Edwards

OCCURRENCE OF PENETRATING IODINE SPECIES IN THE EXHAUST AIR OF PWR POWER PLANTS
H. Deuber, J.G. Wilhelm

KRYPTON RETENTION ON SOLID ADSORBENTS
Paul R. Monson, Jr.

EFFECT OF FLOW RATE ON THE ADSORPTION COEFFICIENT OF RADIOACTIVE KRYPTON ON ACTIVATED CARBON
Lin-Shen Casper Sun, Dwight W. Underhill

DESORPTION OF TEDA FROM IMPREGNATED CHARCOALS
Gerry Wood

NUCLEAR POWER PLANT AIR FILTER MAINTENANCE PROGRAM AND RECORDS
James Fish

REVIEW OF WORK CARRIED OUT 1978-80 ON HEPA FILTERS AND VENTILATION SYSTEMS AT THE DOUNREAY SITE OF THE UKAEA
Ernest Lillyman

OPENING REMARKS OF SESSION CHAIRMAN:

This is the Open End Session. As most of you know, it is intended to include brief technical notes, short presentations of new works in progress that are not yet far enough along to justify a full formal report (such as the papers we have had over the past three days), and, perhaps, to descriptions of puzzling observations that those of you in the audience may like to comment upon from your own experience. We have a number of these presentations, which are most valuable, though brief.

CARBON TETRACHLORIDE DESORPTION FROM ACTIVATED CARBON *

Leonard A. Jonas and Eric B. Sansone
Environmental Control and Research Laboratory
Frederick Cancer Research Center
Frederick, MD 21701

ABSTRACT

Carbon tetrachloride was desorbed from a granular activated carbon subsequent to its adsorption under various vapor exposure periods. The varied conditions of exposure resulted in a range of partially saturated carbon beds which, when followed by a constant flow rate for desorption, generated different forms of the desorbing concentration versus time curve. A method of analyzing the desorption curves is presented which permits extraction of the various desorbing rates from the different desorption curve configurations. The experimental data of desorbing concentration versus time were used to calculate the fractional regeneration of the bed resulting from the desorption and to relate this to the time required for such regeneration. The Wheeler desorption kinetic equation was used to calculate the pseudo first order desorption rate constant for the carbon. The desorption rate constant was found to increase monotonically with increasing saturation of the bed, permitting the calculation of the maximum desorption rate constant for the carbon at 100% saturation. The Retentivity Index of the carbon, defined as the dimensionless ratio of the adsorption to the desorption rate constant, was found to be 681.

Introduction

The movement of an adsorbed gas front through an adsorbent bed under the influence of a flowing inert gas is represented as the desorption wave through the bed. In contrast to the adsorption process, which takes place spontaneously, the desorption process requires that work be done on the system. The work is accomplished by mass transport phenomena involving movement of the adsorbed phase into the flowlines around the sorbent granules, and results in the movement of the adsorbed front through successive portions of the unused bed until the bed is penetrated.

* Research sponsored by the National Cancer Institute under Contract No. NO1-CO-75380, with Litton Bionetics, Inc.

The kinetics of gas desorption from a carbon bed saturated with the adsorbed gas was studied by Wheeler (1) who derived the kinetic equation in terms of t_R, the time in appropriate units required to regenerate an arbitrarily chosen fraction of the saturated bed. The equation can be shown as:

$$\ell n(1/1-f) = -k_d W/\rho_\beta Q + k_d t_R/A'\rho_B \qquad (1)$$

when the carbon bed weight W is constrained to a fixed quantity. In equation (1), A' is a constant of the system (cm^3/g), k_d the pseudo first order desorption rate constant (min^{-1}), Q the volumetric flow rate (cm^3/min), ρ_β the bulk density of the packed bed (g/cm^3), f the chosen fractional regeneration of the carbon, and t_R the time (min) to achieve a specific value of f. A plot of log 1/1-f against t_R should yield a straight line whose slope is equal to $k_d/2.303\ A'\rho_\beta$ and whose y-axis intercept is $-k_d\ W/2.303\ \rho_\beta Q$. The parameters A' and k_d can be obtained directly from the slope and intercept respectively.

The Desorption Curve

The shape of the desorption curve, representing desorbing gas concentrations as a function of time, should vary depending upon the extent of carbon saturation occurring in the adsorption phase. Two basic curve shapes exist. When desorption is initiated after the carbon bed has been fully saturated with the gas in the adsorption phase the shape of the curve will be the mirror image of the sigmoidal gas penetration curve resulting from the continuous challenge of an activated carbon bed until it becomes saturated with adsorbed gas and the exit to inlet gas concentration ratio approaches unity. In this curve the highest desorbing concentrations occur first and the fall-off of concentration becomes a nonlinear function of time. Integration of the area of the curve, multiplied by the flow rate, gives the total quantity of gas desorbed from the carbon.

The shape of the desorption curve resulting from a bed of carbon only partially saturated with gas during the adsorption phase is expected to approximate a bell-shaped or Gaussian curve, which describes, in its symmetry, the coupling of a desorption curve from a saturated bed with the complete adsorption curve. The area under the curve, multiplied by the volumetric flowrate, should provide the total weight of gas desorbed from the carbon, a quantity equal to or less than the quantity challenging the bed during the adsorption phase. Any difference between the inlet and outlet quantities is due to retention of the gas by the carbon.

Retentivity Index

The ratio of the adsorption rate constant k_v to the desorption rate constant k_d, both being pseudo-first-order in kinetics and maximized under the same criteria, results in a dimensionless constant

$$K_R = k_v/k_d \qquad (2)$$

which can be considered the Retentivity Index of the activated carbon for a particular gas. It would be expected that K_R is a function of temperature. The higher the value of K_R the greater will be the overall protective or adsorbing properties of a carbon for a specific gas or vapor.

Results and Discussion

On the basis of previous work using carbon tetrachloride vapor as the adsorbate (2, 3), and the BC-AC lot 0993 activated carbon as the adsorbent, it is known from the adsorption regression equation for the t_b versus W plot that:

$$t_b \text{ (min)} = -27.41 + 31.78\ W$$

from which it has been determined that the adsorption capacity W_e was 0.741 g/g and the adsorption rate constant k_v was 735 min^{-1}.

The operating conditions for the four CCl_4 desorption tests run on the activated carbon granules, as well as the percentage of carbon saturation by carbon tetrachloride adsorption prior to desorption, are shown in Table 1.

In studying the carbon tetrachloride desorption from the BC activated carbon different carbon weights were used in each test run. Since the inlet concentration of CCl_4 remained constant (80.1 - 82.3 $\mu g/cm^3$) on the adsorption side, as did the volumetric flow rate (285 cm^3/min), the quantity of vapor adsorbed by the carbon was varied by varying the time of exposure for each run.

The Wheeler desorption equation, in the form of equation (1), was applied to the desorption data of the test runs only at the time when the desorbing concentration reached its maximum. At this point the desorbing time t_d was set equal to zero and the cumulative quantity of carbon tetrachloride desorbing from the carbon was recorded as a function of time. The rationale for this approach was to obtain the maximum desorption rate of the carbon under the conditions of test. The quantity of carbon tetrachloride remaining on the carbon at $t_d = 0$, and therefore potentially capable of being desorbed, was determined by the relationship:

$$y=C_oQt_c - Q\left[\int_0^{t_c} C_x(t)dt + \int_{t_c}^{t_p} C_x(t)dt\right] \quad (3)$$

where C_o is the inlet gas concentration (g/cm^3), C_x the gas concentration exiting the carbon bed (g/cm^3), Q previously defined, t_c the time of exposure of the carbon to the C_o (min), t_p the time (min) at which the C_x reaches its maximum or peak value (t_p is identical with $t_d = 0$), and y is the quantity (g) of gas remaining on the carbon at $t_d = 0$, the time at which the gas remaining on the carbon can be desorbed at its maximum rate. The first integral in the brackets represents the gas penetrating the carbon bed during its adsorption phase; the second integral represents the gas desorbing from the carbon before its maximum desorbing rate is realized.

When equation (3) was applied to the desorption runs it was found that 0.5923, 0.3645, 0.3680, and 0.7684 g CCl_4 remained at t_p for runs 1-4, respectively. From this point onward the desorption versus time was recorded. For each test run the fractional bed regeneration f (calculated by dividing the cumulative quantity desorbed by the quantity of CCl_4 remaining at t_p) was noted as a function of time t_R. Figure 1 shows the plots of log (1/1-f) versus t_R for runs 1-4. Only those values of log (1/1-f) versus t_R which correspond to a straight line relationship, denoting first order desorption kinetics, were plotted. Beyond this time the points depart from a straight line, indicating the onset of second order kinetics. The smooth lines represent linear regression equations for the calculated data and correspond to the equation:

$$\log (1/1-f) = A + B\ t_R \quad (4)$$

from whose intercept and slope both k_d and A' can be calculated.

The coefficients of the regression equations for the four test runs, as well as the calculated A' and k_d values are shown in Table 2. The percent of carbon tetrachloride saturation, to which the carbon bed had been subjected on the adsorption phase prior to desorption, shown also in Table 2, had a marked effect on the desorption rate constant the carbon exhibited under the test conditions imposed. The desorption rate constants decreased monotonically with decreasing percentage bed saturation on the adsorption side, and are plotted in Figure 2. The quantitative relationship obtained from the plot is:

$$\log (k_d) = -2.127 + 0.0216\ (\%\ CCl_4\ \text{saturation}) \quad (5)$$

The lower desorption rate constants observed with decreasing bed saturation probably results from the lower carbon tetrachloride concentration

present when the adsorbed gas wave reaches the downstream bed - air interface.

We conclude that the maximum desorption rate constant for the BC-AC lot 0993 activated carbon is 1.08 min^{-1}, a value realized after 100% saturation or complete gas adsorption. Thus, the Retentivity Index K_R, obtained for this carbon from equation (2), was found to be 681, a value of the same magnitude found for the desorption of methyl iodide by nuclear grade activated carbon (4). For example, in this referenced work using a 8-16 mesh coal-base charcoal from Sutcliffe and Speakman (Leigh, England) impregnated with a mixture of KI, KIO_3, and hexamethylenetetramine and buffered to a pH of 9-10, the two protected or clean layers of the charcoal-filled bed showed K_R values for methyl ^{127}iodide vapor of 640 and 311 respectively.

References

1. Wheeler, A., 6th Bimonthly Progress Report (Edited by J. Makowski) Army Contract DA18-035-AMC-279(A) p. 85 (Sept. 1965).

2. Jonas, L.A., Sansone, E.B., and Tewari, Y.B., "Prediction of Adsorption Rate Constants of Activated Carbon for Various Vapors", Carbon 17, 345 (1979).

3 Sansone, E.B., Tewari, Y.B., and Jonas, L.A., "Prediction of the Removal of Vapors by Adsorption on Activated Carbon", Envir. Sci. & Tech. 13, 1511 (1979).

4. Jonas, L.A., Deitz, V.R., and Romans, J.B., "Desorption Kinetics of Methyl Iodide from Impregnated Charcoal", Nuclear Technology, 48, 77 (1980).

TABLE 1. TEST CONDITIONS FOR CCl_4 DESORPTION RUNS: FLOW RATE 285 cm^3/min

Run No.	Carbon Weight W (g)	Inlet Conc. C_o ($\mu g/cm^3$)	Carbon Bed Saturation before Desorption (%)
1	0.7973	81.87	97
2	1.6058	82.34	69
3	1.2106	82.34	52
4	1.7681	80.07	6

TABLE 2. DESORPTION PROPERTIES OF BC-AC LOT 0993 CARBON

Run No.	Desorption Equation* Coefficients $\times 10^4$		System Constant A'	Carbon Bed Saturation Before Desorption (%)	Desorption Rate Constant k_d (min^{-1})
	A	B			
1	-24.7	182	49	97	0.98
2	-10.0	15	119	69	0.20
3	-4.0	5	196	52	0.11
4	-0.4	3	24	6	0.01

* $\log (1/1-f) = A + Bt_R$. The correlation coefficient for each regression equation was >0.9999.

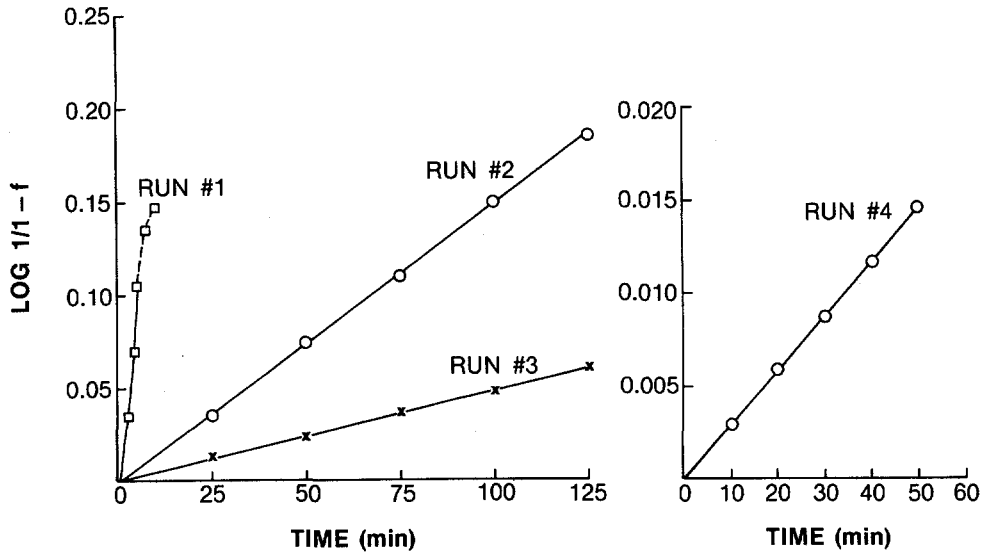

Fig. 1. LOG (1/1-f) VERSUS TIME FOR VARIOUS TEST CONDITIONS.

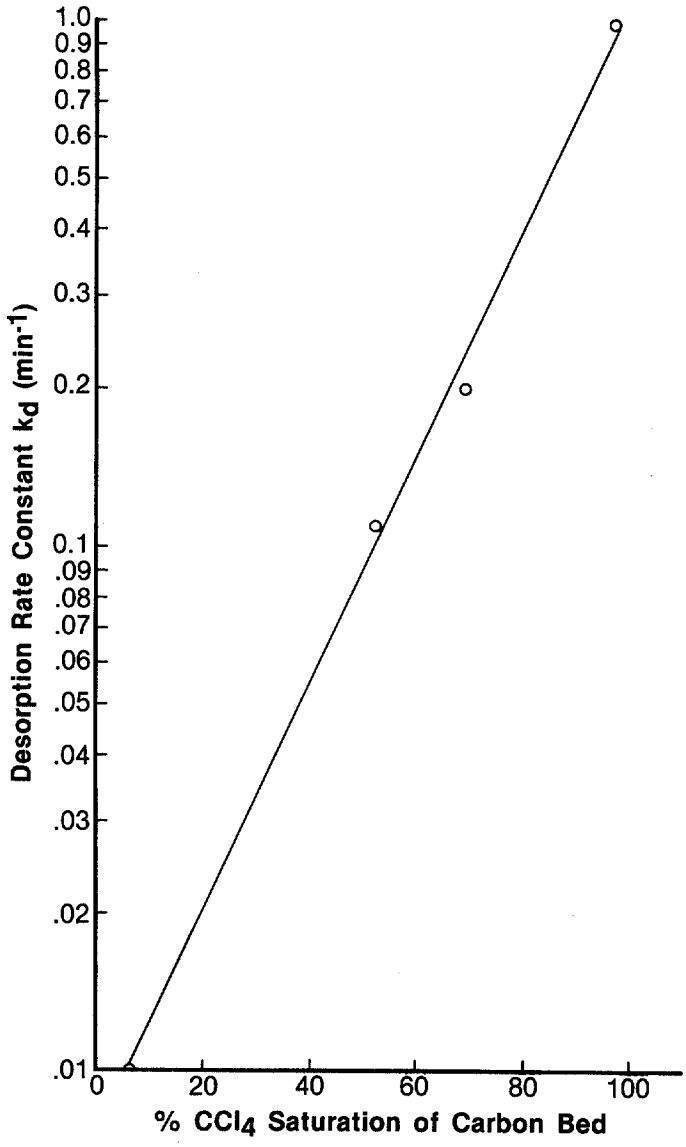

FIG. 2. DESORPTION RATE CONSTANT AS A FUNCTION OF % BED SATURATION.

DISCUSSION

KOVACH: Would you expect to get the same dimensionless number for an impregnated and an unimpregnated carbon with methyl iodide, for example?

JONAS: Perhaps not the same number, but, I think, in the same order of magnitude.

KOVACH: We all know, as an example, that the unimpregnated carbons do not work well on methyl iodide at all. So, how could we compare the effectiveness of a carbon for methyl iodide removal if we get the same number whether it is impregnated or not?

JONAS: I am taking into account only the physical forces on the carbon. If you have isotopic exchange, as you have with the methyl radioiodine, I think we are in another ballpark. But all I have shown is what happens on the physically adsorbed side.

FIRST: Dr. Jonas, how can we use the information you have developed in a practical way to examine carbon residual life?

JONAS: I am not sure I can give an answer to residual life. This is a problem that we are working on separately. I can give the relationship, now, between the desorption rate as a function of saturation. This information may be able to give you an idea of how well your carbon will hold up when you want to load it.

LOADING CAPACITY OF VARIOUS FILTERS FOR LITHIUM FIRE GENERATED AEROSOLS

D. W. Jeppson and J. R. Barreca
Hanford Engineering Development Laboratory
Westinghouse Hanford Company
Richland, Washington

Abstract

The lithium aerosol loading capacity of a prefilter, HEPA filters and a sand and gravel bed filter has been determined. The test aerosol is characterized and was generated by burning lithium in an unlimited air atmosphere. Correlation to sodium aerosol loading capacities are made to relate existing data to lithium aerosol loadings under varying conditions. This work is being conducted in support of the fusion reactor safety program.

Lithium aerosol was generated by burning lithium pools, up to 45 kgs, in a 340 m^3 low humidity air atmosphere to supply aerosol to recirculating filter test loops. The aerosol was sampled to determine particle size, mass concentrations and chemical species. The dew point and gas concentrations were monitored throughout the tests. Loop inlet aerosol mass concentrations ranged up to 5 gr/m^3. Chemical compounds analyzed to be present in the aerosol include Li_2O, LiOH, and Li_2CO_3.

HEPA filters with and without separators and a prefilter and HEPA filter in series were loaded with 7.8 to 11.1 kg/m^2 of aerosol at a flow rate of 1.31 m/sec and 5 kPa pressure drop. The HEPA filter loading capacity was determined to be greater at a lower flow rate. The loading capacity increased from 0.4 to 2.8 kg by decreasing the flow rate from 1.31 to 0.26 m/sec for a pressure drop of 0.11 kPa due to aerosol buildup. The prefilter tested in series with a HEPA did not increase the total loading capacity significantly for the same total pressure drop. Separators in the HEPA had only minor effect on loading capacity. The sand and gravel bed filter loaded to 0.50 kg/m^2 at an aerosol flow rate of 0.069 m/sec and final pressure drop of 6.2 kPa. These loading capacities and their dependence on test variables are similar to those reported for sodium aerosols except for the lithium aerosol HEPA loading capacity dependence upon flow rate.

I. Introduction

Liquid lithium is currently considered for use in fusion reactors as a coolant and/or blanket material and is being used in fusion support facilities. One consideration concerning the use of liquid lithium is potential safety hazards of large volumes of molten lithium. Lithium aerosols are produced when lithium burns in air, nitrogen or carbon dioxide atmospheres.[1] Adequate aerosol control methods will have to be employed to contain these aerosols and any radioactive species associated with them for fusion reactors or support facilities. The Hanford Engineering Development Laboratory (HEDL) is performing a test program which includes providing data on

lithium aerosol containment to support safety and analysis for both normal operating and postulated accident situations and for making appropriate design decisions.

Air cleaning systems including commercial HEPA filters have some application for liquid metal cooled breeder reactors in the containment of sodium aerosols and are expected to be of use for lithium aerosols in the fusion reactor program. Filter systems using commercial HEPA filters have proved reliable and are widely used in the nuclear industry. Information about the lithium aerosol loading capacity of commercial HEPAs and other filters is limited. Lithium pool fires in air have generated aerosols with concentrations up to 18 g/m^3 in contained vessel atmospheres. Up to 8 percent of the burned lithium has become aerosolized in limited air pool fire tests.[1] The objective of this work was to measure the lithium aerosol loading capacity of a prefilter, HEPA filters and a sand and gravel bed filter, and relate these data where possible to existing sodium aerosol loading capacities.

II. Experimental Facilities and Equipment

Facilities and Major Equipment

The lithium aerosol filter loading tests were conducted at the Large Sodium Fire Facility. The aerosol was generated in the Air Cleaning Room (340-m^3 volume) using reaction pans to burn lithium in normal humidity air. The room height is 6.6 m.

The lithium aerosol generated was drawn to the test prefilter and HEPA filters through thirteen meters of 25-cm diameter duct. The filtered air was returned to the Air Cleaning Room by a blower. The room atmosphere was maintained at a slightly negative pressure by exhausting at a small flow rate through a separate ventilation system. An oxygen concentration of greater than 18 percent was maintained in the room by air inleakage. Figure 1 is a schematic of the test arrangement and filter housing for the prefilter and commercial HEPA filters showing the location of the gas and aerosol sampling points, thermocouple, differential pressure and flow measurement locations.

The sand and gravel bed test loop consisted of eight 50-cm diameter (0.204 m^2 surface area), 15 cm thick beds arranged in series as shown in Figure 2, a backup HEPA filter, an orifice for flow measurement and a fan to exhaust the filtered air back to the Air Cleaning Room. The inlet to the sand and gravel bed filter consisted of a one-meter length of 10-cm diameter pipe. Aerosol sampling stations were set up to obtain samples from the inlet and outlet plenums of the sand bed stacks. Pressure taps were located above and below each bed to measure the pressure drops across all of the beds or any combination of beds. Pressure taps were connected to measure the pressure drops across the total beds, beds 1 and 2 and bed 3 throughout the tests.

Samples of the test aerosol were taken through an air-lock arrangement, which allowed the sampling filter or cascade impactors to be inserted directly into the Air Cleaning Room. The aerosol mass concentration in the room was determined by using weighed filters; lithium concentration was determined by titration of the

filter samples with hydrochloric acid. Lower levels of lithium were measured on cascade impactors and a downstream sampler by atomic absorption. Oxygen, hydrogen, and water were measured by on-line instruments and supplemented with thief samples analyzed by mass spectrometry.

Cascade impactors were used for aerosol particle size measurement, and electron microscope grids were exposed for particle shape information. Air flow, temperature, and pressure drop at the test filters were recorded by a 100-channel data logger on paper and magnetic tape for subsequent plotting and calculation. Deposition pans placed at various locations on the room floor measured the total aerosol deposition on the floor area.

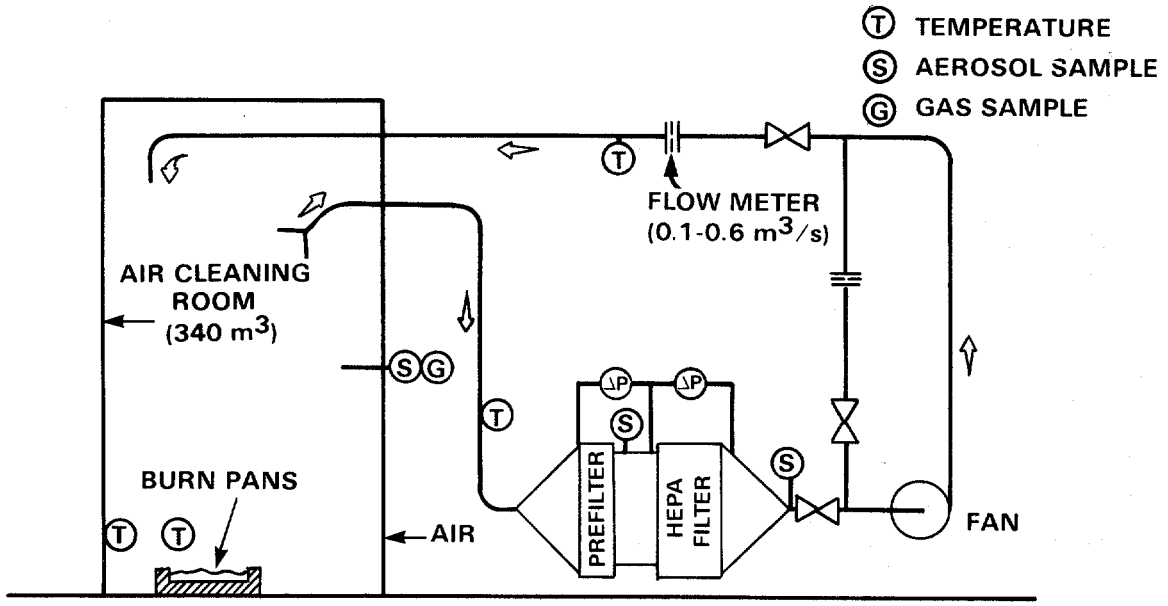

FIGURE 1. Schematic of Filter Loading Test Equipment.

Test Filters

The HEPA filters tested consisted of a glass media with and without nonmetallic separators. They were HEPA/HPS (Hanford Plant Standards) Type C, having an efficiency of ≥99.97% for 0.3 μm DOP particles. The HEPA filters were all 60 x 60 cm face area, 30 cm thick. One knitted stainless steel metal mesh prefilter with face area of 60 x 60 cm and thickness of 13 cm was tested.

The sand and gravel beds tested consisted of various sized aggregate and sand particles as shown in Figure 2. The beds were arranged in series such that the aerosol contacted the largest aggregate sized bed first and then the progressively smaller sized aggregate and sand particle beds thereafter. Flow of aerosol was directed upward through the beds to favor loading of aerosol on the lower section of the beds. This arrangement provided the ability to measure the effectiveness of each gravel or sand particle size with respect to other beds in removing aerosol.

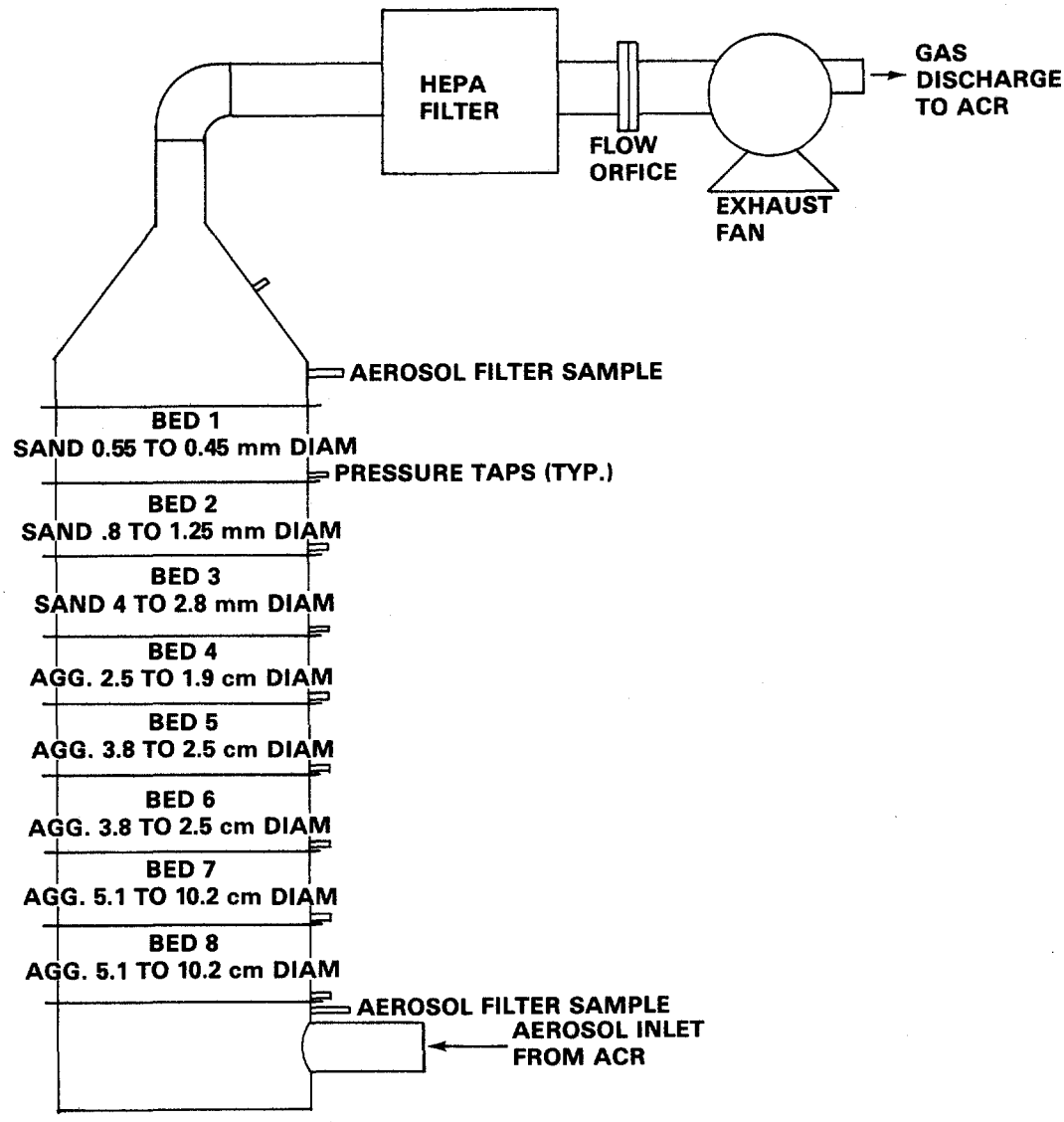

FIGURE 2. LSB-1 Sand and Gravel Filter Loop Schematic

III. Test Procedure

Two test series were performed, LFL-1 and LFL-2. In the first series (LFL-1), eighteen kilograms of lithium were heated to 300°C in two heater pans under an argon atmosphere and then exposed to air (0.4 m^2 surface area) to ignite the lithium and generate aerosol. The aerosol concentration was monitored until it reached 0.50 g/m^3 -- at which time the commercial filter test loop fan was activated to draw aerosol from the room to the preweighed test filter. The flow rate was maintained at 0.472 m^3/sec until the test filter was loaded (ΔP across filter reached 5 kPa). Aerosol concentrations in the duct were measured before and after the test filter. After loading a test filter, flow was discontinued, the filter was removed and weighed, another preweighed filter was placed in the loop, and flow was resumed. During this test series, two filters were loaded and a third was partially loaded.

In the second series, LFL-2, about 45 kilograms of 230°C lithium was added to a reaction pan and allowed to ignite and burn in the Air Cleaning Room to generate aerosol. The commercial filter test loop was loaded with a preweighed prefilter and a preweighed HEPA filter with separators. When the room aerosol concentration exceeded 0.5 g/m^3 the commercial filter test loop and the sand and gravel bed test loop were activated to draw aerosol from the room. Flow at 0.47 m^3/sec to the commercial filters was maintained until the filters were loaded to a total pressure drop of about 5 kPa. Flow was then discontinued and the filters removed and weighed to determine the aerosol loading. A sleeve was then placed in the prefilter location of the loop and a preweighed HEPA without separators was placed in the test loop. Aerosol flow to this HEPA was started at 0.47 m^3/sec and maintained until the filter was loaded to a ΔP of about 0.3 kPa at which time the aerosol in the room was depleted. The flow was discontinued and the filter weighed.

The sand and gravel bed filters were tested concurrently with the commercial filters as part of test LFL-2. These tests were initiated by starting flow at 0.014 m^3/sec through the first stack LSB-1A when the room aerosol concentration reached 0.5 g/m^3. The flow was maintained steady during the loading period with the exception of a 9 minute period that the flow was stopped to establish a pressure drop reading across the backup HEPA. The flow was terminated when the sand and gravel bed filter total ΔP reached 6.5 kPa. This loaded stack was removed and a second stack LSB-1B was placed in the loop. The backup HEPA filter was also replaced with a second HEPA. The aerosol flow was started at 0.001 m^3/sec and maintained constant until the aerosol concentration in the room decreased below 0.4 g/m^3 at which time it was terminated.

IV. Test Variables and Aerosol Characterization

The test variables examined in these tests were:

- Filter flow rate
- Aerosol generation conditions

Table I. Initial and Final Room Atmosphere Conditions

Filter #	Filter	Stage	Room Atm. Tem. °C	Rel. Hum.	Concentration Mole % O_2	N_2	CO_2	H_2	Time	Room Aerosol Conc. g/m^3
LFL-1	HEPA	Initial	42	26	20	78.5	0.15	<.01	13:10	0.40
A	W/sep	Final	61	4	19	78.5	0.15	<.01	13:59	3.4
B	HEPA	Initial	65	3	19	78.5	0.15	<.01	14:02	3.6
	W/sep	Final	65	3	18.5	78.6	0.16	<.01	14:33	3.95
C	HEPA	Initial	65	3	18.5	78.6	0.16	<.01	14:37	3.4
	W/sep	Final	53	9	18.5	78.6	0.16	<.01	15:00	0.6
LFL-2	Prefilter &	Initial	42	<1	20.9	78.1	0.07	<.01	10:00	0.75
A	HEPA w/sep	Final	67	<1	20.3	78.7	0.04	0.01	10:51	4.7
B	HEPA	Initial	67	<1	20.7	78.2	0.08	<.01	11:02	5.0
	WO/sep	Final	68	<1	20.5	78.5	0.07	0.01	12:21	1.3
C	HEPA	Initial	70	<1	18.6	80.3	0.04	0.07	12:33	2.2
	WO/sep	Final	50	<1	20.5	78.5	0.05	0.04	15:10	0.3
LSB-1	Stack	Initial	43	<1	20.8	78.2	0.06	<0.01	10:10	0.8
	A	Final	67	<1	20.6	78.6	0.04	0.01	10:59	4.8
LSB-2	Stack	Initial	65	<1	20.5	78.5	0.07	0.01	11:56	0.5
	B	Final	50	<1	20.5	78.5	0.05	0.04	15:10	0.3

- Commercial filter construction, with or without separators
- Effect of prefilter on HEPA performance.

The initial and final atmosphere conditions for each of the filters tested are listed in Table I. Plots of the room aerosol concentration during the tests is shown in Figure 3 with the times of each filter loading period and lithium add times.

The ratio of lithium mass to total aerosol mass is shown in Figure 4 for the room aerosol during Test LFL-2. This ratio tends to decrease with time suggesting that the aerosol reacts to form a carbonate and/or hydrate.

The aerosol Aerodynamic Mass Median Diameter (AMMD) and standard deviation for various times during each test are listed in Table II.

Table II. AMMD and Standard Deviation of Test Aerosols

Time Minutes From Ignition	LFL-1 AMMD µm	LFL-1 Standard Deviation	LFL-2 AMMD µm	LFL-2 Standard Deviation
24	1.58	3.35		
44	3.4	4.41	0.79	5.25
86	4.4	4.3		
103			3.6	2.41
143			2.27	2.25
200			3.50	2.30

After each test series the aerosol collected in the deposition pans was weighed and titrated, and the results along with the filter loading data used to determine the total aerosol generation.

V. Experimental Results

The test results include mass loading capacities of the filters, final pressure drop across the filters and removal efficiencies measured. These test results are summarized in Table III for the commercial filters and Table IV for the sand and gravel bed filters. The average aerosol mass concentration at the filter inlet as determined by the total mass divided by the total volume throughout is also listed in these tables.

Mass Loading Capacity of Filters

The HEPA mass loading ranged from 2.8 to 4.0 kg (7.8 to 11.1 kg/m^2) at a pressure drop of 5 kPa for lithium aerosol generated in normal humidity air. The loading capacity appeared to be dependent upon the period of aerosol generation and the flow rate of aerosol to the filters but not greatly influenced by the presence of a prefilter or of separators in the HEPA filter. These loading parameters had similar effects on loading as those reported by McCormack for

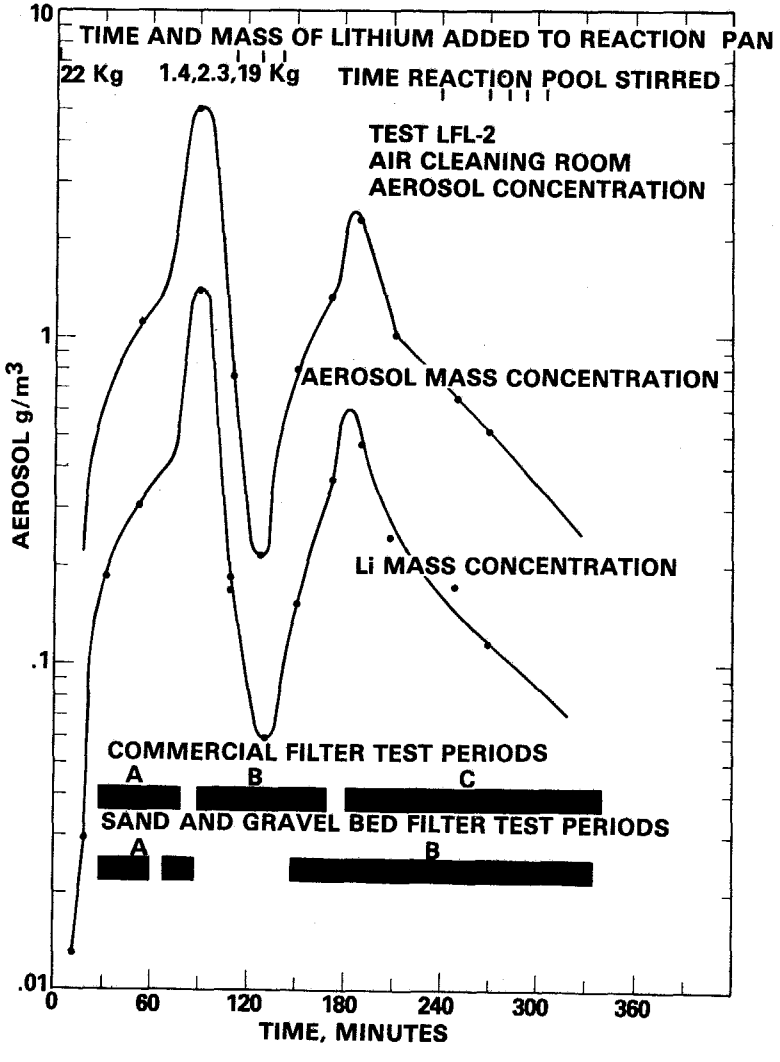

FIGURE 3 (a). Air Cleaning Room Atmosphere Aerosol Concentration.

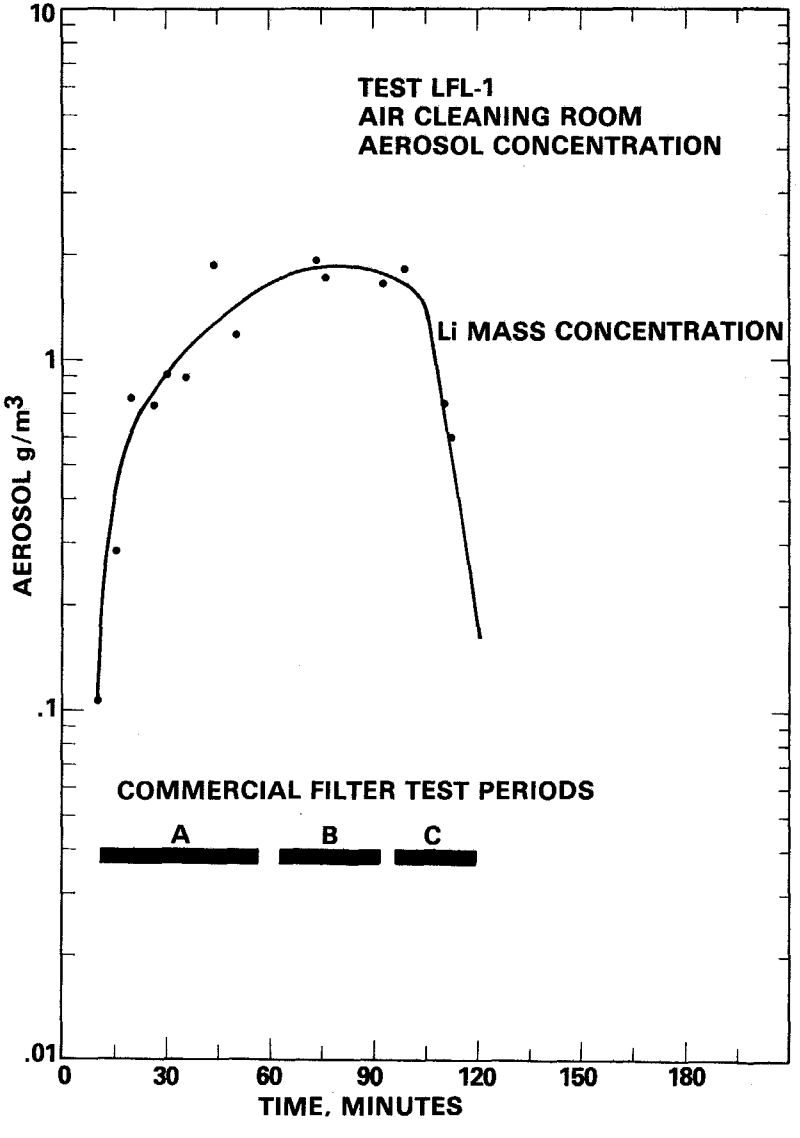

FIGURE 3 (b). Air Cleaning Room Atmosphere Aerosol Concentration.

TABLE III. Filter Loading Test Results

Test #	Filter Arrangement		Flowrate	ΔP kPa		Measured Mass Aerosol Collected kg			Proj. Mass Loading (kg) at ΔP=5 kPa	Aerosol Removal Eff. %	Average Aerosol in Inlet Duct g/m³
	Pre-filter	HEPA	m³/sec	Pre-filter	Total	Pre	HEPA	Total			
LFL-1											
A	None	With Separators	0.47		5.0		2.8		2.8	>99.99	1.6
B	None	With Separators	0.47		5.0		3.7		3.7	>99.99	3.4
C	None	With Separators	0.47		1.2		1.5			>99.99	1.8
LFL-2	Metal Mesh 13 cm Thick										
A		Without Separators	0.47	1.7	5.7	1.91	1.49	3.4	3.1	>99.99	2.0
B	None	Without Separators	0.47		4.4		3.85		4.0	>99.99	1.5
C	None	With Separators	0.09		0.2		0.86			>99.99	1.0

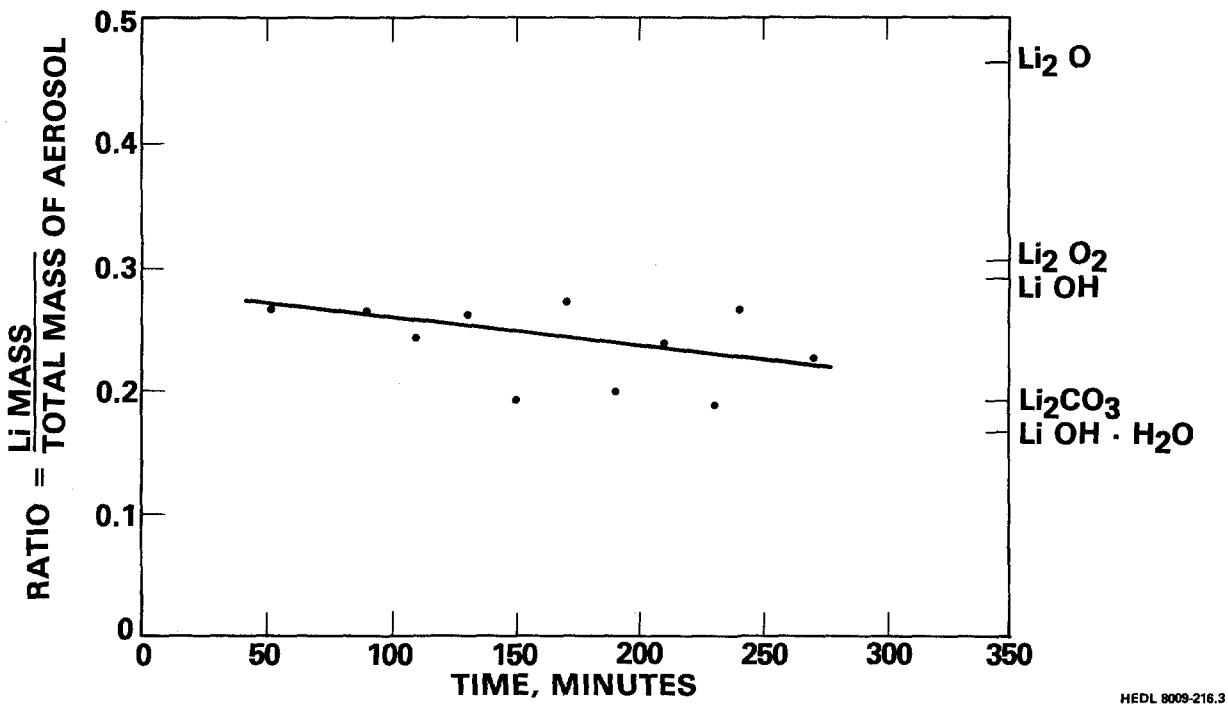

FIGURE 4. Air Cleaning Room Lithium Mass Ratios for Test LFL-2 Aerosol

sodium aerosols with the exception of flow rate.[2] The sand and gravel bed filter loaded to 0.13 kg/m^2 at a pressure drop of 6.2 kPa.

Period of Aerosol Generation

The filters loaded during early periods of aerosol generation, LFL-1-A and LFL-2-A, had the lowest aerosol loading (2.8 and 3.1 kg respectively at a pressure drop of 5 kPa). The reason for this smaller loading is thought to be the small particle size of the initial aerosol generated as was shown by the AMMDs in Table II. The filters loaded during later periods of aerosol generation, LFL-1-B and LFL-2-B, were loaded to 3.7 and 4.0 kg at a pressure drop drop of 5 kPa.

Flow Rate Effect on Loading

The loading capacity of HEPAs for lithium aerosol appeared to be increased by decreasing the flow rate of aerosol laden gas. For 0.09 m^3/sec flow rate the LFL-2-C filter was loaded to 0.86 kg of aerosol with only 0.2 kPa pressure drop before the aerosol in the Air Cleaning Room was depleted. At the HEPA nominal flow rate of 0.47 m^3/sec the filter (LFL-1-C) pressure drop increased by 1.2 kPa with 1.5 kg of aerosol. For this filter the loading to 0.86 kg corresponded with a pressure drop increase of 0.6 kPa which is greater than that for LFL-2-C indicating that a greater mass load can be obtained with a lower flow rate.

The loading of two identical sand bed filters at the two flow velocities, stack A at 0.069 m/sec and stack B at 0.0047 m/sec indicates that this particular arrangement of beds will load more aerosol at the lower flow rate than at the higher. The low flow rate test was terminated at a 0.02 kPa pressure drop because of a lack of available aerosol. Table IV shows a much greater percentage of aerosol buildup in filter B large aggregate sized beds 6, 7, and 8 than does A. Filter A shows a 68% buildup in fine aggregate sized bed 3 which caused its large pressure buildup.

Filter Efficiencies and Pressure Drop

All commercial HEPAs and the prefilter and HEPA series combination tested were determined to have removed >99.99% of the aerosol. The sand and gravel bed filter was determined to have a greater efficiency (99.69) at a face velocity of 0.069 m/sec. The lithium content of the aerosol in the inlet and outlet gas flow to the sand and gravel filter is shown in Table V as determined by aerosol samples and by averaging the lithium collected on the sand and gravel filter for the inlet concentration and on the backup HEPA filter for the outlet concentration. The efficiency of the sand and gravel filter is also shown in this table at the various sample times as determined from the respective sample results. The average efficiencies determined by total amounts collected on the sand and gravel filter versus the HEPA filter are also listed. The pressure drop across the commercial filters tested are shown in Figure 5. The pressure drop across the sand and gravel bed stacks tested are shown in Figure 6. A photograph of typical loaded filters is shown in Figure 7.

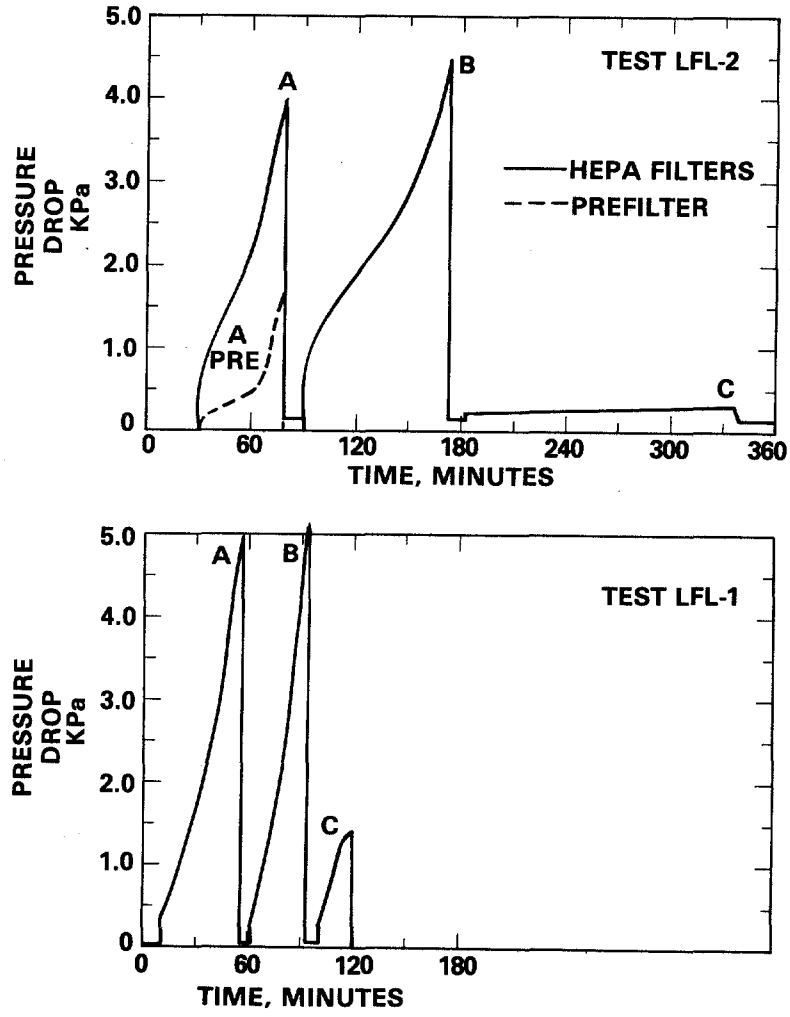

FIGURE 5. Pressure Drop Across Commercial Test Filters.

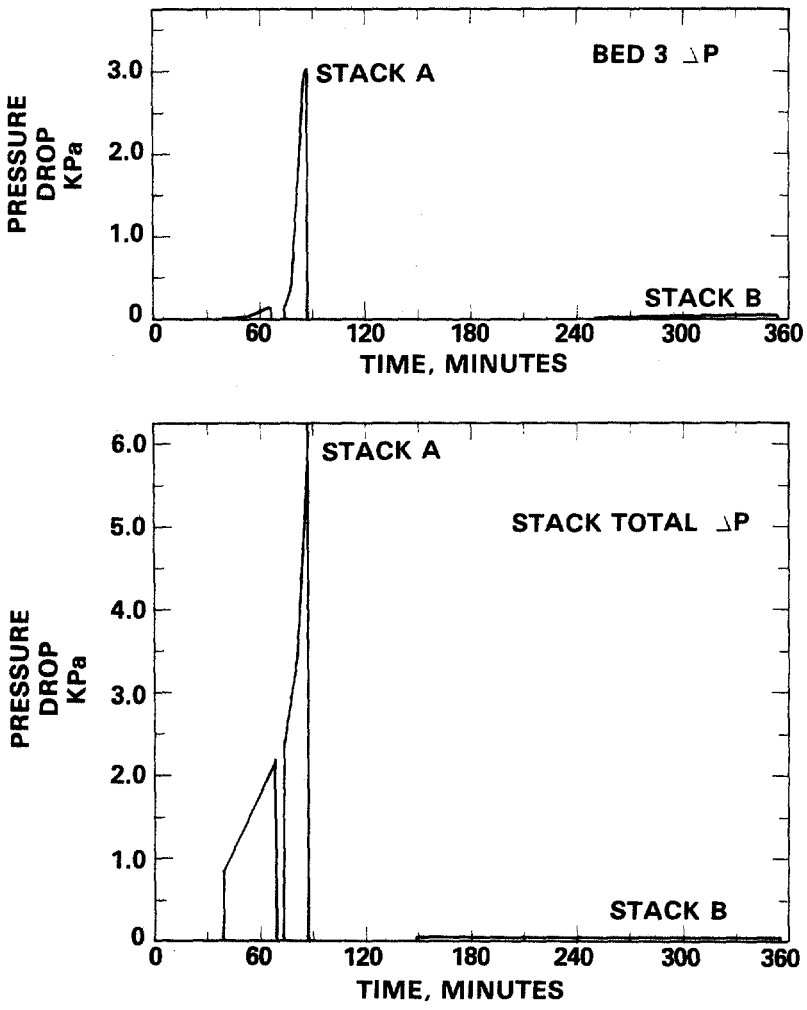

FIGURE 6. Sand and Gravel Bed Test Pressure Drop.

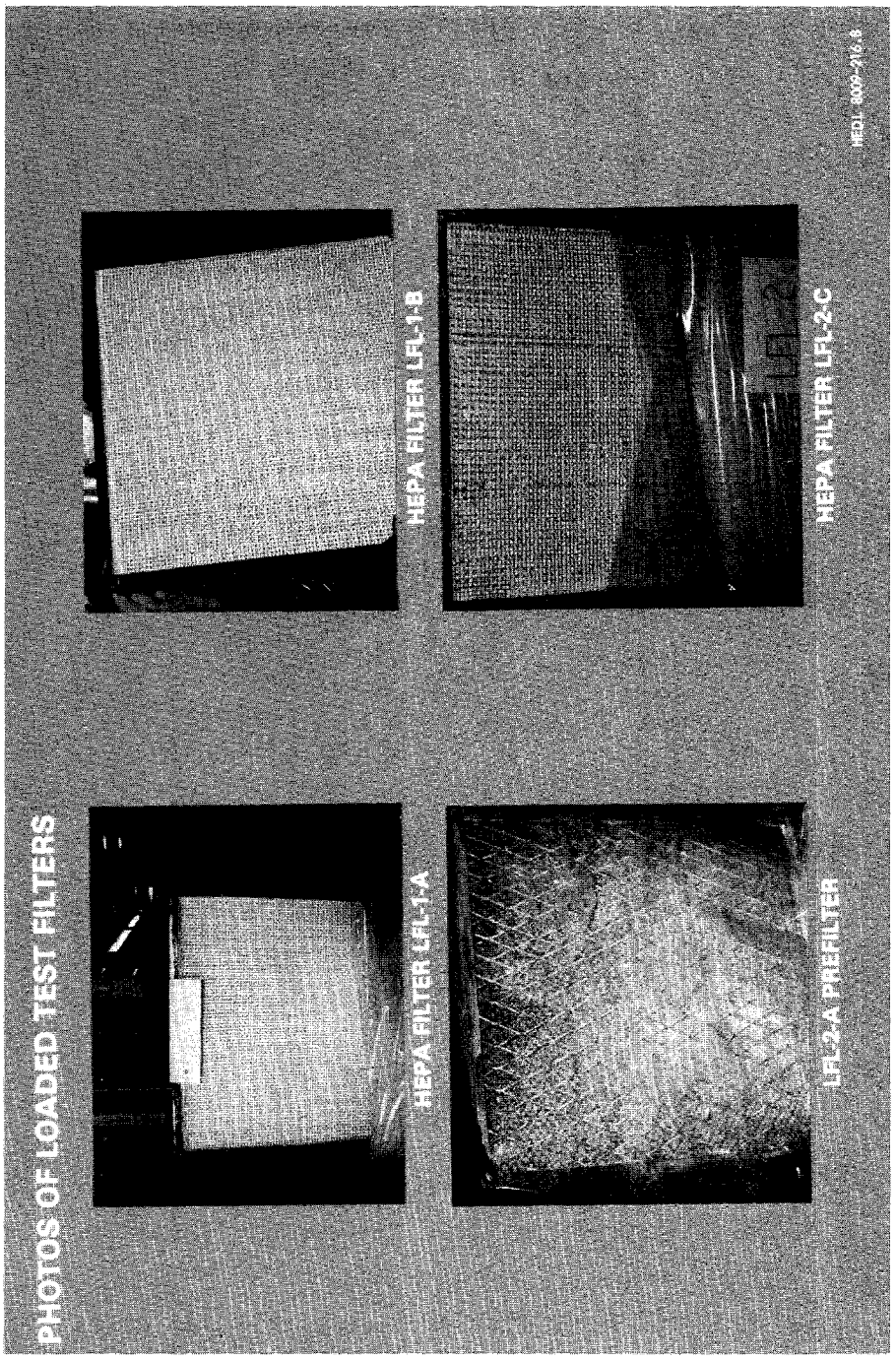

FIGURE 7. Photos of Loaded Test Filters.

TABLE IV. Lithium Sand Bed Loading

Stack Flowrate, m/sec	A 0.069	B 0.047
Bed	gr Li Collected	gr Li Collected
1	0.21	.06
2	3.21	.15
3	17.42	.11
4	1.03	.09
5	1.06	.12
6	1.14	.28
7	0.61	.42
8	0.86	.44
Inlet	.70	.31
Outlet	<.001	<.001
HEPA	.0798	.0294
Total Collected g on beds 1-8	25.54	1.68
Lithium Mass Loading		
g Li/m^2	126	8.28
g Li/m^3	103	6.80
Efficiency	99.69	98.23
Final Pressure Drop kPa	6.2	0.02
Average Aerosol Concentration in Inlet g Li/m^3	0.60	0.15

TABLE V. Sand and Gravel Bed Loading Efficiencies

Stack	Total Time of Flow Min.	Sample Time Into Loading Min.	Aerosol Concentration g Li/m³ Inlet By Sample	Inlet Average By Loading	Outlet By Sample	Outlet By HEPA Loading	Efficiency By Gas Sample	Efficiency Average HEPA Loading
A		15	0.393		.00218		99.55	
0.069 m/sec	50							
		36	1.085					
		41			.0009		>99.99	
		48	2.09					
				0.60		0.00186		99.69
B		5	0.212		.00791		96.27	
0.0047 m/sec	195	35	.254		.00184		99.28	
		65	.141		.00088		99.38	
		95	.092		.0011		98.80	
		125	.103		.00116		98.87	
		155	.077		.00102		98.67	
		185	.042		.00062		98.52	
				0.15		.00265		98.23

Aerosol Release and Duct Collection

The lithium was allowed to burn to completion during each test. The total aerosol generated was determined by summing up the aerosol collected on the test filters, that settled on the floor of the Air Cleaning Room and in the duct to the HEPA filters. The aerosol settled on the floor was determined by measuring the mass and lithium content of aerosol collected in several deposition pans placed throughout the room. The aerosol collected in the duct was determined by washing the duct with water at the conclusion of the test and titrating for lithium. In test LFL-1, 17 percent of the lithium was released as an aerosol and in test LFL-2 10 percent of the lithium was released. The difference in quantity of aerosol generated was thought to result because of the external heat applied to the reaction pans in test LFL-1 where none was applied in test LFL-2.

Thirteen percent of the aerosol entering the 13 meter length of 25 cm diameter duct plated out on the wall of the duct. The inlet duct included a 10-m horizontal length, a 3.4-m vertical length. Two 90° ells, one 45° ell and a one-meter 30° tapered inlet section.

VI. Conclusions

A number of preliminary conclusions about the loading capacities of filters loaded with lithium aerosols generated by burning lithium in normal humidity air are:

- HEPA/HPS type C loading capacities range between 2.8 and 4.0 kg when loading at a nominal 0.47 m^3/sec flowrate and to a pressure drop of 5 kPa.
- HEPAs without separators have about a 10 percent greater loading capacity.
- The prefilter tested was not effective in increasing the combined filter holding capacity.
- The holding capacity was increased for both the HEPA and sand and gravel bed filters by reducing the flowrate.
- The aerosol generated during the first period of a lithium fire causes a greater pressure drop across a HEPA per unit mass collected than the aerosol collected at later periods.
- The sand and gravel bed filter arrangement loaded with 0.414 kg/m^2 at a flowrate of 0.069 m/sec.
- The sand and gravel bed filter efficiency increased as it was loaded with aerosol.
- The loading capacity of the sand and gravel bed filter may be increased by selecting improved particle sizes for the beds for a given flowrate.

- HEPA filter loading was considerably greater than for the sand and gravel bed filter tested. 11.6 kg aerosol/m^2 at 1.31 m/sec flow and 5 kPa pressure drop versus 0.48 kg aerosol/m^2 at 0.069 m/sec flow and 6.2 kPa pressure drop.

- These conclusions are in close agreement with those reported for sodium aerosols with the exception of flow rate for HEPA filters. It has been reported that the holding capacity is not strongly increased by using lower than nominal flow for sodium aerosols.

VII. REFERENCES

1. D. W. Jeppson, "Interactions of Liquid Lithium With Various Atmospheres, Concretes, and Insulating Materials; and Filtration of Lithium Aerosols," HEDL-TME 79-7. April, 1978.

2. J. D. McCormack, R. K. Hilliard, J. R. Barreca, "Loading Capacity of Various Filters for Sodium Oxide/Hydroxide Aerosols," Proceedings of the 15th DOE Nuclear Air Cleaning Conference, CONF 780819.

3. J. R. Barreca, J. D. McCormack, "Sodium Fire Aerosol Loading Capacity of Several Sand and Gravel Filters, "Proceedings of 16th DOE Nuclear Air Cleaning Conference, San Diego, California. October, 1980.

DISCUSSION

BURCHSTED: Were these mass efficiencies?

JEPPSON: Yes, they were.

DIETZ: Some rather serious explosions have been experienced in lithium high-capacity storage batteries. Have you seen any effect of dirty air, containing carbon dust or hydrocarbon, during the experimentation you have reported?

JEPPSON: We have not looked for that, and have not seen anything that would indicate that it is occurring.

WILHELM: Did you see any corrosion on the glass fibers from lithium hydroxide? Did you perform tests at average or higher relative humidities?

JEPPSON: No, we did not. We did use nonmetallic separators to get away from corrosion.

HOLLOMAN: I noticed in the conclusion that the use of separator-type or separatorless-type filters had an effect.

JEPPSON: About a 10% difference. This is very little. effect.

HOLLOMAN: But it was an increase?

JEPPSON: An increase for the one without the separators.

A UNIQUE APPROACH TO CARBON SAMPLING

by

DANIEL D. Whitney

Rancho Seco Nuclear Generating Station
Sacramento Municipal Utility District
P.O. Box 15930
Sacramento, California 95813

with

James R. Edwards

Charcoal Service Corporation
P.O. Box 3
Bath, North Carolina 27808

SUMMARY

To comply with Nuclear Power Plant Standard Technical Specifications, operating nuclear power plants are required to verify that the radioiodine removal efficiency of installed adsorber beds meets or exceeds acceptance criteria every 720 hours of adsorber bed operation.

Anytime the integrity of the adsorber bank is violated as a result of maintenance, or testing, an in-place bank bypass-leakage efficiency test is required. Such testing is time consuming and expensive, hence, Rancho Seco has devised a charcoal test tray which exposes adsorber samples to the bed environment and allows sampling without the necessity for violating the integrity of the filter bank.

INTRODUCTION

The Rancho Seco Nuclear Generating Station has one Pressurized Water Reactor of 913 MWe net. As is typical of many such facilities, the unit utilizes the CS-8T Type II Charcoal Adsorber Tray in its ventilation exhaust and post-accident air cleanup systems. It is the policy of the Nuclear Regulatory Commission to require new nuclear power plants to utilize the Standard Technical Specifications when they apply for their operating license, and for operating plants to incorporate these Standard Technical Specifications as changes or revisions are requested. These new specifications require adsorber radioiodine efficiency determination every 720 hours (one month) of adsorber operation, whereas previous requirements were "...once every refueling, not to exceed 18 months." Previous methods of obtaining adsorber samples required removing a tray from the installed bank. This violated the filter bank integrity and therefore required another test, the in-place leakage efficiency determination, to requalify the bank for service. In a facility like Rancho Seco, such sampling and retesting would constitute a continuous program requiring considerable manpower and expense. Developing a test tray which provides the appropriate and similar service conditions for the adsorber, and which would not require violating adsorber bank integrity when obtaining a sample, offered significant manpower and economic incentives.

CHARCOAL TEST TRAY

The Charcoal Test Tray is designed to replace a typical Type II Adsorber Tray, one built to CS-8T. Replacing the Type II Tray is a stainless steel frame which acts as the structural supports for the entire device, the sample canisters being mounted on a air-tight plenum cantilevered in front of the "normal" filter face. See Figure 1. Sample canisters are located only on the horizontal faces of the plenum, thus they duplicate the orientation and airflow directions found in a typical Type II tray. The feature which allows sampling without violation of the filter bank integrity is that the test tray plenum extends out into the access region on the downstream face of the filter bank. In this position, a technician can enter the unit, remove a sample canister, and replace it with a blank and return the unit to service. There is no requirement for in-place leakage efficiency testing as the maximum opening presently by an un-blanked sample port will not pass enough air to exceed the allowable bypass flow for most systems. Subsequent laboratory testing with radioactive methyl iodine is done directly on the adsorber in its sample canister without need to open or disturb.

It is important that the test tray be provided with sufficient sample canisters to provide the number of samples for the projected life of the adsorber material they are representing. Obviously, the sample canisters must be filled with the same "lot" of adsorber and see the same operating time as that of the filters they are representing. The sample canisters are shown in ANS I N509, 1980 Nuclear Power Plant Air-Cleaning Units and Components, and are the same two inch depth as the beds in a typical Type II adsorber tray.

APPLICATION AT RANCHO SECO

Rancho Seco has installed charcoal test trays in the following systems:

System	Number of Type II Trays	Airflow, cfm	Number of Test Cartridges
In-Containment - Safeguards A	126	40,000	12
In-Containment - Safeguards B	126	40,000	12
Reactor Bldg. Purge Exhaust	192	74,000	24
Auxiliary Bldg. Exhaust A	126	42,300	24
Auxiliary Bldg. Exhaust B	126	42,300	24
Auxiliary Bldg. Grade Level Exhaust	60	20,000	24

Measurements made on the installed canisters show that the design goal of 40 ft/min through the adsorber test canister is achieved if care is exercised in filling the canister with the adsorber. Packing full is necessary to allow for subsequent settling and to better represent the flow resistance of the tightly packed Type II beds.

Experience at Rancho Seco has confirmed the ease of installation and sampling. The reduction by one in the number of Type II trays installed in each bank does not have a significant effect on the flow through the remaining trays. Care was exercised in selecting the physical location of the test tray to insure that it was in a position seeing airflow representative of the average for the entire filter bank.

CONCLUSIONS AND RECOMMENDATIONS

Rancho Seco has found that the introduction of this charcoal test tray provides representative adsorber samples in a timely and cost effective manner, without imposing additional testing or maintenance requirements.

The Sacramento Municipal Utility District, owners of Rancho Seco, have applied for a patent on this concept, and have entered into an exclusive license with Charcoal Service Corporation of Bath, North Carolina, to manufacture and sell trays of this type.

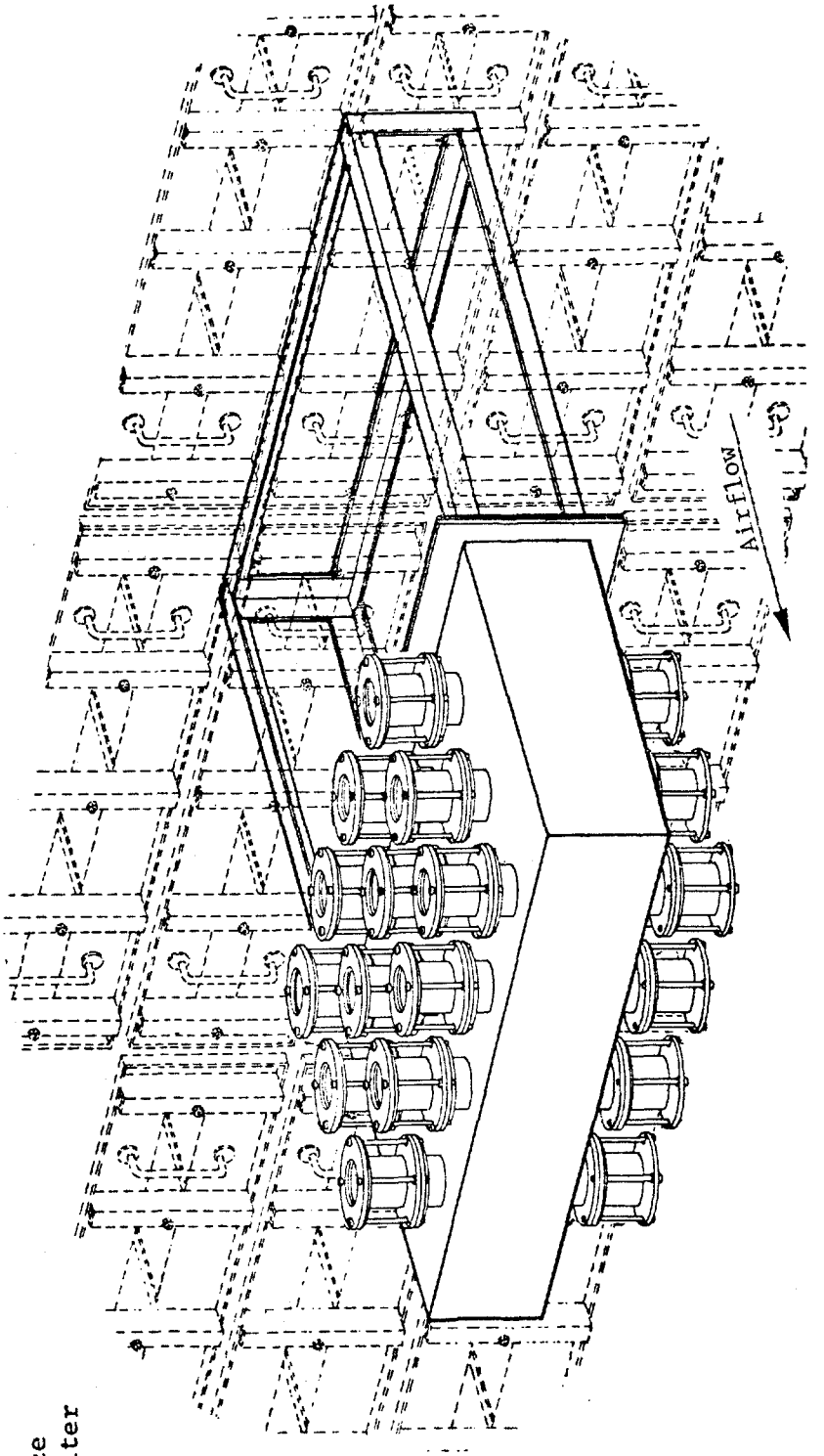
TRAY-TYPE
ADSORBENT SAMPLER
Airflow
Downstream Face
of Type II Filter
Bank

Figure 1

DISCUSSION

EVONIUK: Does the insertion of a sample affect the flow characteristics of the bed such that the adsorption characteristics of the test charcoal would be different than what would be representative of the total bed itself?

WHITNEY: No, it does not. One of the beauties of this design is that we maintain a geometric orientation of the beds, or the trays themselves, that is representative. We maintain the same geometry, the same orientation, and the air distribution and air flow through the test cell, or cartridge, is the same as in the actual charcoal bed.

FIRST: Will you tell us how you have determined that it is the same?

WHITNEY: We have made some measurements by going in and measuring the air flow through each one of the various test cells. We have also taken the trouble to locate the test tray in a position that we previously determined to be at the average flow rate for the entire bank.

DEITZ: We have exposed four 2 inch columns of carbon in parallel to a flow of high humidity air and then determined the methyl iodide-131 penetration through each. The four samples should have shown the same penetration. It was found that the 2 inch canisters must be packed equally in order to assure equal air flow through each.

WHITNEY: We also noticed quite a difference when we first ran some of these tests depending upon the amount of carbon and how it was packed into the tray. And so, we have taken pains to insure that the same quantity is packed to the same compaction in all of the trays.

EDWARDS: I have one more thing I would like to add, using a figure. Sometimes a small system does not have the room to cantilever the unit out into the access plenum. Figure 1 shows the same arrangement Mr. Whitney showed, but with usable charcoal in either side. With this arrangement, you lose only about 30% of the charcoal. The next figure, No. 2, is the one that is of interest, and the one I would like to talk about. Typically, an emergency control room ventilation system, such as Farr would manufacture, does not have an access plenum. We have designed the cartridges into the plenum of the bed itself. We just recessed the carbon back about 8 inches and installed the cartridges in that recess.

FEATURES

- No In-Place Test Of Filter Bank Required After Sampler Is Removed.
- Unit Fits Into Slot Vacated By Standard Type II Cell.
- Various Quantity Of Samplers Available For Any Size Filter Bank.
- Samplers Are Accessable For Quick And Easy Removal.
- The Sample May Be Tested For Iodine Efficiency Without Disturbing The Adsorbent In The Sampler.

TECHNICAL DATA

- All T-304 Stainless Steel Construction.
- Weight Of Unit Is Approx. The Same As A Filled Type II Cell (i.e., 85lbs.)
- Rated Flow Of 30" Long Unit At 40FPM Thru Charcoal Bed Is 214 CFM.
- Canister Geometry Meets The Requirements Of ANSI/ASME N509-1976

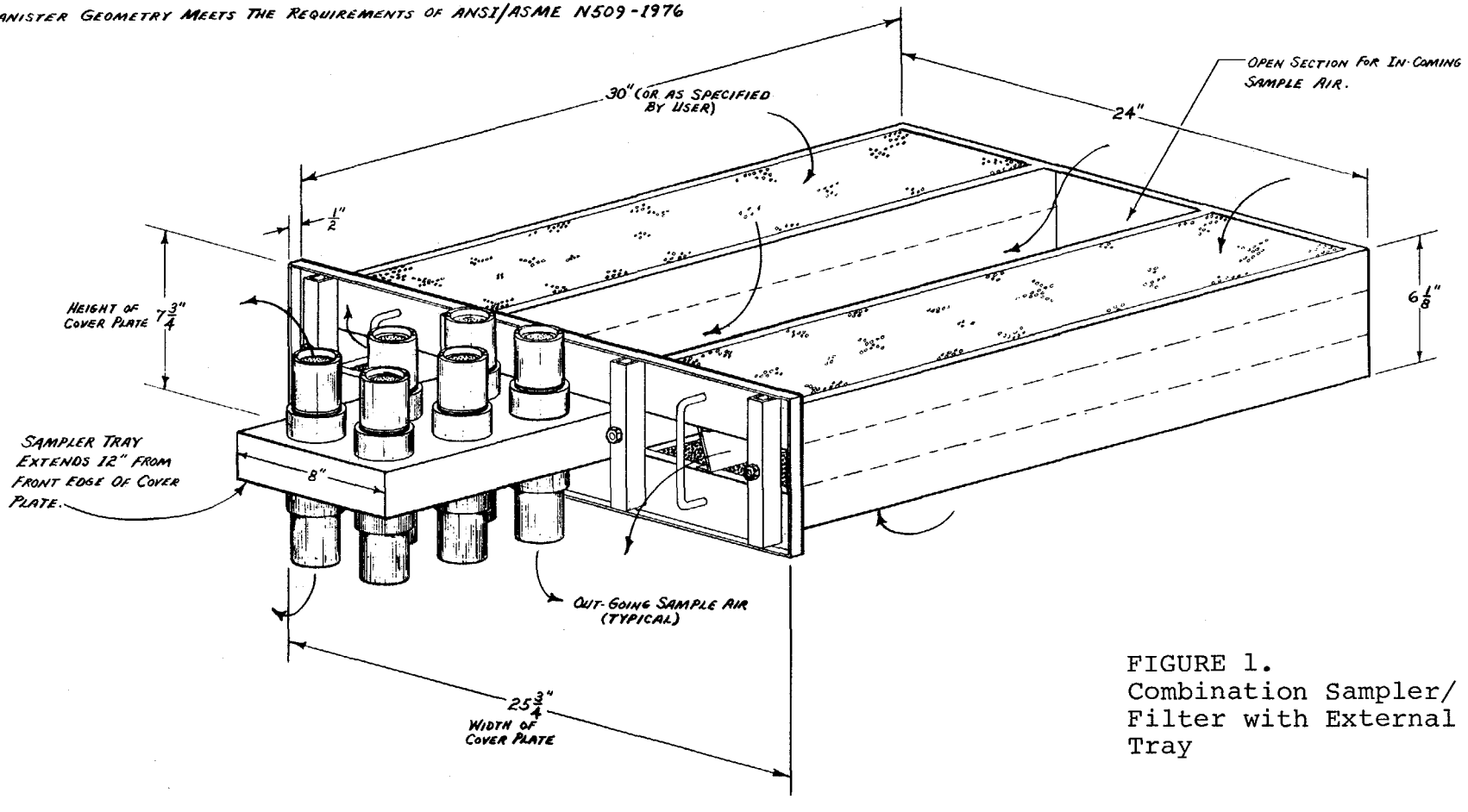

FIGURE 1.
Combination Sampler/
Filter with External
Tray

FEATURES

- No In-Place Test Of Filter Bank Required After Sampler Is Removed.
- Unit Fits Into Slot Vacated By Standard Type II Cell.
- Various Quantity Of Samplers Available For Any Size Filter Bank.
- Samplers Are Accessable For Quick And Easy Removal.
- The Sample May Be Tested For Iodine Efficiency Without Disturbing The Adsorbent In The Sampler.
- Samplers Do Not Project Out Into Access Area.

TECHNICAL DATA

- All T-304 Stainless Steel Construction.
- Weight Of Unit Is Approx. The Same As A Filled Type II Cell (i.e., 85lbs.)
- Rated Flow Of 30" Long Unit At 40 FPM Thru Charcoal Bed Is 279 CFM.
- Canister Geometry Meets The Requirements Of ANSI/ASME N509-1976

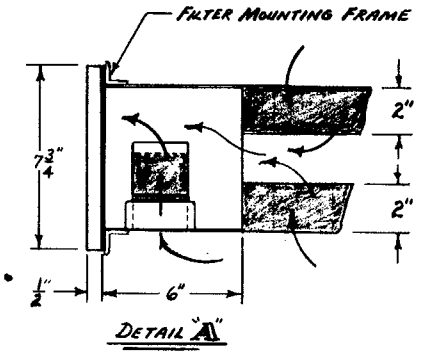

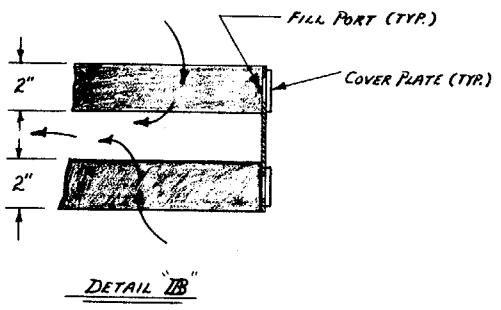

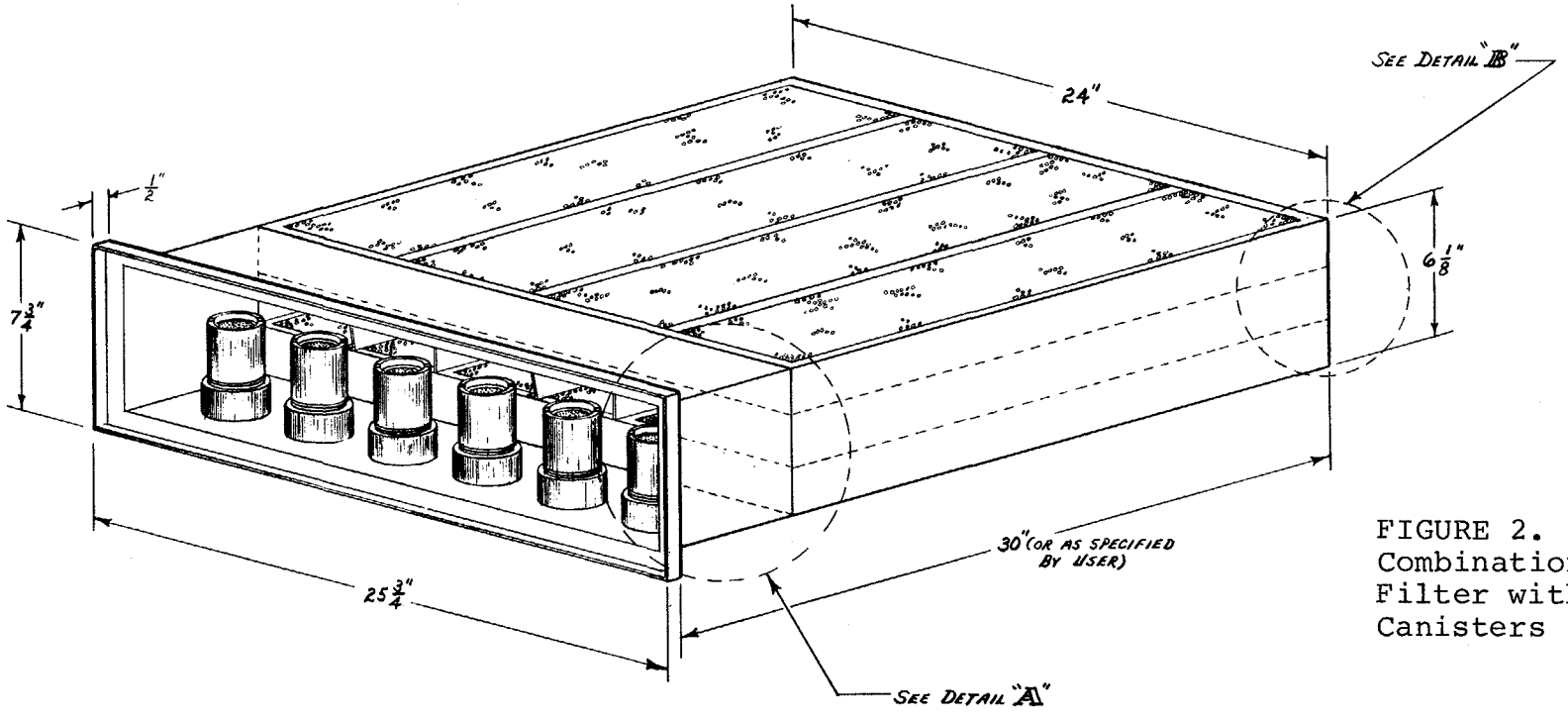

FIGURE 2.
Combination Sampler/
Filter with Recessed
Canisters

OCCURRENCE OF PENETRATING IODINE SPECIES IN THE EXHAUST AIR OF PWR POWER PLANTS

H. Deuber, J.G. Wilhelm
Laboratorium für Aerosolphysik und Filtertechnik,
Kernforschungszentrum Karlsruhe GmbH,
Postfach 3640, D-7500 Karlsruhe 1,
Federal Republic of Germany

Abstract

Because of controversial or missing data the sorption of the potentially penetrating iodine species hypoiodous acid (HOI) and iodine benzene (C_6H_5I) by various iodine sorbents was investigated. (C_6H_5I was chosen as a model substance for aromatic iodine compounds.) An estimation was performed of the occurrence of these species in the exhaust air of PWRs by investigating the sorption of iodine by these sorbents.

The species mentioned were found to desorb to a substantial extent from iodine sorbents at extended purging. It was concluded that the fractions of these compounds are not significant in the exhaust air of PWRs.

Table of contents

1. Introduction

In the event of poor iodine removal by iodine filters, apart from aging the occurrence of penetrating iodine species has been frequently discussed. A potentially penetrating iodine compound is hypoiodous acid, HOI [1,2]. The retention efficiency of iodine sorbents for this compound has been examined [3]. It was found that the removal efficiency of impregnated activated carbons is higher than that of sorbents based on inorganic materials. Moreover, desorption of HOI with extended purging was observed.

The occurrence of HOI in the exhaust air of light water reactors has been investigated [4,5]. Average fractions of 20 % for BWRs and of 40 % for PWRs were found. However, in other investigations no HOI was detected in the exhaust air of PWRs [6].

Because of the low concentration of radioiodine in the exhaust air of nuclear power plants, the investigations on the occurrence of HOI were performed with radioiodine species samplers in which the iodine species are retained on particulate filters and specific sorbents respectively [7,8,9,10]. This is an indirect measurement. Also in laboratory investigations HOI has been identified indirectly only. The indirect evidence of gaseous HOI may be one of the reasons why the data on retention and occurrence of this species are not beyond controversy.

Other potential penetrating iodine species are aromatic iodine compounds, such as iodine benzene, C_6H_5I [11]. Data on retention and occurrence of these compounds seem to be very limited.

Because of controversial or missing data investigations were carried out which aimed at:

(a) determination of the adsorption and desorption behavior of HOI and C_6H_5I with sorbents used in iodine filters and iodine species samplers;

(b) estimation of the occurrence of these compounds in different exhausts of PWRs by the adsorption and desorption behavior of iodine with these sorbents.

2. Laboratory tests

2.1. General

Test sorbents

The sorbents investigated for retention of iodine species are listed in Table I. They comprise sorbents used in iodine filters and eligible for iodine species samplers (CG 0.8, AC 6120) and sorbents used in iodine species samplers only (DSM 11, CDI, IPH).

Test agents

Apart from hypoiodous acid (HOI) and iodine benzene (C_6H_5I) elemental iodine (I_2) and methyl iodide (CH_3I) were used in the tests on removal efficiency. The knowledge of the retention of I_2 and CH_3I is essential for judging the retention of the other iodine compounds and for judging the iodine fractions obtained with iodine species samplers.

The iodine species were tagged with ^{131}I. I_2, CH_3I and HOI were generated by standard methods:

$$6\ K\ ^{131}I + K_2Cr_2O_7 \rightarrow 3\ ^{131}I_2 + Cr_2O_3 + 4\ K_2O;$$

$$K\ ^{131}I + (CH_3)_2\ SO_4 \rightarrow CH_3\ ^{131}I + CH_3\ K\ SO_4;$$

$$^{131}I_2 + H_2O \rightarrow HO^{131}I + H^+ + {}^{131}I^-.$$

C_6H_5I was prepared from aniline via diazotozation [12].

The purity of I_2, CH_3I and C_6H_5I, as inferred from penetration profiles, was high: the fractions of the impurities were << 1 %. In the case of HOI, the fraction of impurities (organic iodides) was 10 to 20 %.

Test conditions

The test conditions are given in Table II. The carrier concentration (^{127}I) was 10^{-3} g/m^3 in the tests with I_2 and CH_3I. Due to the preparation method, the carrier concentration was different for HOI and C_6H_5I. However, the carrier concentration has been shown to have no influence on retention over a very wide range.

Many of the tests described in this account were conducted either at 40°C and 50 % R.H. or at 30°C and 20 % R.H. The temperature of 40°C and the relative humidity of 50 % are standard average conditions for testing sorbents eligible for iodine species samplers in our laboratory. The standard total range in this context is 10 to 70°C and 20 to 80 % R.H. (DSM 11 has been tested in this range [6].) 30°C and 20 % R.H. are typical conditions of the exhausts of the PWRs investigated. These conditions were used in tests with HOI when the strong influence of temperature and relative humidity on the retention of HOI had become apparent. The activated carbon tests were performed under the most adverse relative humidity, i.e. at 98 to 100 % R.H.

Limiting values

The detection limit for ^{131}I, measured with a NaI(Tl) detector, was 10^{-11} Ci per bed (100 % error at the 3 σ confidence level). Total activities of 10^{-3} Ci ^{131}I were used in the cases of I_2, CH_3I, C_6H_5I and, due to the generation method, of 10^{-8} Ci ^{131}I in the case of HOI. These values translate to a minimum detectable penetration of 10^{-6} % in the first three cases and of 10^{-1} % in the last case.

Interpretation of results

The results of the retention tests are presented as accumulative removal efficiencies in the tables and as accumulative penetrations in the figures. (Penetration [%] is equal to 100 minus removal efficiency [%].)

When interpreting the semilogarithmic graphs of penetration versus bed depth, one should keep in mind the following principles:

(a) the type of an individual compound with respect to its sorption behavior is characterized by the slope of the corresponding straight line (possibly after resolving the curve);

(b) the percentage of an individual compound is given by the point of intersection of the corresponding straight line with the ordinate axis.

These principles apply if no desorption occurs. With desorption it is more difficult to interpret these graphs.

2.2. Tests with I_2 and CH_3I

2.2.1. Results

The results for the sorbents used in iodine filters are presented, together with the data for other iodine compounds, in Figs. 4, 5 and 8. The results for the sorbents used in iodine species samplers are given in Tables III and IV and in Figs. 1 to 3.

Sorbents for iodine filters

The retention of I_2 by CG 0.8 and AC 6120 is very high, even at a high relative humidity. The retention of CH_3I, strongly dependent on the relative humidity, is much lower. The values given apply to a purging time of 2 h. However, at purging times of 1 week essentially the same values hold.

Sorbents for iodine species samplers

I_2 is strongly retained by DSM 11, CDI and IPH, even at a purging time of 1 week. The small desorption found at the long purging time could be caused by impurities. CH_3I is retained to a very small extent by these sorbents.

2.2.2. Conclusions

According to the tests performed, at a residence of about 0.1 s DSM 11 and CDI are suitable for specifically retaining I_2 in the presence of CH_3I. As regards IPH, when used for specifically retaining HOI, I_2 would disturb, not however CH_3I. I_2 has therefore to be removed previously.

With CDI and IPH the results are consistent with other reported data except for the retention of I_2 by CDI for which a much lower value has been indicated (80 to 90 % at a residence of about 0.1 s) [9].

2.3. Tests with HOI

2.3.1. Results

The results for CG 0.8, AC 6120, DSM 11 and IPH are shown in Tables V and VI and in Figs. 4 to 7. CDI has not yet been investigated for retention of HOI in our laboratory.

Sorbents for iodine filters

In the case of CG 0.8, at a short purging time HOI is retained nearly as strongly as I_2. With increasing purging the penetration of HOI increases substantially and may become similar to that of CH_3I.

As regards AC 6120, at a short purging time the penetration of HOI is similar to that of CH_3I. At a long purging time the penetration of HOI is very high. Nearly complete desorption of HOI may occur. (The organic impurities are retained.)

Sorbents for iodine species samplers

With DSM 11 little HOI is removed, the amount diminishing with rising purging time.

IPH adsorbs HOI strongly at a short purging time: at a residence of 0.1 s the adsorption is nearly complete. (The organic impurities are not retained.)

At a long purging time the retention is much lower. It has to be mentioned that at slightly more adverse conditions (40°C, 50 % R.H.) nearly complete desorption was detected at a purging time of 1 week.

2.3.2. Conclusions

HOI is much better retained by CG 0.8 than by AC 6120. Analogous results are to be found in the literature (3). Because of the relatively strong desorption of HOI even from impregnated activated carbons, this compound could be a problem for iodine filtration if it occurred in high percentages in the exhausts to be filtered.

According to the tests conducted, at a residence time of about 0.1 s there is little interference by HOI in the specific retention of I_2 by DSM 11 in the presence of other iodine species. With the low retention of HOI by CDI reported in the literature (9), the same applies to CDI.

IPH can not be reliably used for quantitative retention of HOI (after removing I_2) over a wide range of conditions. In the literature both high and low retention of HOI by IPH is reported (9).

Information on the relative amounts of HOI can be conveniently obtained by establishing the extent of desorption from AC 6120 with purging.

2.4. Tests with C_6H_5I

2.4.1. Results

The data for CG 0.8 are to be found in Table VII and in Fig. 8, for AC 6120 and DSM 11 in Table VIII.

With CG 0.8 at a short purging time the penetration of C_6H_5I approximates that of I_2, at a long purging time the penetration of C_6H_5I is higher, but still much lower than that of CH_3I.

With AC 6120 and DSM 11 nearly complete penetration occurs.

2.4.2. Conclusions

C_6H_5I can be effectively retained by activated carbon only. Although desorption occurs, this species should be no problem in iodine filtration because its penetration can be expected to be much lower than that of CH_3I over long purging times.

In iodine species samplers C_6H_5I can be adequately retained by CG 0.8. If CG 0.8 is preceded by AC 6120, differentiation of CH_3I and C_6H_5I is possible.

3. In-plant tests

3.1. General

Exhausts investigated

A great number of tests were performed in the exhausts of a modern German PWR ("PWR3").These exhausts are characterized in Table IX. Some of the tests were also conducted in the exhausts of another PWR ("PWR 2").

Test conditions

Two groups of iodine species samplers used in the tests can be distinguished. They are called normal and special samplers in this context. The normal samplers contained media for retaining, in order of flow, particulate iodine, I_2, HOI and organic iodine. The group of normal samplers comprised two types of samplers, the difference consisting mainly of the media used. Detailed information can be obtained from the tables and figures containing the results.

The special iodine species samplers featured a different sequence of sorbents or other sorbents to obtain additional information on the iodine species contained in the exhaust investigated. In particular, AC 6120 was used instead of IPH to obtain information on the occurrence (a) of HOI by desorption of iodine from this sorbent during purging after sampling and (b) of C_6H_5I by migration of iodine through this sorbent (without purging after sampling). Details are contained in the tables and figures presenting the results.

Additional important informations pertaining to the in-plant tests are given in tables I and X.

Mostly a higher face velocity was used in the in-plant tests as compared to the laboratory tests to increase the ^{131}I activity collected in the samplers. However, this difference has been found to be irrelevant at the same residence time.

Usually the samplers were operated over a period of 7 days with no purging afterwards. However, in certain cases they were operated for 1 day only and purged over a period of 7 days under ambient conditions. Generally two or more samplers were run in parallel.

Limiting values

The detection limit for ^{131}I, measured with Ge(Li) detectors, was 10^{-12} Ci per sampler component (100 % error at the 1 σ confidence level). Total activities of 10^{-6} to 10^{-7} Ci ^{131}I were collected in the samplers operated in the equipment room exhaust and of 10^{-9} to 10^{-10} Ci ^{131}I in the samplers run in the hood and plant exhausts of PWR 3. Therefore, the minimum detectable percentage of ^{131}I per sampler component was ≤ 0.001 % in the case of equipment room exhaust samplers and ≤ 1 % in the case of hood and plant exhaust samplers.

3.2. Tests for HOI

3.2.1. Results

In the following sections only typical results obtained in PWR 3 are given. Those achieved in PWR 2 are quite similar.

Equipment room exhaust

The results for the normal samplers are presented in Table XI and in Figs. 9 and 10, for the special samplers in Tables XII to XIV and in Figs. 11 to 19.

In the two types of normal samplers the activities collected per sampler section differ to a high extent.

As regards the special samplers, with the samplers which differed in the type of I_2 sorbent (DSM 11 or CDI), there is a great difference in the activities found on the I_2 sorbent and on AC 6120. No influence of the purging time was detected with these samplers. With the samplers which featured a different order of DSM 11 and IPH, essentially the same activity distribution was detected. With the samplers which contained different sorbents downstream of CDI, a high activity was found on DSM 11 if this sorbent followed CDI directly, but a low activity was detected on DSM 11 if IPH had been placed between CDI and DSM 11.

Other exhausts

The findings are presented in Tables XV and XVI and in Figs. 20 to 25.

As in the equipment room exhaust, in the two types of normal samplers the activities found per sampler section differ substantially.

In the special samplers little activity was found on CG 0.8 placed downstream of AC 6120.

3.2.2. Conclusions

The conclusions can be summarized as follows:

(a) With different I_2 sorbents (DSM 11 or CDI) in iodine species samplers different fractions of iodine species can be found.

(b) In the exhausts investigated HOI was not present in significant proportions. At least two reasons can be offered. Firstly, because the activity passing both DSM 11 and CDI was strongly retained by AC 6120 (from which HOI desorbs easily), even after extended purging. Secondly, because when DSM 11 and IPH (which differ in removal efficiency for HOI) were used as first sorbents in samplers, essentially the same activity was found on each of the sorbents.

(c) The iodine which penetrated DSM 11 and was strongly retained by AC 6120 consisted mainly of CH_3I.

(d) The iodine which migrated through CDI and was strongly adsorbed by both AC 6120 and DSM 11 consisted mainly of CH_3I and I_2. (Penetration of CDI by I_2 to a high extent is in contradiction to the laboratory findings and can presently not be accounted for.)

3.3. Tests for C_6H_5I

The results from the samplers containing AC 6120 can be used for estimating the fractions in which C_6H_5I occurred in the exhausts investigated. In these samplers C_6H_5I would be collected on CG 0.8 downstream of AC 6120. The activity found on CG 0.8 downstream of AC 6120 corresponds therefore to the upper limit of C_6H_5I. According to the tests conducted this limit is 1 to 5 %.

4. Summary

In laboratory tests HOI (hypoiodous acid) and C_6H_5I (iodine benzene) were found to desorb from sorbents used in iodine filters to a substantial extent at long purging. In the case of HOI this result compares favorably with literature data. (For C_6H_5I no published data are known to exist.)

The retention efficiency of impregnated activated carbon for HOI may fall short of that for CH_3I. HOI could therefore be a problem for iodine filtration if this species occurred in substantial proportions in the exhausts to be filtered. Because of higher retention, C_6H_5I should be no problem.

From investigations with special iodine species samplers in the exhausts of PWRs it is concluded that the fractions of HOI and C_6H_5I are not significant. For HOI this conclusion is not in agreement with results to be found in the literature. (According to one publication the fraction of HOI may average 40 % in the exhausts of PWRs.)

As regards iodine species samplers, it is concluded that I_2 may partially pass the section for I_2 and be retained in the section for HOI. On the other hand HOI may partially penetrate the section for HOI and be adsorbed in the section for organic iodine. Thus, the presently used samplers may fail to adequateley differentiate the iodine species.

Acknowledgements

Most of the tests were performed by K. Bleier and R. Butz. The tests with HOI were conducted by G. Birke. C_6H_5I was prepared by H.E. Noppel.

References

1) Cartan, F.O., et al., "Evidence for the existence of hypoiodous acid as a volatile iodine species produced in water-air mixtures," CONF-680 821, p. 342 - 353 (1968).

2) Keller, J.H., et al., "Hypoiodous acid: an airborne inorganic iodine species in steam-air mixtures," CONF-700 816, p. 467 - 481 (1970).

3) Kabat, M.J., "Testing and evaluation of absorbers for gaseous penetrative forms of radioiodine," CONF-740 807, p. 765 - 799 (1974).

4) Pelletier, C.A., et al., "Sources of radioiodine at boiling water reactors," EPRI NP-495 (1978).

5) Pelletier, C.A., et al., "Sources of radioiodine at pressurized water reactors," EPRI NP-939 (1978).

6) Deuber, H., Wilhelm, J.G., "Determination of the physico-chemical ^{131}I species in the exhausts and stack effluent of a PWR power plant," CONF-780 819, p. 446 - 475 (1978).

7) Keller, J.H., et al., "A selective adsorbent sampling system for differentiating airborne iodine species," CONF-700 816, p. 621 - 634 (1970).

8) Keller, J.H., et al., "An evaluation of materials and techniques used for monitoring airborne radioiodine species," CONF-720 823, p. 322 - 330 (1972).

9) Emel, W.A., et al., "An airborne radioiodine species sampler and its application for measuring removal efficiencies of large charcoal adsorbers for ventilation exhaust air," CONF-760 822, p. 389 - 431 (1976).

10) Kabat, M.J., "Selective sampling of hypoiodous acid," CONF 760 822, p. 490 - 506 (1976).

11) Wilhelm, J.G., et al., "Head-end iodine removal from a reprocessing plant with a solid sorbent," CONF 760 822, p. 447 - 477 (1976).

12) Murray, A., Williams, D.L., "Organic synthesis with isotopes," Pt. 2, p. 1129 - 1131 (1958).

Table I Sorbents employed

Name	Main use	Base material	Size	Impregnant	Supplier
CG 0.8	iodine filters	activated carbon	0.8 mm (pellets)	KI	CEAG (Dortmund, F.R.G.)
AC 6120	iodine filters	silicid acid	1 - 2 mm (beads)	$AgNO_3$	Südchemie AG (Munich, F.R.G.)
DSM 11	iodine species samplers (specific retention of I_2)	silicid acid	1 - 2 mm (beads)	mainly KI	
CDI	iodine species samplers (specific retention of I_2)	diatomaceous earth	20 - 40 mesh	CdI_2	Science Applications, Inc. (Nuclear Environmental Services, Rockville, Md., U.S.A.)
IPH	iodine species samplers (specific retention of HOI after removal of I_2)	activated alumina	20 - 40 mesh	4-Iodophenol	

Table II Parameters of the laboratory tests

Parameter	Unit	Value [a]
Carrier concentration I_2, CH_3I tests	g/m^3	10^{-3}
Carrier concentration HOI tests	g/m^3	10^{-8}
Carrier concentration C_6H_5I tests	g/m^3	10^{-1}
Temperature	^oC	30 or 40
Relative humidity	%	20, 50 or 98
Face velocity	cm/s	25
Bed depth [b]	cm	1.25
Residence time per bed [b]	s	0.05
Preconditioning time	h	$\geq$ 16
Injection time	h	1
Purging time	h	2 or 168

a) Deviations are indicated in the respective tables and figures.

b) Mostly 8 successive test beds were used of depth 1.25 cm corresponding to a total residence time of 0.4 s. As back-up, heated beds of impregnated activated carbon were used with a total residence time of 0.9 s.

Table III Removal efficiency of the sorbents [a] DSM 11, CDI and IPH for ^{131}I in the form of I_2

Temperature : 40°C
Relative humidity: 50 %
Other parameters : see Table II

Sorbent	Bed depth (cm)	Removal efficiency (%)	
		2 h [b]	168 h [b]
DSM 11	1.25	99.89	99.87
	2.5	99.990	99.987
	3.75	99.991	99.989
	5.0	99.992	99.990
	6.25	99.993	99.990
	7.5	99.993	99.990
	8.75	99.994	99.991
	10.0	99.994	99.991
CDI	1.25	99.03	98.6
	2.5	99.983	99.961
	3.75	99.990	99.981
	5.0	99.990	99.982
	6.25	99.991	99.983
	7.5	99.991	99.983
	8.75	99.991	99.984
	10.0	99.991	99.984
IPH	1.25	99.85	99.62
	2.5	99.995	99.85
	3.75	99.998	99.924
	5.0	99.9990	99.952
	6.25	99.9992	99.963
	7.5	99.9994	99.968
	8.75	99.9995	99.971
	10.0	99.9996	99.973

a) Sorbents are described in Table I

b) Purging time

Table IV Removal efficiency of the sorbents DSM 11, CDI and IPH for ^{131}I in the form of CH_3I

Temperature : 40°C
Relative humidity: 50 %
Purging time : 2 h
Other parameters : see Table II

Sorbent	Bed depth (cm)	Removal efficiency (%)
DSM 11	1.25	0.04
	2.5	0.08
	3.75	0.12
	5.0	0.16
	6.25	0.20
	7.5	0.24
CDI	1.25	0.001
	2.5	0.002
	3.75	0.003
	5.0	0.004
	6.25	0.005
	7.5	0.006
IPH	1.25	0.001
	2.5	0.002
	3.75	0.003
	5.0	0.004
	6.25	0.005
	7.5	0.006

Table V Removal efficiency of the activated carbon CG 0.8 for ^{131}I in the form of HOI [a)]

Temperature : 40°C

Relative humidity: 98 - 100 %

Other parameters : see Table II

Bed depth (%)	Removal efficiency (%)	
	2 h [b)]	189 h [b)]
0.625	96.0	70.0
1.25	97.6	80.1
2.5	98.3	90.7
3.75	98.5	95.7
5.0	98.5	98.0

a) Including impurities

b) Purging time

Table VI Removal efficiency of the sorbents AC 6120, DSM 11 and IPH for ^{131}I in the form of HOI

Temperature : 30°C
Relative humidity: 20 %
Other parameters : see Table II

Sorbent	Bed depth (cm)	Removal efficiency (%)	
		2 h [a]	> 100 h [a, b]
AC 6120	1.25	87.9	30.5
	2.5	93.8	33.2
	5.0	95.7	34.3
	7.5	96.4	34.7
	10.0	96.9	35.1
DSM 11	2.5	10.3	2.7
	5.0	18.0	3.7
	7.5	22.0	4.5
	10.0	24.7	5.1
IPH	1.25	82.3	67.7
	2.5	88.2	74.7
	5.0	91.9	76.4
	7.5	93.0	77.1
	10.0	93.6	77.5

a) Purging time

b) AC 6120: 120 h, DSM 11: 143 h, IPH: 189 h

Table VII Removal efficiency of the activated carbon CG 0.8 for ^{131}I in the form of C_6H_5I [a]

Temperature : 30°C
Relative humidity: 98 - 100 %
Other parameters : see Table II

Bed depth (cm)	Removal efficiency (%)	
	2 h [b]	168 h [b]
1.25	99.979	99.22
2.5	99.99985	99.9939
3.75	99.99991	99.9983
5.0	99.99993	99.9990
6.25	99.99993	99.9994
7.5	99.99994	99.9997
8.75	99.99994	99.9998
10.0	99.99995	99.9999

Table VIII Removal efficiency of the sorbents AC 6120 and DSM 11 for ^{131}I in the form of C_6H_5I [a]

Sorbent	Temperature (°C)	Relative humidity (%)	Maximum removal efficiency [c] (%)
AC 6120	30	70	0.1
DSM 11	40	50	0.006

a) Iodine benzene

b) Purging time

c) Bed depth 2.5 cm

Table IX Exhausts investigated (PWR 3) [a]

Name	Origin	^{131}I concentration (Ci/m^3)	Remarks
Equipment room exhaust	Containment	10^{-9}-10^{-11}	Main source of ^{131}I; after iodine filtration minor contributor to ^{131}I released from plant; continuous vent even during power operation
Hood exhaust	Box in which primary coolant is sampled; hood in which primary coolant is analyzed	10^{-10}-10^{-12}	Main source of elemental ^{131}I (so far generally no iodine filtration)
Plant exhaust [b]	Reactor building, auxiliary building	10^{-11}-10^{-13}	Turbine building exhausted separately

a) More information is given elsewhere (6)

b) Also called stack exhaust

Table X Parameters of the in-plant tests

Parameter	Unit	Value [a]
Temperature	^{o}C	30
Relative humidity	%	20-40
Air flow	m^3/h	3.6 (ca. 2.5)
Face velocity	cm/s	50 (ca. 28)
Bed depth	cm	2.5 (ca. 2.5)
Residence time per bed	s	0.05(ca.0.09)
Number of beds per sampler section	-	3 or 5 (1)
Residence time per sampler section	s	0,15 or 0.25 (ca.0.09)
Operating time	d	7
Purging time	-	0

a) Deviations are indicated in the respective tables and figures. Numbers in parentheses apply to the samplers of Science Applications, Inc. (RADeCO, San Diego, Cal., U.S.A.), and correspond to an air flow of 1.5 cfm [9].

Table XI Distribution of ^{131}I in parallel iodine species samplers

Exhaust : equipment room exhaust
Residence time per bed
sampler 1 : 0.05 s
sampler 2 : 0.09 s
Other parameters : see Table X
^{131}I in samplers [a]
sampler 1 : $9.1 \cdot 10^{-7}$ Ci
sampler 2 : $4.8 \cdot 10^{-7}$ Ci

Fraction of ^{131}I (%) per sampler component [b]	
Sampler 1	Sampler 2 [c]
GF/A	F-700
1 < 0.1	1 < 0.1
DSM 11	CDI
2 26.9	
3 3.0	2 6.2
4 1.7	
2-4 31.6	
IPH	IPH
5 3.5	
6 1.3	3 25.5
7 1.0	
5-7 5.8	
CG 0.8	AGX
8 49.4	
9 6.9	4 65.7
10 4.4	
11 1.6	AC
12 0.4	
8-12 62.6	5 2.5

a) Calculated for end of sampling period.

b) The numbers on the left side of each column are the numbers of the sampler components counted in order of flow.
The numbers on the right side of each column are the corresponding fractions of ^{131}I.
The sampler components are (compare Table I):
GF/A, F-700 : particulate filters,
DSM 11, CDI : sorbents for retaining I_2,
IPH : sorbent for retaining HOI,
CG 0.8, AGX, AC : sorbents for retaining organic I
(AGX: molecular sieve in silver form,
AC : impregnated activated carbon).

c) Sampler of Science Applications, Inc.

Table XII Distribution of ^{131}I in parallel iodine species samplers

Exhaust : equipment room exhaust

Operating time : 1 d

Purging time
samplers 1 and 3: 0 d
samplers 2 and 4: 7 d

Other parameters : see Table X

^{131}I in samplers
sampler 1 : $1.4 \cdot 10^{-7}$ Ci
sampler 2 : $1.3 \cdot 10^{-7}$ Ci
sampler 3 : $1.2 \cdot 10^{-7}$ Ci
sampler 4 : $1.3 \cdot 10^{-7}$ Ci

Sampler component	Fraction of ^{131}I (%)			
	Sampler 1	Sampler 2	Sampler 3	Sampler 4
	GF/A	GF/A	GF/A	GF/A
1	< 0.1	< 0.1	< 0.1	< 0.1
	DSM 11	DSM 11	CDI	CDI
2	25.9	24.8	5.9	4.8
3	3.3	2.9	2.0	1.8
4	1.8	1.7	1.4	1.3
2-4	31.0	29.3	9.3	7.9
	AC 6120	AC 6120	AC 6120	AC 6120
5	60.1	62.9	82.9	84.3
6	3.1	2.7	2.5	2.4
7	0.9	0.5	0.7	0.5
5-7	64.1	66.2	86.1	87.1
	CG 0.8	CG 0.8	CG 0.8	CG 0.8
8	4.5	3.7	4.3	4.2
9	0.3	0.6	0.2	0.6
10	< 0.1	< 0.1	< 0.1	< 0.1
11	< 0.1	< 0.1	< 0.1	< 0.1
12	< 0.1	< 0.1	< 0.1	< 0.1
8-12	4.9	4.4	4.5	4.9

Table XIII Distribution of ^{131}I in parallel iodine species samplers

Exhaust : equipment room exhaust

Parameters : see Table X

^{131}I in samplers
sampler 1 : $1.6 \cdot 10^{-7}$ Ci
sampler 2 : $1.5 \cdot 10^{-7}$ Ci

Sampler component	Fraction of ^{131}I (%)	
	Sampler 1	Sampler 2
	GF/A	GF/A
1	0.1	< 0.1
	DSM 11	IPH
2	26.0	22.0
3	2.4	6.7
4	1.3	4.7
2-4	29.8	33.3
	IPH	DSM 11
5	4.2	2.7
6	2.1	0.8
7	1.2	0.6
5-7	7.5	4.0
	CG 0.8	CG 0.8
8	55.8	56.3
9	6.1	5.4
10	0.7	0.7
11	0.1	0.1
12	< 0.1	< 0.1
8-12	62.6	62.6

Table XIV Distribution of ^{131}I in parallel iodine species samplers

Exhaust : equipment room exhaust

Parameters : see Table X

^{131}I in samplers

sampler 1 : $1.3 \cdot 10^{-7}$ Ci

sampler 2 : $1.4 \cdot 10^{-7}$ Ci

sampler 3 : $1.3 \cdot 10^{-7}$ Ci

Fraction of ^{131}I (%) per sampler component		
Sampler 1	Sampler 2	Sampler 3
GF/A	GF/A	GF/A
1 0.2	1 0.1	1 0.2
CDI	CDI	CDI
2 3.2	2 3.4	2 3.7
3 1.6	3 1.5	3 1.7
4 1.3	4 1.2	4 1.0
2-4 6.2	2-4 6.1	2-4 6.5
CG 0.8	DSM 11	IPH
5 90.7	5 27.7	5 21.2
6 2.7	6 2.7	6 7.1
7 0.2	7 0.9	7 5.8
8 < 0.1	5-7 31.3	5-7 34.1
9 < 0.1		
5-9 93.7	CG 0.8	DSM 11
	8 59.1	8 2.5
	9 3.1	9 0.5
	10 0.2	10 0.2
	11 < 0.1	8-10 3.2
	12 < 0.1	
	8-12 62.5	CG 0.8
		11 53.7
		12 2.1
		13 0.2
		14 < 0.1
		15 < 0.1
		11-15 56.1

Table XV Distribution of ^{131}I in iodine species samplers (parallel in the same exhaust)

Exhaust : Hood exhaust, plant exhaust, respectively
Residence time per bed
samplers 1 and 3: 0.05 s
samplers 2 and 4: 0.09 s
Other parameters : see Table X
^{131}I in samplers
sampler 1 : $3.0 \cdot 10^{-10}$ Ci
sampler 2 : $1.5 \cdot 10^{-10}$ Ci
sampler 3 : $2.3 \cdot 10^{-10}$ Ci
sampler 4 : $8.4 \cdot 10^{-11}$ Ci

Fraction of ^{131}I (%) per sampler component			
Hood exhaust		Plant exhaust	
Sampler 1	Sampler 2 a)	Sampler 3 b)	Sampler 4 a)
GF/A 1 1.4	F-700 1 4.2	GF/A 1 0.6	F-700 1 < 1.6
DSM 11 2 61.4 3 16.0 4 < 0.4 2-4 77.4	CDI 2 55.1	DSM 11 2 33.0 3 2.9 4 < 0.6 2-4 35.9	CDI 2 13.3
IPH 5 4.8 6 < 0.4 7 < 0.4 5-7 4.8	IPH 3 20.0	IPH 5 5.1 6 < 0.6 7 < 0.6 5-7 5.1	IPH 3 32.3
CG 0.8 8 16.4 9 < 0.4 10 < 0.4 8-10 16.4	AGX 4 20.7 AC 5 < 0.9	CG 0.8 8 58.5 9 < 0.6 10 < 0.6 8-10 58.5	AGX 4 52.2 AC 5 2.2

a) Sampler of Science Applications, Inc. (compare Table XI)
b) Air flow 7.2 m^3/h, face velocity 100 cm/s, bed depth 5.0 cm

Table XVI Distribution of ^{131}I in iodine species samplers (not parallel)

Exhaust : hood exhaust, plant exhaust, respectively

Residence time per bed: 0.075 s

Other parameters : see Table X

^{131}I in samplers
sampler 1 : $9.4 \cdot 10^{-10}$ Ci
sampler 2 : $1.8 \cdot 10^{-10}$ Ci

Sampler component	Fraction of ^{131}I (%)	
	Sampler 1 (hood exhaust)	Sampler 2 [a] (plant exhaust)
	GF/A	GF/A
1	0.4	< 0.7
	DSM 11	DSM 11
2	67.4	47.9
3	3.9	12.6
2-3	71.3	60.5
	AC 6120	AC 6120
4	22.9	33.8
5	4.1	2.4
4-5	26.9	36.2
	CG 0.8	CG 0.8
6	1.4	3.4
7	< 0.1	< 0.7
6-7	1.4	3.4

a) Air flow 7.2 m^3/h, face velocity 100 cm/s, bed depth 5.0 cm

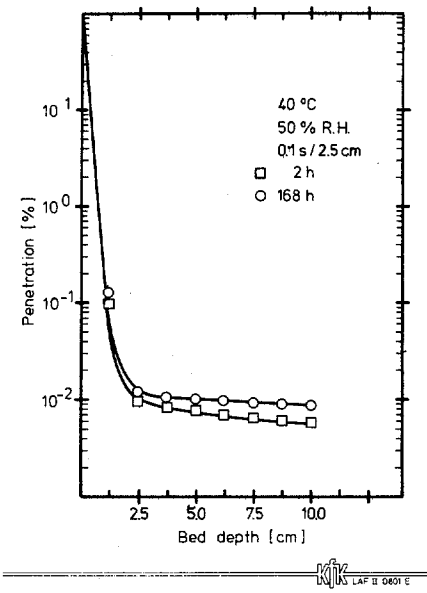

Penetration of DSM 11 for ^{131}I in the form of I_2 with different purging times

Fig. 1 a)

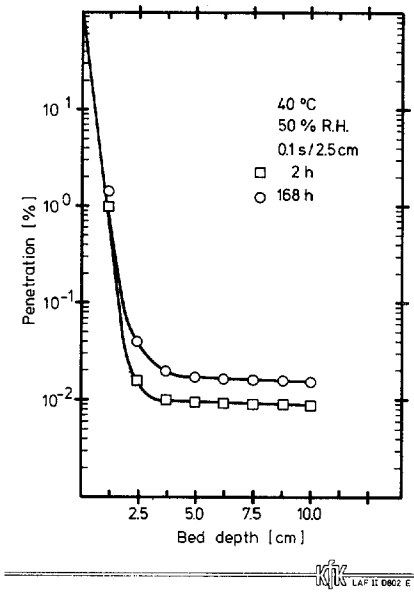

Penetration of CDI for ^{131}I in the form of I_2 with different purging times

Fig. 2 a)

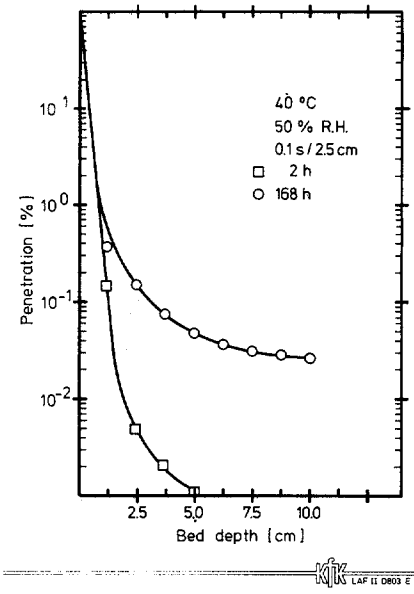

Penetration of IPH for ^{131}I in the form of I_2 with different purging times

Fig. 3 a)

a) The sorbents are described in Table I.
The test conditions are indicated in Table II
(residence time 0.1 s per 2.5 cm).
The corresponding removal efficiencies are given in the respective tables.

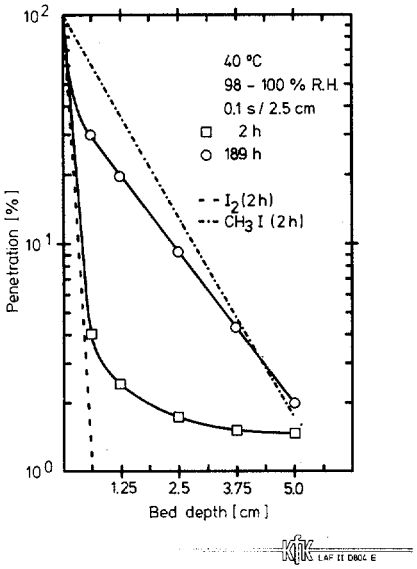

Penetration of CG 0.8 for ^{131}I in the form of HOI with different purging times

Fig. 4 a, b)

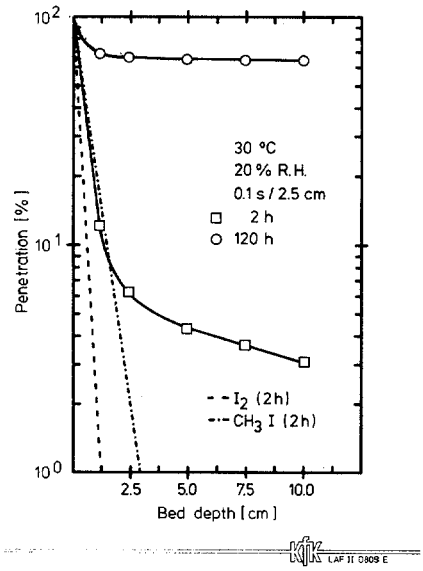

Penetration of AC 6120 for ^{131}I in the form of HOI with different purging times

Fig. 5 a, b)

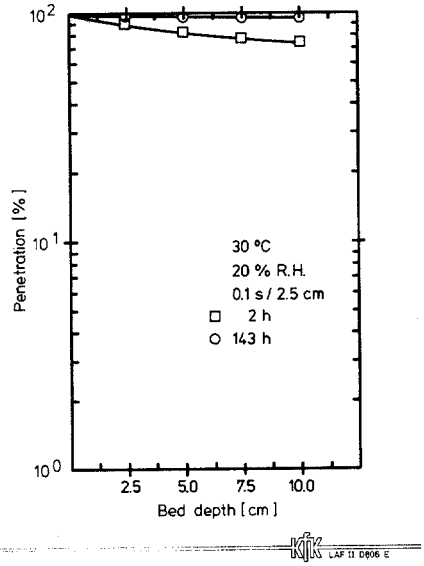

Penetration of DSM 11 for ^{131}I in the form of HOI with different purging times

Fig. 6 a)

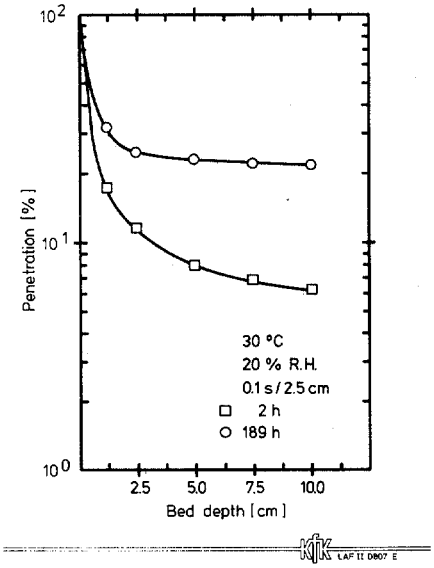

Penetration of IPH for ^{131}I in the form of HOI with different purging times

Fig. 7 a)

a) The fraction of impurities (organic iodides) was 10 to 20 %.

b) The penetration for ^{131}I in the form of I_2 and CH_3I at a purging time of 2 h is included for comparison.

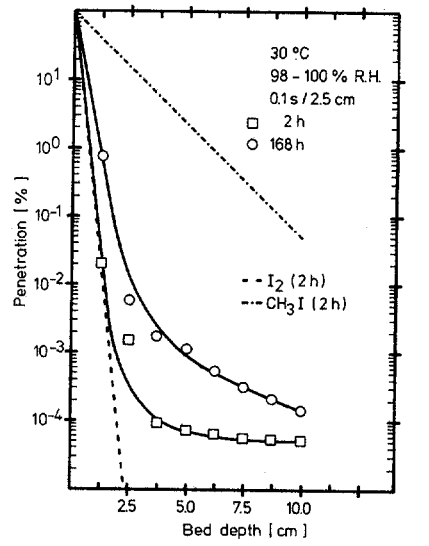

Penetration of CG 0.8 for ^{131}I in the form of C_6H_5I with different purging times

Fig. 8 a)

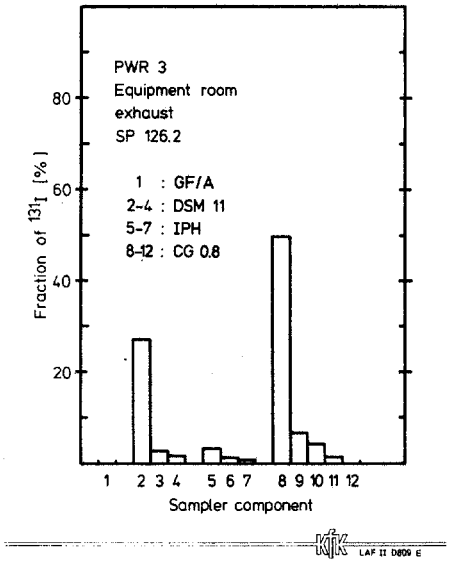

Distribution of ^{131}I in the radioiodine species sampler

Fig. 9 b)

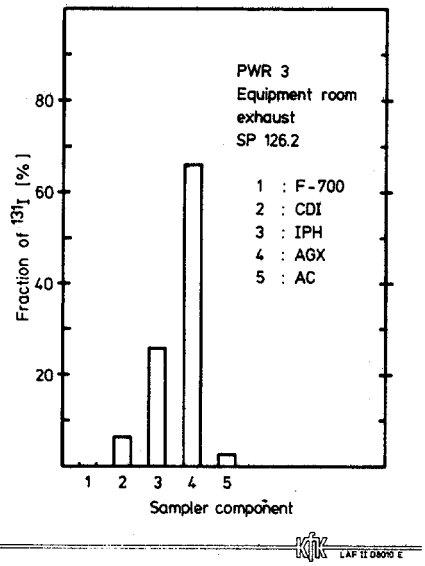

Distribution of ^{131}I in the radioiodine species sampler

Fig. 10 b, c)

a) The penetration of ^{131}I in the form of I_2 and CH_3I at a purging time of 2 h is included for comparison.

b) The exhausts are characterized in Table IX.
The sorbents are described in Tables I and XI.
The test conditions are indicated in Table X.
Samplers of the same sampling period (SP) were operated in parallel.

c) Sampler of Science Applications, Inc.

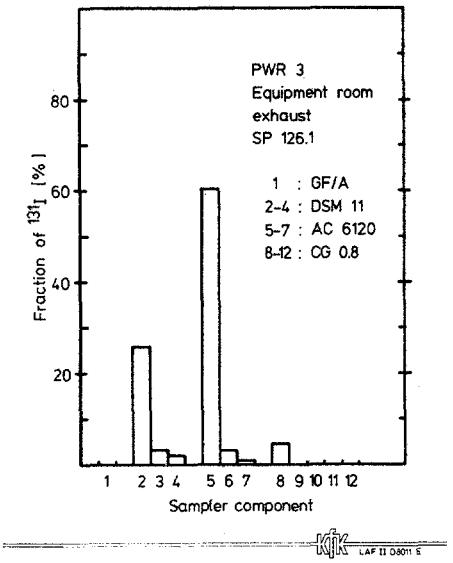

Distribution of ^{131}I in the radioiodine species sampler

Fig. 11 a, b)

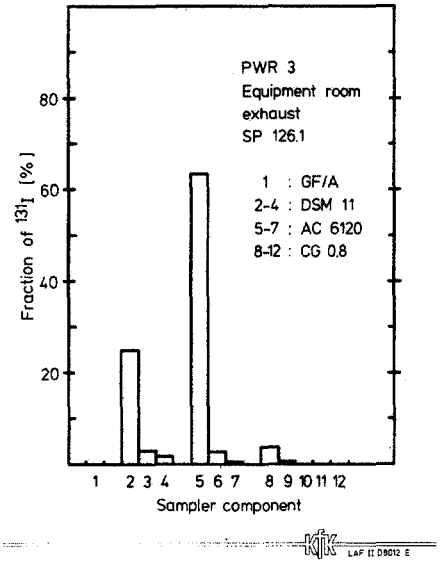

Distribution of ^{131}I in the radioiodine species sampler

Fig. 12 a, c)

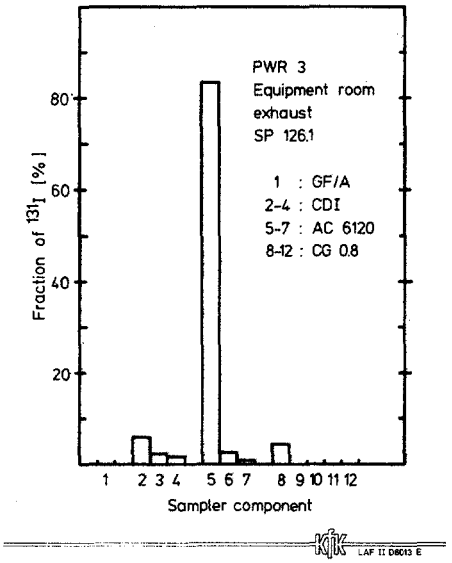

Distribution of ^{131}I in the radioiodine species sampler

Fig. 13 a, b)

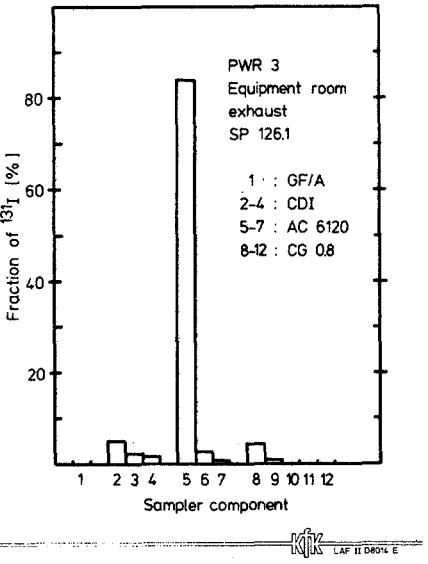

Distribution of ^{131}I in the radioiodine species sampler

Fig. 14 a, c)

a) Operating time 1 d

b) No purging after sampling

c) Purging of 7 d after sampling

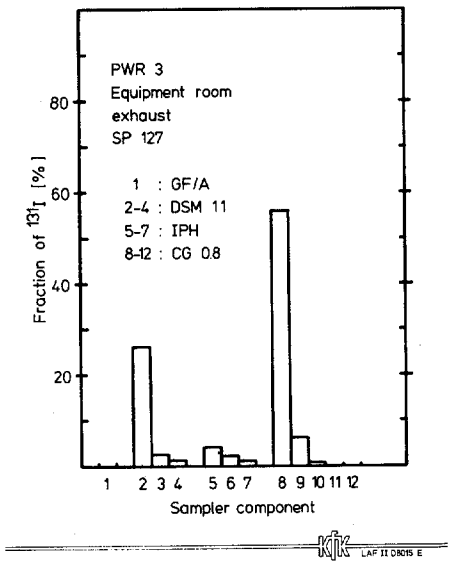

Distribution of ^{131}I in the radioiodine species sampler

Fig. 15

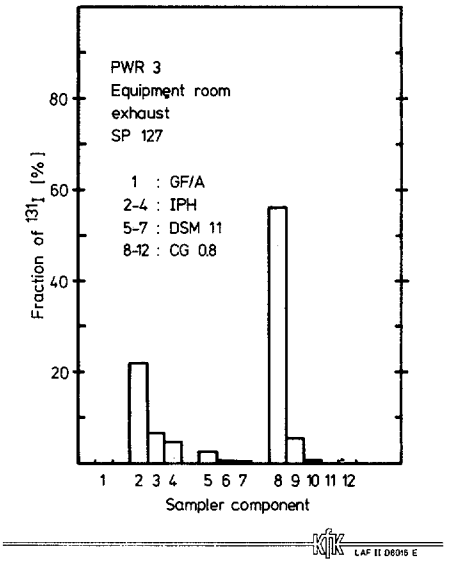

Distribution of ^{131}I in the radioiodine species sampler

Fig. 16

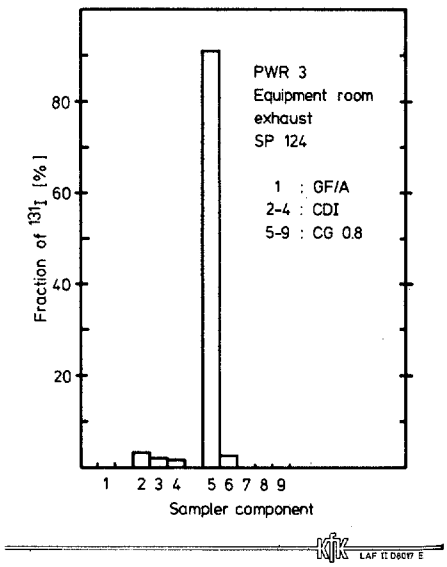

Distribution of ^{131}I in the radioiodine species sampler

Fig. 17

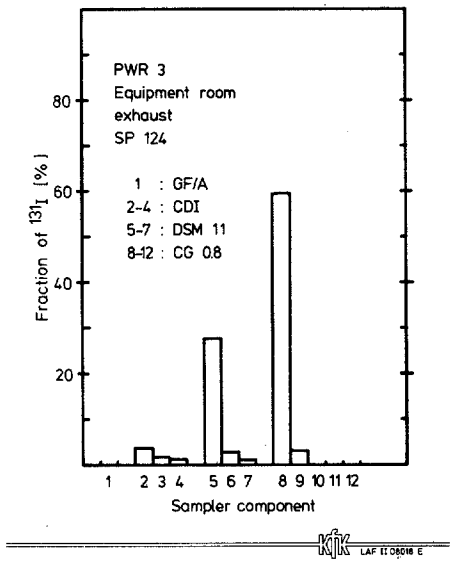

Distribution of ^{131}I in the radioiodine species sampler

Fig. 18

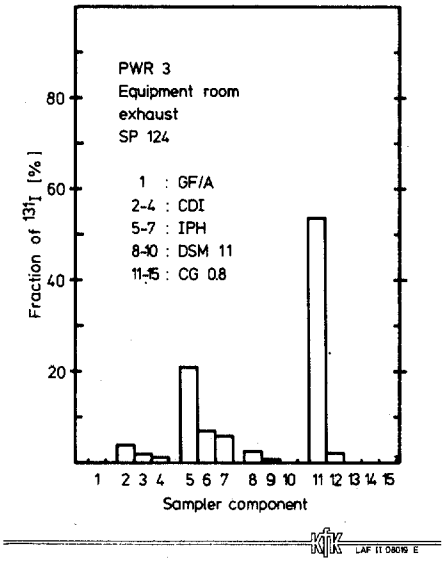

Distribution of ^{131}I in the radioiodine species sampler

Fig. 19

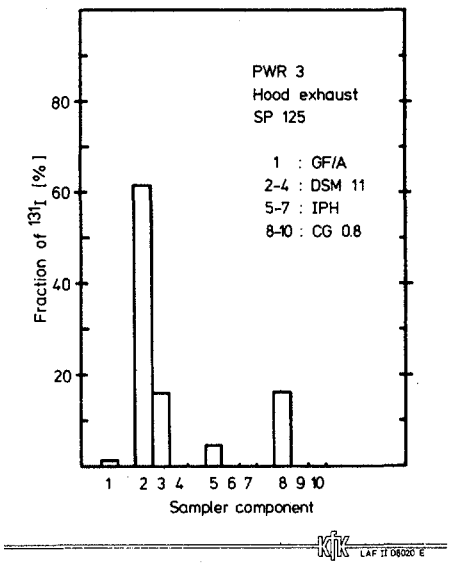

Distribution of ^{131}I in the radioiodine species sampler

Fig. 20

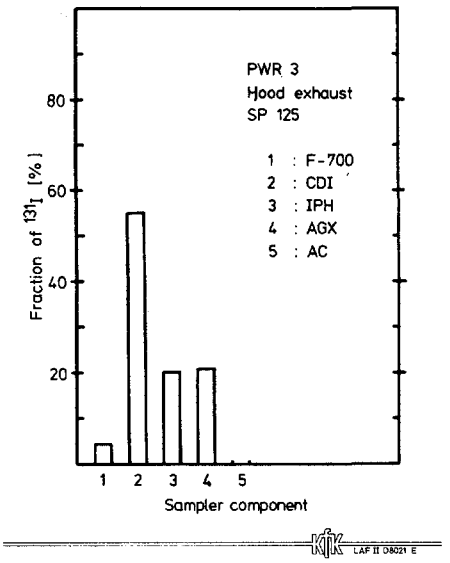

Distribution of ^{131}I in the radioiodine species sampler

Fig. 21 a)

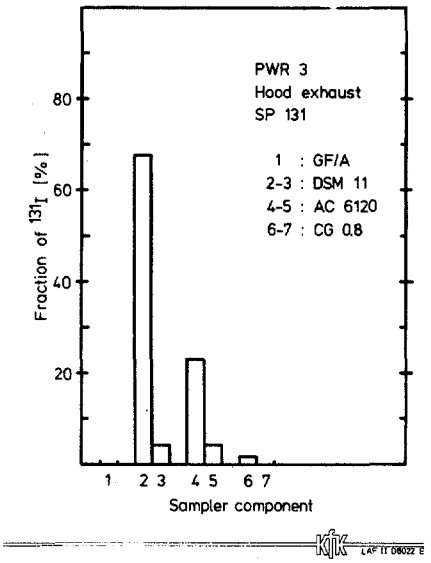

Distribution of ^{131}I in the radioiodine species sampler

Fig. 22 b)

a) Sampler of Science Applications, Inc.

b) Residence time 0.075 s per bed

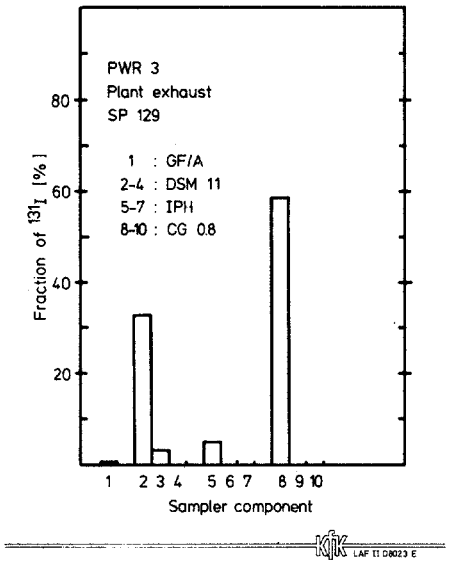

Distribution of ^{131}I in the radioiodine species sampler

Fig. 23

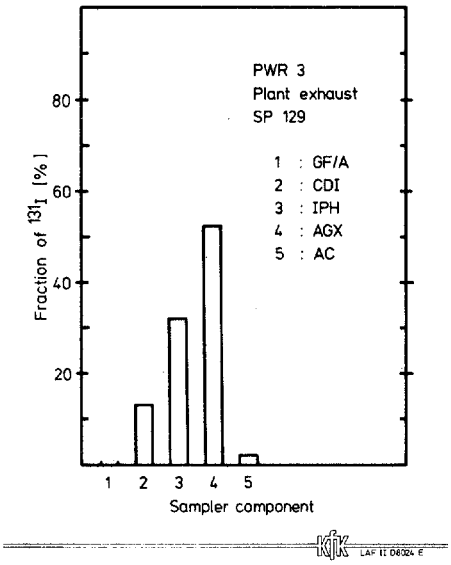

Distribution of ^{131}I in the radioiodine species sampler

Fig. 24 a)

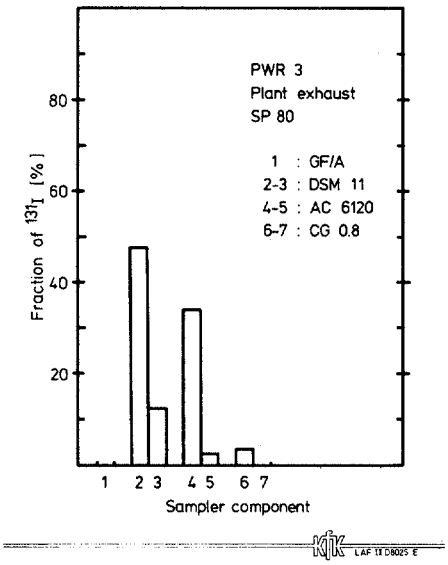

Distribution of ^{131}I in the radioiodine species sampler

Fig. 25 b)

a) Sampler of Science Applications, Inc.

b) Residence time 0.075 s per bed

DISCUSSION

EVONIUK: At what temperature did you run the AC 6120 sampler?

DEUBER: The experiments with AC 6120 and HOI in the laboratory were run at the same conditions as those found in the exhaust air, that is, 30°C and 20% relative humidity.

EVONIUK: Would you expect that if you ran the AC 6120 at a higher temperature, it would retain more of the iodine in the form of HOI?

DEUBER: I imagine that at a higher temperature HOI may decompose, and therefore, retention may be higher. Otherwise, I think that, generally, inorganic substances are poor adsorbers for HOI. But what is important, according to our measurements, is that in the exhaust air of pressurized water reactors, HOI does not exist in significant amounts.

KRYPTON RETENTION ON SOLID ADSORBENTS*

P. R. Monson, Jr.
E. I. du Pont de Nemours & Co.
Savannah River Laboratory
Aiken, SC 29808

Abstract

Radioactive krypton-85 is released to the atmosphere in the off-gas from nuclear reprocessing plants. Three main methods have been suggested for removal of krypton from off-gas streams: (1) cryogenic distillation, (2) fluorocarbon absorption, and (3) adsorption on solid sorbents. Use of solid adsorbents is the least developed of these methods, but offers the potential advantages of enhanced safety and lower operating costs.

An experimental laboratory program was developed that will be used to investigate systematically many solid adsorbents (such as zeolites, i.e., mordenites) for trapping krypton in air. The objective of this investigation is to find an adsorbent that is more economical than silver-exchanged mordenite.

Various physical and chemical characteristics such as adsorption isotherms, decontamination factors, co-adsorption, regeneration, and the mechanism and kinetics of noble gas adsorption were used to characterize the adsorbents. In the experimental program, a gas chromatograph using a helium ionization detector was used to measure the krypton in air before and after the adsorbent bed. This method can determine directly decontamination factors greater than 100.

Introduction

The Savannah River Laboratory has a long-range program to develop the technology required for retaining the radioactive gaseous effluents (^{3}H, ^{14}C, ^{85}Kr, and ^{129}I) from nuclear fuel reprocessing. This paper will report studies of krypton retention.

Three methods [(1) cryogenic distillation, (2) fluorocarbon absorption, and (3) adsorption on solids] are under development for krypton retention. Our work was to develop adsorption on solids. This is the least developed method but one promising a low energy consumption, low initial cost, and a safe system with decontamination factors (DF) up to 500. Our goal is a DF of about 100.

There are three key problems with the solid adsorbent system (Table 1). Dallas Pence of Science Applications, Inc., reported that silver mordenite has the highest krypton adsorption capacity, but this adsorbent is very expensive. Also, the system operates at cryogenic temperatures to enhance the capacity, which increases operating maintenance. In addition, little is known about the mechanism of noble gas adsorption. Our program is designed to solve these key problems by finding less expensive absorbents that are effective above cryogenic

* The information contained in this article was developed during the course of work under Contract No. DE-AC09-76SR00001 with the U. S. Department of Energy.

temperatures (but perhaps below-ambient temperature) and by investigating adsorption mechanisms.

Experimental Approach

Our experimental approach (Table 2) has several parts. First we surveyed a variety of adsorbents using small columns (containing 6 to 10 grams of the adsorbents) in a gas chromatograph. This technique allowed us to determine krypton adsorption isotherms and heats of adsorption, and to study cation exchange - seeking ions about the same size as silver in silver mordenite.

We are studying three types of solid adsorbents:

1. Zeolite molecular sieves (mordenites are a form of zeolite), which are crystalline aluminosilicates with cage-type structures that selectively trap the gaseous species, depending on their atomic or molecular size and the size of the cage openings. Cage size can be controlled by the choice of zeolite and by the cation in its structure which influences the size of the cage opening.

2. Amorphous adsorbents such as silica gel and activated carbon.

3. Hydrophobic molecular sieves such as silicalite produced from alkyl-bearing cations.

Unlike zeolites, which are hydrophilic, these materials preferentially adsorb nonpolar molecules, like krypton.

We used two methods to investigate the mechanism of krypton adsorption:

1. Powder x-ray diffraction to determine cell parameters of the crystalline adsorbents as a function of cation exchange.

2. High-resolution electron microscopy to actually "see" the pores of the zeolites and the positions of the cations in the cages.

The most promising adsorbents, in the small column GC studies, will be tested in larger columns (kilograms). These tests will determine: (1) decontamination factors by measuring the krypton in the entering and exiting stream, (2) regeneration conditions and rates, (3) co-adsorption of krypton when other gases are present in the stream, and (4) behavior with a simulated dissolver off-gas stream.

All developmental work will be with nonradioactive krypton; when the system has been thoroughly evaluated, radioactive krypton will be used.

Instrumentation is relatively simple (Fig. 1), consisting of a Varian dual column and a dual helium-ionization detector, gas chromatograph output to a dual pen recorder. Instruments were calibrated by injecting known amounts of the pure gas into an exponential dilution flask which was continually flushed through the sample loop with helium. Gases were then injected at precise times after placing the standard into the flask.

Discussion of Results

Fig. 2 shows a typical qualitative chromatogram showing the separation of the gases, H_2, O_2, Ar, N_2, Kr, and Xe on sodium mordenite.

Most gases are relatively easy to detect between 1 and 10 ppb with the helium-ionization detector. However, direct detection of krypton in air is much more difficult because air normally contains only 1.14 ppm krypton in the presence of 78% nitrogen and 21% oxygen. To determine krypton decontamination factors of up to 100 directly (without pre-concentration of the sample), we must be able to detect 0.01 ppm krypton in air. Fig. 3 shows the detection of 1.14 ppm krypton in air on silver mordenite at 25°C. The N_2 and O_2 on an attenuation of 1024 are far offscale while krypton on an attenuation of 1 is easily detected. With newly acquired electronics, we will be able to greatly reduce the noise level and increase the sensitivity by a factor of 10, which will allow us to detect krypton at the required 0.01 ppm.

Fig. 4 shows the gas chromatographic scan following Slide 5 but with 300 ppm krypton added to the air stream. Note the attenuation of 256 for krypton, which verifies the peak as krypton.

The gas chromatographic data can be used to obtain the krypton adsorption isotherm (Fig. 5), the adsorption capacity for krypton as a function of the krypton partial pressure at a constant temperature. This plot shows three sets of data that we have measured covering 8 orders of magnitude in partial pressure. Previously, the adsorption capacity was available at only one point (SAI) for silver mordenite; our data for silver mordenite (AgZ) are in agreement. AgZ had been thought to have a krypton adsorption capacity of 100 times that for any other material; however, as our data show, AgZ has only 3 to 5 times greater capacity than either sodium or hyrogen mordenite. Thus, the much cheaper commercial mordenites (sodium and hydrogen) are worthy of further study.

Fig. 6 shows the krypton adsorption isotherms for silver mordenite at 303°K, 328°K, and 373°K. The expected trend of increasing capacity with temperature is observed.

Fig. 7 shows the initial data on the temperature dependence of AgZ versus the sodium and hydrogen forms of the synthetic mordenites. Although limited, the data indicate the capacity of the sodium form may approach that of the silver mordenite at subambient temperatures. We are now extending the measurements to lower temperatures to investigate this phenomenon.

Another important property, the heat of adsorption, can also be determined by gas chromatography. Fig. 8 shows the heat of adsorption of krypton on AgZ at five values of the adsorption capacity. The heat of adsorption is the amount of heat given off when krypton is adsorbed. From the Clausius-Clapeyron equation, a plot of ln p versus 1/T is linear with slope equal to the heat of adsorption (Q). This figure shows that Q varies from 6.5 kcal/mole at 10^{-10} moles/gram to 7.0 kcal/mole at 10^{-8} moles/gram. This information is important in determining how much cooling is necessary to prevent desorption or capacity reduction from heating of the column.

Summary

In conclusion, we have:

- Developed a sensitive technique for the detection of the permanent gases and can measure krypton in air.
- Measured adsorption isotherms and heat of adsorption over a wide range of partial pressures.
- Surveyed several commercially available and cation exchanged zeolites for their krypton adsorption properties.
- Developed techniques for "tailoring" absorbents for optimal krypton retention.

Reference

1. Pence, D. T., Chou, C. C., and Paplawsky, W. J., An Integrated Off-Gas Treatment System Design for Nuclear Fuel Reprocessing Plants Using Selective Adsorption, SAI/00979-2, August 1979.

TABLE 1

KEY PROBLEMS WITH PRESENT SOLID ADSORBENTS

- High Cost of Silver Exchanged Mordenites
- Cryogenic Temperatures Used to Enhance Capacity
- Basic Understanding of Mechanism of Noble Gas Adsorption

TABLE 2

EXPERIMENTAL APPROACH

- Small Column Studies Using GC
- Solid Adsorbents
- Mechanism of Krypton Adsorption
- Large Column Laboratory Studies

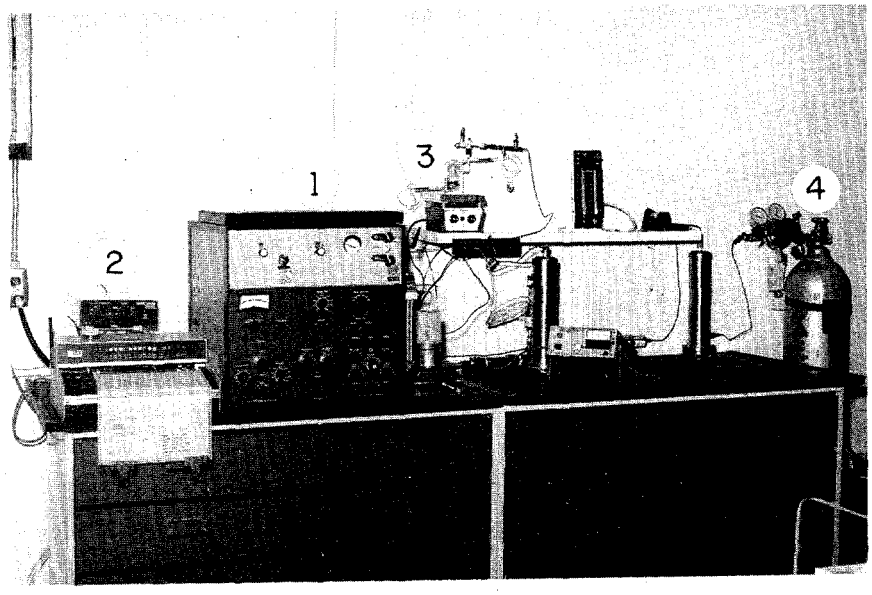

FIGURE 1.

EXPERIMENTAL APPARATUS

1. Gas Chromatograph (Dual Column, Dual Helium Ionization Detectors)
2. Dual Channel Strip-Chart Recorder
3. Exponential Dilution Flask
4. Ultrahigh Purity Helium

FIGURE 2

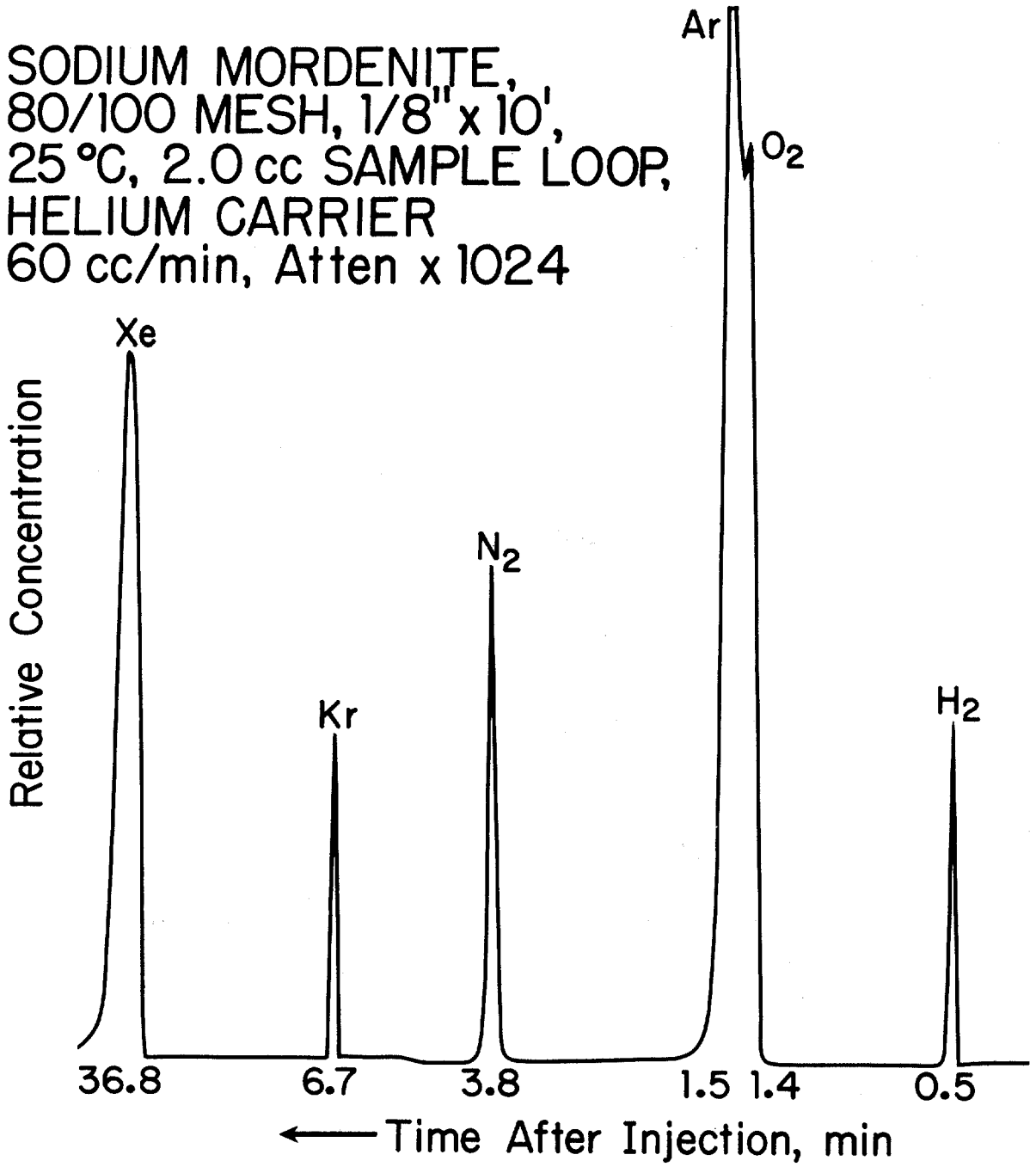
SODIUM MORDENITE,
80/100 MESH, 1/8" x 10',
25 °C, 2.0 cc SAMPLE LOOP,
HELIUM CARRIER
60 cc/min, Atten x 1024
Relative Concentration
Xe
Kr
N2
Ar
O2
H2
36.8
6.7
3.8
1.5
1.4
0.5
← Time After Injection, min

FIGURE 3

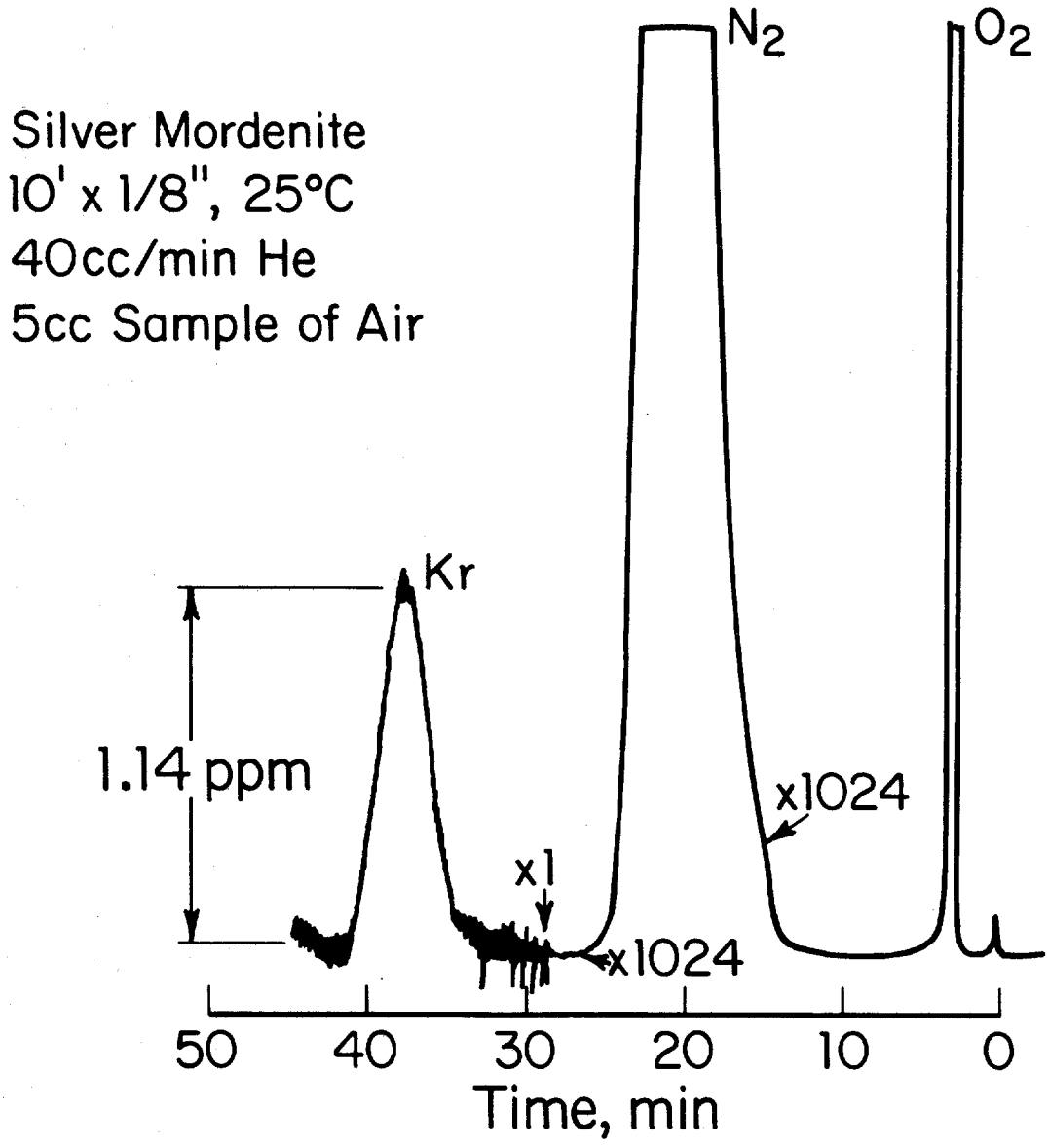
Silver Mordenite
10' x 1/8", 25°C
40cc/min He
5cc Sample of Air
N2
O2
Kr
1.14 ppm
x1024
x1
x1024
50
40
30
20
10
0
Time, min

FIGURE 4

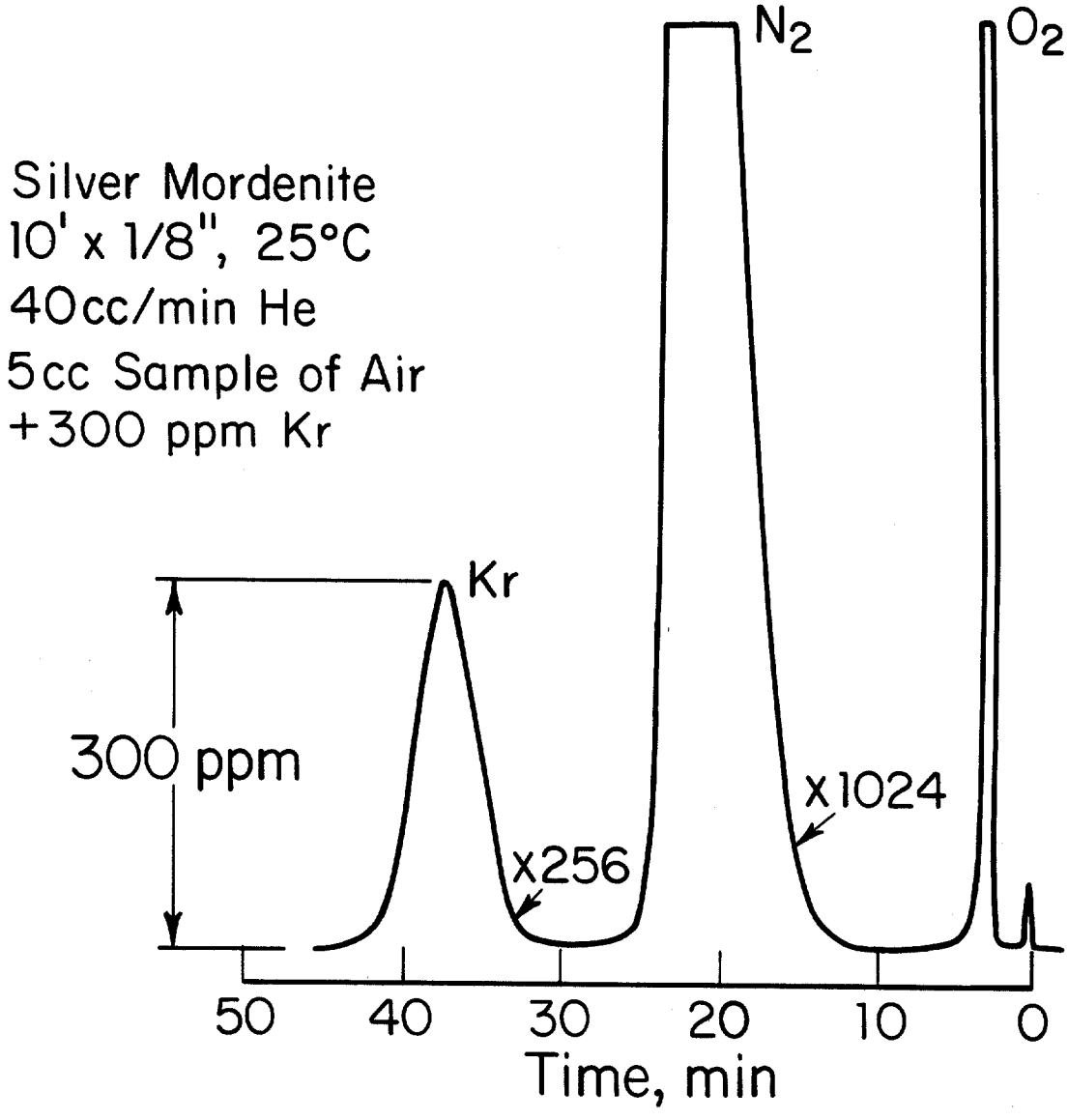
Silver Mordenite
10' x 1/8", 25°C
40cc/min He
5cc Sample of Air
+300 ppm Kr
N2
O2
Kr
300 ppm
x256
x1024
50
40
30
20
10
0
Time, min

FIGURE 5

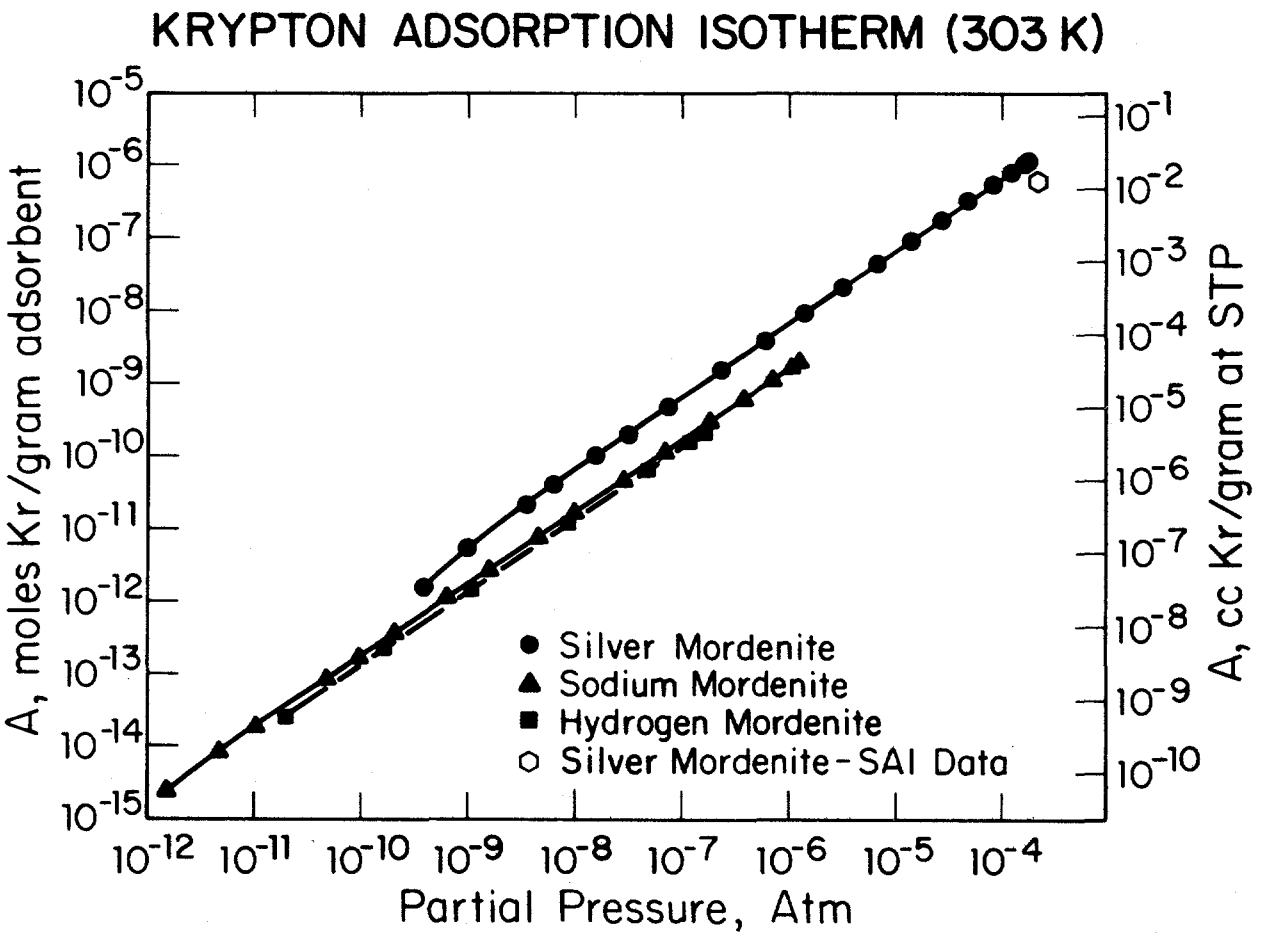
KRYPTON ADSORPTION ISOTHERM (303 K)
A, moles Kr/gram adsorbent
A, cc Kr/gram at STP
Partial Pressure, Atm
Silver Mordenite
Sodium Mordenite
Hydrogen Mordenite
Silver Mordenite - SAI Data

FIGURE 6

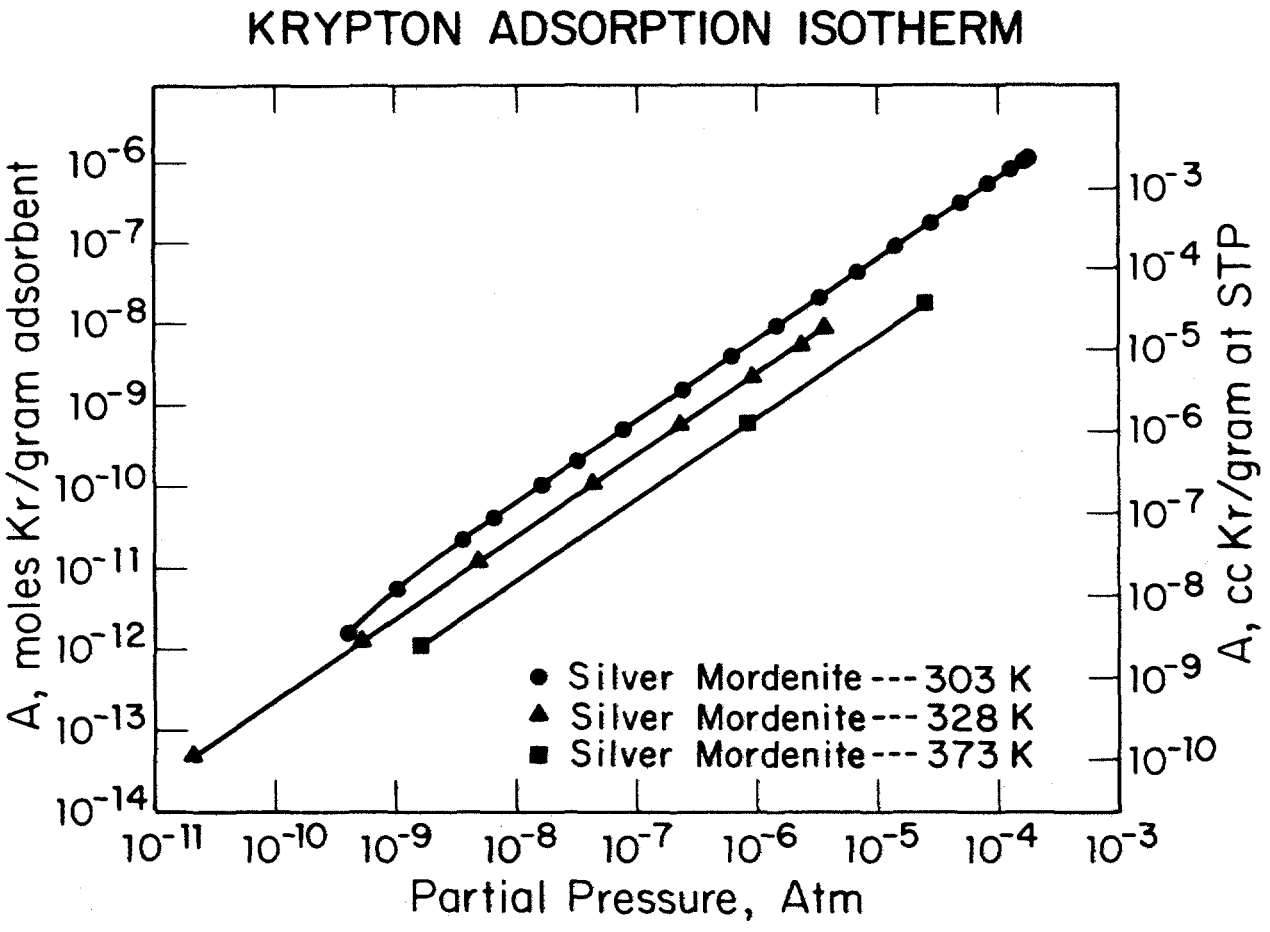
KRYPTON ADSORPTION ISOTHERM
A, moles Kr/gram adsorbent
A, cc Kr/gram at STP
Partial Pressure, Atm
Silver Mordenite --- 303 K
Silver Mordenite --- 328 K
Silver Mordenite --- 373 K

FIGURE 7

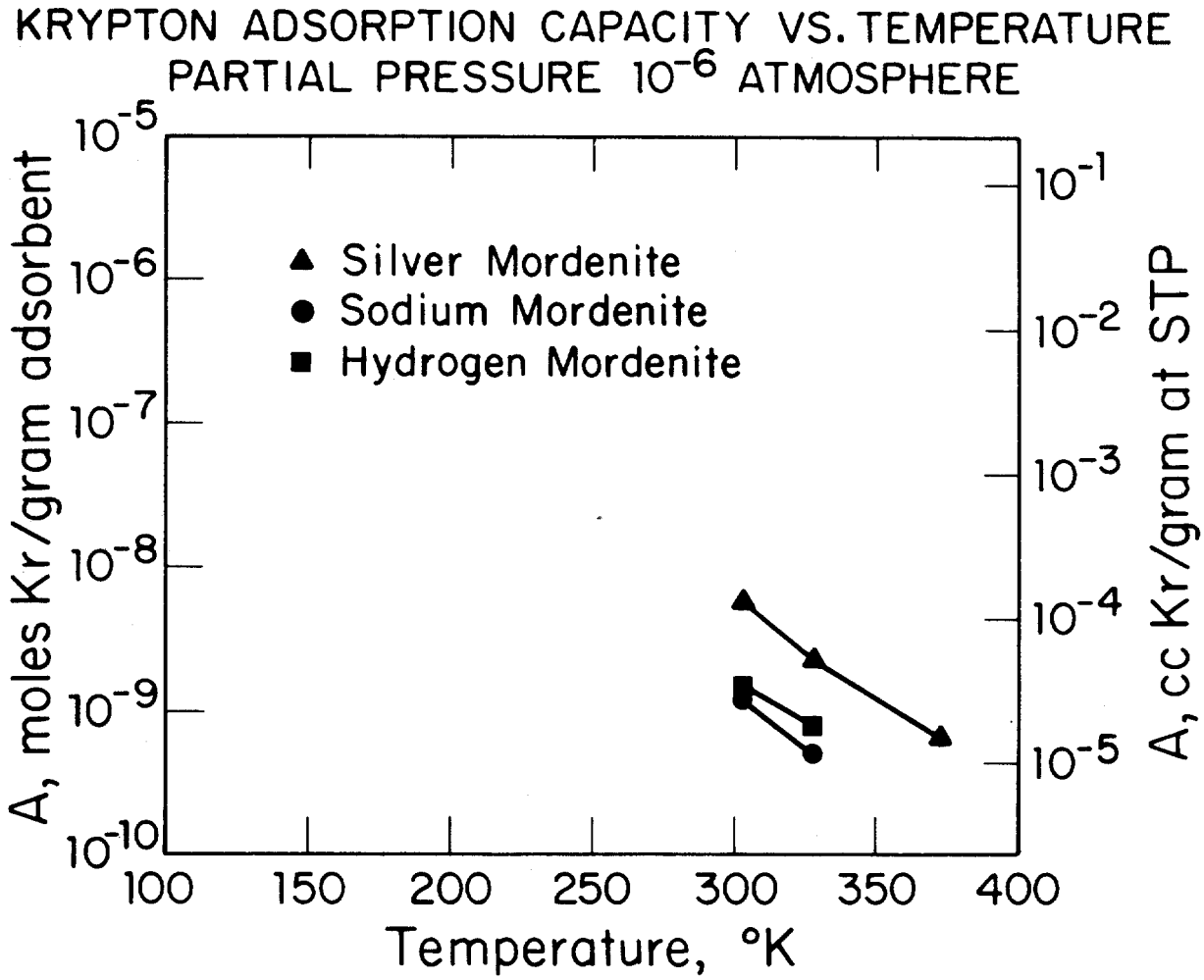
KRYPTON ADSORPTION CAPACITY VS. TEMPERATURE
PARTIAL PRESSURE 10^{-6} ATMOSPHERE
A, moles Kr/gram adsorbent
10^{-5}
10^{-6}
10^{-7}
10^{-8}
10^{-9}
10^{-10}
▲ Silver Mordenite
● Sodium Mordenite
■ Hydrogen Mordenite
10^{-1}
10^{-2}
10^{-3}
10^{-4}
10^{-5}
A, cc Kr/gram at STP
100
150
200
250
300
350
400
Temperature, °K

FIGURE 8

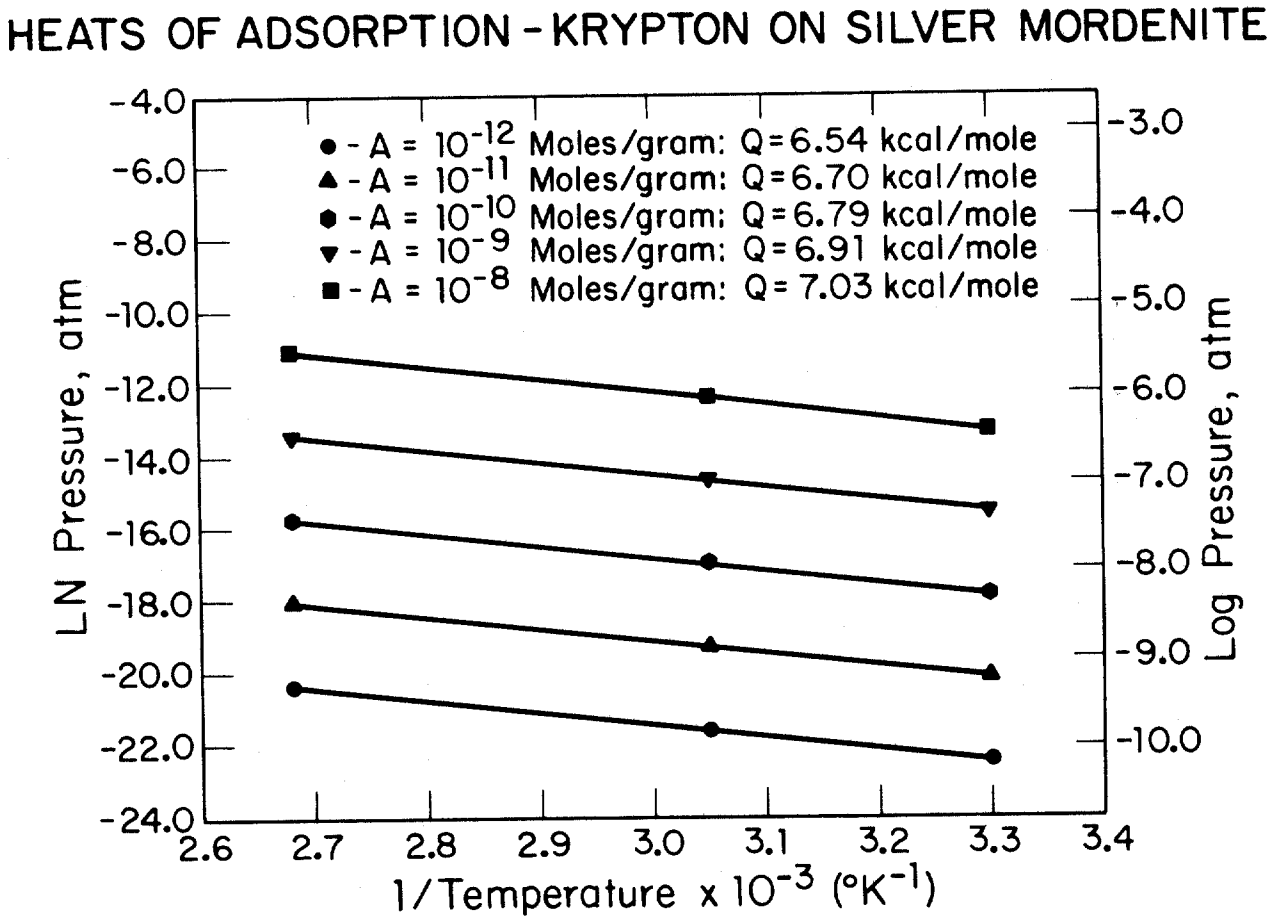
HEATS OF ADSORPTION - KRYPTON ON SILVER MORDENITE
● - A = 10^-12 Moles/gram: Q = 6.54 kcal/mole
▲ - A = 10^-11 Moles/gram: Q = 6.70 kcal/mole
⬢ - A = 10^-10 Moles/gram: Q = 6.79 kcal/mole
▼ - A = 10^-9 Moles/gram: Q = 6.91 kcal/mole
■ - A = 10^-8 Moles/gram: Q = 7.03 kcal/mole
LN Pressure, atm
Log Pressure, atm
-4.0
-6.0
-8.0
-10.0
-12.0
-14.0
-16.0
-18.0
-20.0
-22.0
-24.0
-3.0
-4.0
-5.0
-6.0
-7.0
-8.0
-9.0
-10.0
2.6
2.7
2.8
2.9
3.0
3.1
3.2
3.3
3.4
1/Temperature x 10^-3 (°K^-1)

DISCUSSION

SRIDHAR: Following Dr. Pence's excellent review of krypton retention technology, I mentioned that we have also started in a very modest way to investigate krypton adsorption techniques and technology. We agree with your opening statement and it is our evaluation that when it comes to krypton abatement in reprocessing plants, the cryogenic distillation process as well as the fluorocarbon absorption process are first generation types of well developed processes with clearly identifiable disadvantages and advantages. But we do see the potential of the inorganic solid sorbent system in terms of safety and cost, as you have mentioned. The other point I would like to note is that we started our initial experiments sometime in January 1978, and we have identified certain sorbents (molecular sieves) at this stage as most promising. We think we are in a position to go to small-scale units. What do you think is your time factor to go to such kinds of experiments? I wonder if it would be worthwhile collaborating on this particular aspect.

MONSON: Our plans are to finish the small-scale studies early this coming year. We have done a lot more work than is presented in this paper. The omission is because of DOE timing for clearance. Work is continuing, including going to lower temperatures, which I did not discuss. In the coming year we hope to scale up our experiments and perform hot tests either during the coming year, or the year after, using a simulated dissolver material and a high level cave situation. I think, if DOE is willing, we would be glad to collaborate.

SRIDHAR: Have you looked at any of the decationated zeolites yet?

MONSON: No, we have looked at other cation exchanged varieties of hydrogen mordenite such as potassium and cerium, but not the decationated zeolites.

FIRST: I wonder if Mr. Monson would care to comment on the relative effectiveness of charcoal and the zeolites he has worked with?

MONSON: From a purely effectiveness standpoint, activated carbon has a greater adsorption constant than the zeolites (see also Paper 3-3). However, in a reprocessing offgas stream with the possibility of NO_x and O_2 being present at the krypton separation step, the inorganic sorbents are preferred from a safety viewpoint.

SRIDHAR: In our krypton separation studies on molecular sieves presented at this Conference earlier (Paper 3-3) we had indeed carried out a comparison of the relative effectiveness of the carbons and the zeolites. (See Fig.5, in Paper 3-3). Results show that Kr selectivity values for de-aluminated H-Mordenite is quite comparable to the best of activated carbons for which data are available. In fact, a modest extrapolation of data suggests that at temperatures below 200°K the selectivity of de-aluminated H-Mordenite may be even greater than that of the activated carbon. For Purex-type dissolver offgases containing O_2 and NO_x, carbon beds pose a fire hazard and from that point of view, zeolites are preferable in a reprocessing plant.

EFFECT OF FLOW RATE ON THE ADSORPTION COEFFICIENT OF RADIOACTIVE KRYPTON ON ACTIVATED CARBON

by

Lin-Shen Casper Sun, Fellow
Advisory Committee on Reactor Safeguards
U. S. Nuclear Regulatory Commission

and

Dwight W. Underhill, Associate Professor
University of Pittsburgh

Abstract

For some time, there have been questions relative to the effect of carrier gas velocity on the adsorption coefficient for radioactive noble gases on activated charcoal. Resolution of these questions is particularly important in terms of developing standard procedures for determining such coefficients under laboratory conditions. Studies at the Harvard Air Cleaning Laboratory appear to confirm that the adsorption coefficient for radioactive krypton on activated charcoal is independent of the velocity of the carrier gas.

I. Introduction

Although charcoal adsorption beds are in wide use for the removal of short lived krypton and xenon isotopes, and although it is recognized that the effectiveness of these beds depends directly on the adsorption coefficient of krypton and xenon, there is yet no standard procedure for measuring these coefficients on selected samples of charcoal. The purpose of this present work is to determine the factors necessary for an accurate measurement of the dynamic adsorption coefficient. The factor considered here in detail is the effect of the carrier gas velocity on the measured dynamic adsorption coefficient, for if it were to be found that the results depend on this factor, then the carrier gas velocity would also have to be specified in the design of a standardized test procedure.

II. Theoretical Analysis

Because the vast majority of adsorption sites are located internally, apart from the flow paths of the carrier gas, it would appear to be a logical assumption that the carrier gas velocity has no effect on the adsorption coefficient. At the 15th Nuclear Air Cleaning Conference, Lovell and Underhill[1] demonstrated that in theory the adsorption coefficient will be independent of the carrier gas velocity when the input is in the form of a step function. Also, in the case of a pulse input, if the adsorption isotherm were linear, the adsorption coefficient will be independent of the carrier gas velocity. But a pulse injection in the case of a highly nonlinear adsorption isotherm may lead to a situation where the carrier gas velocity affects the measured adsorption coefficient. In this case, however, the results are essentially meaningless because there is no way to deter-

mine the concentration to which this adsorption coefficient corresponds.

III. Previous Work

Wirsing, et al.[2] conducted extensive measurements at the Brookhaven National Laboratory on the adsorption of krypton and xenon on charcoal from air and nitrogen at low temperature. Parish[3] showed that the adsorption coefficients obtained in these experiments were strongly dependent on the carrier gas velocity. Although data taken from the lowest flow regime used by Wirsing, et al., agreed with proprietary data of Parish, at higher carrier gas velocities the adsorption coefficients obtained by Wirsing, et al. sharply decreased as the carrier gas velocity increased. Not only do the data of Wirsing, et al., show a velocity effect, but they also have a high degree of scatter. Parish believes that at higher velocities, Wirsing, et al. encountered fluidization and that this influenced their breakthrough curves. If fluidization is the explanation for their erratic results, Underhill and Moeller[4] noted that this difficulty could have been avoided if the carrier gas had been passed down, rather than up, through the adsorbent bed.

Other data from the Brookhaven National Laboratory are in sharp contrast to the results reported by Wirsing, et al. Kenney and Eshaya[5] and Eshaya and Kalinowski[6] observed that increasing the carrier gas velocity increased the adsorption coefficient. This is the opposite of the effect reported by Wirsing, et al.[2]

In the experiments of Kenney and Eshaya[5], Eshaya and Kalinowski[6] and Wirsing, et al.[2], step function inputs were used. Under this condition there seems to be no possible explanation other than experimental error, for the reported effect of the carrier gas velocity on the adsorption coefficient.

Data reported by Koch and Grandy[7] also show a strong decrease in the adsorption coefficient as the carrier gas velocity is increased. The same effect is apparent in data reported by Kahn, et al.[8] In these latter two reports, the authors state that pulse inputs were used. But under the conditions of these experiments the noble gas isotherms are so nearly linear that the possibility that nonlinearity had any measurable influence on these results can be discounted.

There are, on the other hand, a number of studies in which the carrier gas velocity was observed to have no effect on the adsorption coefficient. Rozhdestvenskaya, et al.[9], for example, observed no effect of the carrier gas velocity on the adsorption coefficient in tests with superficial velocities ranging from 0.8 to 4 cm/sec. Additionally, Siegwarth, et al.[10] found the adsorption coefficient to be independent of the carrier gas velocity. Finally, the results of Kawazoe[11] indicate that, if the adsorption coefficient is affected by the carrier gas velocity, the effect is not great.

IV. Experimental Data

The breakthrough curves obtained in the laboratory are slightly skewed as the result of normal mechanisms of mass transfer. For

purposes of evaluation, the adsorption coefficient, k, of the absorbent in the bed, can be calculated using the following equation:

$$k = \frac{\int_0^\infty C\,V\,dV}{m\int_0^\infty C\,dV} - (\text{Void Space})/m$$

Where C is the radionuclide concentration in the effluent stream;
V is the volume of the effluent stream; and
m is the mass of absorbent.

This equation has been applied to data recently obtained at the Harvard Air Cleaning Laboratory on the absorption of radioactive krypton on charcoal under the following conditions:

1. Absorption bed: 7.6 cm diameter by 33.0 cm long, containing 556.4 grams of commercial brand charcoal;
2. Operating temperature: 25°C;
3. Operating pressure: 1 Atm.;
4. Moisture content: 1% by weight of the charcoal, corresponding to a relative humidity of 6.1%;
5. Carrier gas: air.

The void space from the point of krypton injection to the outlet of the recording ionization chamber was 1220 cm^3.

The experimental data are summarized in Table I. As may be noted, the superficial flow velocities ranged from 0.18 to 0.91 cm/sec, representing a five-fold difference. The calculated dynamic adsorption coefficients ranged from 96.69 to 99.43 cm^3/gm, with an overall average of 98.06 cm^3/gm and a standard deviation of 1.20. The correlation coefficient, r, between the dynamic adsorption coefficient, $\bar{k}$, and the carrier gas flow velocity, $\bar{v}$, was calculated as follows:

$$r = \frac{\frac{1}{N}\Sigma kv - \bar{k}\,\bar{v}}{\sigma_k\,\sigma_v} = 0.52$$

where

$$\sigma_k = \sqrt{\frac{1}{N}\Sigma k^2 - (\bar{k})^2} \qquad \text{and} \qquad N = 5$$

$$\bar{v} = 0.614 \text{ cm/sec}$$

$$\sigma_v = \sqrt{\frac{1}{N}\Sigma v^2 - (\bar{v})^2} \qquad \sigma_v = 0.65 \text{ cm/sec}$$

$$\bar{k} = 98.06 \text{ cm}^3/\text{gm}$$

$$\sigma_k = 2.41 \text{ cm}^3/\text{gm}$$

For such a calculation, Fisher's z transformation is:

$$z = \tfrac{1}{2}\ln\left(\frac{1+r}{1-r}\right) = 0.58$$

This has a standard error of $z\,(N-3)^{\frac{1}{2}}$ or 0.82 and therefore r is not statistically provable to be different from zero. Therefore, from a

statistical standpoint, the assumption that the adsorption coefficient, k, is indepencent of the superficial carrier gas velocity, v, appears to be strongly supported.

V. Conclusions

From the work reported here it has been shown that dynamic adsorption coefficients for the adsorption of radioactive krypton on activated charcoal can be measured precisely and that the results are valid for a wide range of carrier gas velocities. Even allowing for a few percent error in the experimental measurements, these data appear to confirm that the adsorption coefficient is independent of the velocity of the carrier gas and that adsorption coefficients determined under standardized conditions at one carrier gas velocity should be valid over a wide range of carrier gas velocities.

Table I. Experimental Data

Flow Velocity, v (cm/sec)	Retention Volume, $\bar{V}$ (liters)	Dynamic Adsorption Coefficient, k (cm^3/gm)
0.18	55.71	97.94
0.37	55.25	97.11
0.73	55.02	96.69
0.88	56.37	99.12
0.91	56.54	99.43

$\bar{v} = 0.614$; $\bar{k} = 98.06$; $s = 1.20$.

References

1. Lovell, R. and Underhill, D. W. "Experimental Determination of Fission Gas Adsorption Coefficient", U. S. ERDA Report CONF-780819, pp. 893-900.(1979).

2. Wiring, E., Jr., Hatch, L. P., and Dodge, B. F. "Low Temperature Adsorption of Krypton on Solid Adsorbents", U. S. AEC Report, BNL-50254, T-586.(1970).

3. Parish, H. Personal Communication. (1979).

4. Underhill, D. W. and Moeller, D. W. "The Effect of Temperature, Moisture, Concentration, Pressure and Mass Transfer on the Adsorption of Krypton and Xenon on Activated Charcoal", U. S. Nuclear Regulatory Commission, NUREG-0678,Chap. 6:11-13.(1980).

5. Kenney, W. F. and Ashaya, A. M. "Adsorption of Xenon on Activated Charcoal", U. S. AEC Report, BNL-689, T-235. (1960).

6. Eshaya, A. M. and Kalinowski, W. L. "Adsorption of Krypton and of Mixed Xenon and Krypton on Activated Charcoal", U. S. AEC Report, BNL-724, T-258. (1961).

7. Koch, R. C. and Grandy, G. L. "Retention Efficiencies of Charcoal Traps for Fission Gases", U. S. AEC Report, NSEC-7. (1957).

8. Khan, A. A., Deshingkar, D. S., Ramarathinam, K. and Kishore, A. G. "Evaluation of Activated Charcoal for Dynamic Adsorption of Krypton and Xenon", Bhabha Atomic Research Centre, Bombay, India. Report BARA-839. (1976).

9. Rozhdestvenskaya, A. G., Cherepov, B. R., Keir, B. R., Chechetkin, Yu., and Kizin, V. D. "Effect of Ammonia on Adsorption of Krypton and Xenon on SKT-M Carbon, II. Determination of the Equilibrium Adsorption Coefficients of the Inert Gases Under Dynamic Conditions", J. Phys. Chem. (USSR) 49, pp. 1500-1502. (1975).

10. Siegwarth, D. P., Neulander, C. K., Pao, R. T. and Siegler, M. "Measurement of Dynamic Adsorption Coefficients for Noble Gases on Activated Carbon", U.S. AEC Report CONF-720823, pp. 28-47. (1973).

DISCUSSION

PARISH: I thank you for referencing our analysis as reported by Underhill in NUREG-0678. I agree with your conclusions but I just want to clarify one point, namely that we do not subscribe to the concept of a dynamic adsorption coefficiency dependency on velocity. As you pointed out, we did analyze the BNL data by Wirsing et al. (as referenced in NUREG-0678), and the results of the analysis did indicate a fairly drastic effect with flow. But we did not really consider that the apparent result was correct and looked for some explanation. After reviewing the literature and the Wirsing report in quite a bit of detail and talking with some of the authors, we concluded that there was a plausible explanation in that they used upflow through the bed as opposed to downflow and, furthermore, did not have a very effective means of supporting the top of the bed to restrain the carbon. We also calculated a critical velocity that would lead to bed fluidization which, unfortunately, corresponded with the lowest flow that they used and reported on. But it is interesting that the data taken at that flow rate represented their maximum dynamic adsorption coefficient which corresponded very closely to ones that we measured. Our conclusion was that the reason for the apparent effect of flow rate on the dynamic adsorption coefficient was due to fluidization of the bed. The extent of bed fluidization (and probably resultant flow channeling) would be expected to increase with increasing flow rate, which in turn could readily explain the apparent decrease in dynamic adsorption coefficient.

DESORPTION OF TEDA FROM IMPREGNATED CHARCOALS*

Gerry Wood
Industrial Hygiene Group
Los Alamos Scientific Laboratory
University of California
Los Alamos, New Mexico 87545

Abstract

Triethylenediamine (TEDA) is one of the most effective charcoal impregnants for trapping organic forms of radioiodine from air. It is used in air cleaning adsorbers, air samplers, and air purifying respirator canisters and cartridges for airborne radioiodine. Volatility of the pure crystals suggested the possibility of significant TEDA desorption in these applications, resulting in toxic levels of amine and/or degradation of sorbent efficiency.

Measurements of TEDA desorption rates were made for four commercial charcoals. Temperatures of 70-120°C were used to give levels detectable with a photoionization detector. Extrapolations to temperatures nearer normal ambient were made by using Clapeyron equation plots.

Among three charcoals with the same 5% level of TEDA impregnation, desorption rates varied over factors as great as 10. Slopes of Clapeyron plots were similar, giving an average 25 kcal/mol heat of desorption. This corresponds to a doubling of the TEDA desorption rate with each 5°C (9°F) rise in temperature. Desorption rates were directly proportional to airflow rates or velocities through the test beds and independent of humidity. Desorption rates per unit weight of charcoal decreased exponentially with bed depth, presumably due to TEDA readsorption.

Calculations based on this data and the geometry of a standard adsorber cell showed that at normal ambient temperatures: (1) concentrations of TEDA in effluent air are well below expected toxic levels; and (2) losses of TEDA may be significant. At elevated temperatures TEDA desorption rates are high enough to affect methyl iodide trapping efficiencies and, possibly, charcoal ignition temperatures.

I. Introduction

Triethylenediamine (TEDA; 1,4-diazabicyclo[2.2.2] octane; $N(C_2H_4)_3N$) has long been recognized as an effective charcoal impregnant for the trapping from air of organic forms of radioiodine. TEDA-impregnated charcoals are used in air cleaning adsorbers, air purifying respirator canisters, and in air samplers. This compound has a normal boiling point of 174°C, but is known to sublime readily at room temperatures.

*Work supported by the Nuclear Regulatory Commission and performed at the Los Alamos Scientific Laboratory operated under the auspices of the U. S. Department of Energy, Contract No. W7405 ENG-36.

This volatility of the pure crystals has brought up the question of the volatility of TEDA impregnated in activated charcoals. The first reason for this concern is the possible release of significant amounts of this amine of unestablished toxicity from sorbents, especially in air purifying canister applications. A second reason for concern is the loss of TEDA from air cleaning adsorbers over long periods of use, resulting in degraded performance. Another concern for air cleaning adsorbers is heating due to high loading of radioactively decaying ^{131}I after an accidental release, resulting in TEDA desorption and possible ignition.

To supply data to answer these concerns we have measured TEDA desorption rates from commercial impregnated charcoals.

II. Experimental Details

Apparatus

The detector for TEDA in air was a photoionization detector (HNU Systems, Inc., Model PI-52-02), through which air samples were drawn at 22 cm^3/min. Detector response was amplified and attenuated with the electrometer component and recorded on a strip chart. The detector was calibrated by sublimation of TEDA crystals at 30.0°C into flowing air. Weight loss rate (4.80 µg/min) and diluent air flow rates (60-2000 cm^3/min) were measured and used to calculate calibration concentrations.

A gas chromatograph oven was used to control temperatures (70-120°C) of test beds, the air entering them, and the sampling lines. Temperature was monitored by a digital thermometer (±0.2°C). Charcoal samples of 1-4 cm^3 volume were packed into 0.95-cm-i.d. stainless steel tubes and held in place by glass wool. This resulted in bed depths of 1.4-5.6 cm.

Compressed air from cylinders was passed through a filter of activated charcoal before use. It was quite dry initially. For higher humidity studies a fraction or all of the airflow was passed through the headspace of a water reservoir. Resulting relative humidities were determined using a dew point hygrometer (General Eastern Model 1200). Airflow rate (100-400 cm^3/min) through the test beds was adjusted using an electronic bubble flowmeter (Mast Development Co., Model 823-1). Linear flow velocities varied 2.35-9.40 cm/s; bed contact times varied 0.3-1.2 s.

Experimental Charcoals

Test charcoals were identified by their commercial sources as 8-16 mesh range with the impregnants given in Table I.

Table I. Experimental Charcoals

Source	Impregnants (Weight Percents)
Barnebey Cheney Co.	5% TEDA
Scott Health/Safety Products	5% TEDA
Norton Safety Products	5% TEDA
Mine Safety Appliances Co.	2% TEDA + 5% KI_3
Mine Safety Appliances Co.	5% KI_3

Procedures

Two charcoal beds were placed in the oven in such a way that the airflow could be switched by a valve to either. One bed contained unimpregnated activated charcoal and the other the test charcoal. Air flowed through the former to the detector during oven equilibration. Upon reaching a steady detector baseline signal the airflow was switched to the test bed. An upscale signal shift occurred. When a constant level was attained, the airflow was switched back to the unimpregnated charcoal. Such signal shift measurements were repeated at the same conditions, often using a fresh bed. At least three temperatures were used for each charcoal. Signal shifts recorded on the strip chart were measured with a ruler, multiplied by attenuation factors, and compared with calibration curves to get TEDA concentrations (μg/L). Desorption rates (μg/g-min) were then calculated from charcoal densities and airflow rates.

III. Results

Charcoal Variation

Desorption rates (D) at 4.7 cm/s airflow velocity and 90°C varied from 0.9 to 9 μg/g-min for the three 5% TEDA charcoals. The 2% TEDA, 5% KI_3 charcoal desorption rate was 1.2 μg/g-min at the same conditions. No iodine or other desorbing vapors were detected from the 5% KI_3 (only)-impregnated charcoal up to 120°C.

The differences in desorption rates for the three 5% TEDA charcoals are significant. They may be due to impregnation methods or due to the charcoal base characteristics (activity, surface area, pore structure, pore size, etc.). These differences, however, do not affect the efficiencies of these sorbents for methyl iodide trapping. We have measured essentially equal efficiencies for the highest and the lowest TEDA desorption rate charcoals in this test group.

Temperature Variation

Clapeyron (or Van't Hoff) equation plots (log D vs 1/T) for TEDA desorption rates at 4.7 cm/s are shown in Figure 1. These are linear plots, as expected from analogy with evaporation and sublimation processes. The slopes of these plots are similar, implying similar heats of desorption, ΔH_D. The range of ΔH_D values was 23 to 29 kcal/mol with an average of 25 kcal/mol. This is much higher than the 14 kcal/mol heat of TEDA sublimation from pure crystals. The difference is due to TEDA-charcoal interactions. The 25 kcal/mol corresponds to a doubling of the desorption rate with every 5°C rise in temperature.

Another use of the Clapeyron equation plots is extrapolation to lower temperatures where TEDA desorption is too small to measure directly. Such extrapolations yielded desorption rates of 0.0009 to 0.008 μg/g-min for the three 5% TEDA charcoals and 0.002 μg/g-min for the 2% TEDA, 5% KI_3 charcoal at 25°C.

Airflow Velocity Variation

The 5% TEDA charcoal with the highest desorption rate was used to study effects of varying airflow velocity (2.35-9.40 cm/s). Results for two temperatures are shown in Figure 2. Desorption rate was directly proportional to airflow velocity. This implies that the limiting process in TEDA loss was removal of vapor by flowing air, rather than the volatilization step itself.

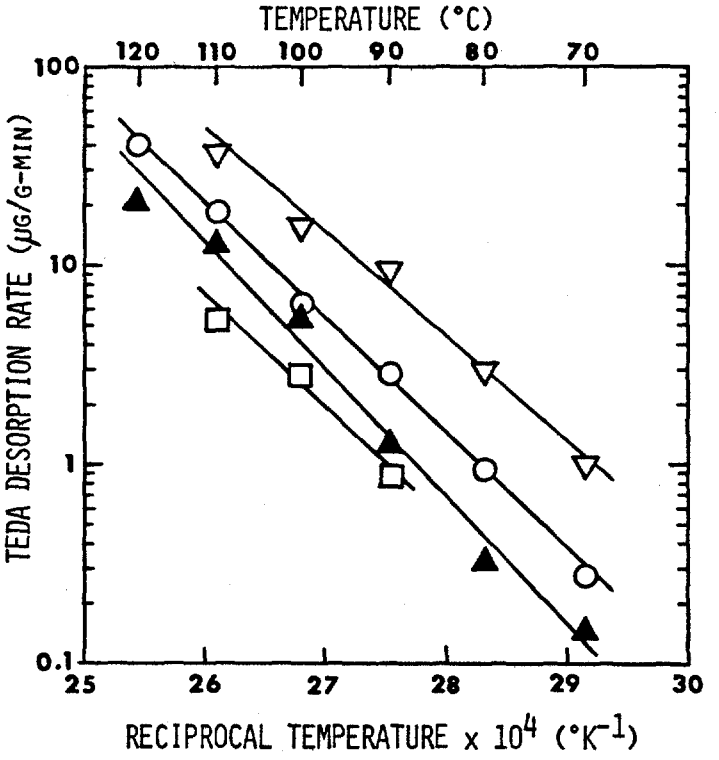

FIGURE 1
EFFECT OF TEMPERATURE ON TEDA DESORPTION RATE FROM THREE 5% TEDA CHARCOALS (▽,○,□) AND A 2% TEDA, 5% KI_3 CHARCOAL (▲)

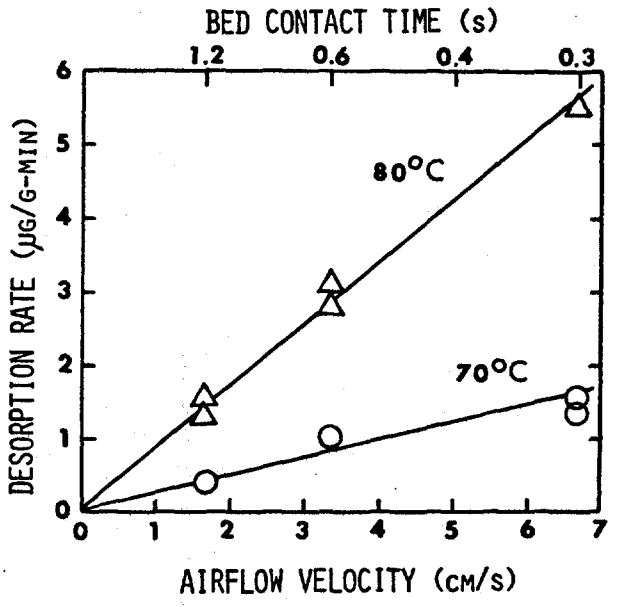

FIGURE 2
EFFECT OF AIRFLOW VELOCITY ON TEDA DESORPTION RATE

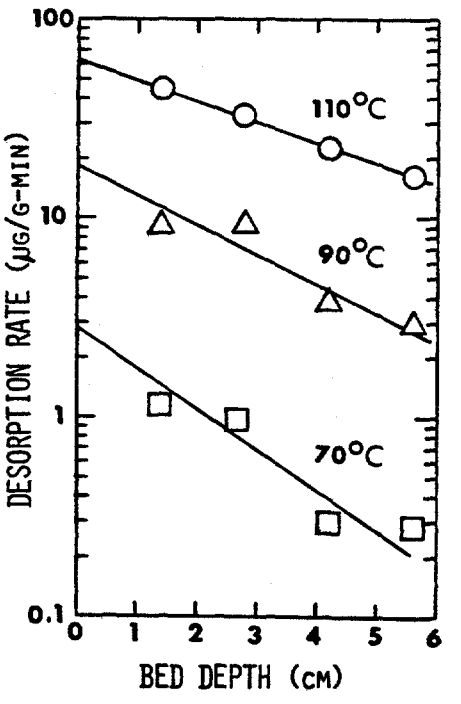

FIGURE 3
EFFECT OF BED DEPTH ON TEDA DESORPTION RATE

A general equation for desorption rate can be derived from the effects of temperature and flow velocity:

$$D = V \exp [a - \Delta H/RT]$$

Data from 21 measurements using this charcoal at 5 temperatures and 4 airflow velocities was fit to this equation to give a = 34.8 (std dev = 1.3) and ΔH = 24.9 kcal/mol (std dev = 0.9).

Humidity Variation

In one series of measurements with the highest desorption rate charcoal water vapor content of the air was varied. Dew points of -18 ± 4°C, 15.1 ± 1.4°C, and 24.8 ± 0.7°C were measured at test conditions of 70°C, 90°C, and 110°C. At 25°C these dew points correspond to relative humidities of 4%, 54%, and 99%. Increasing water vapor concentrations decreased the response of the photoionization detector. When this response change was taken into account, no detectable changes in TEDA desorption rates were observed over these ranges of experimental parameters. Only dry air was used in other experiments.

Bed Depth Variation

In another series of measurements with the highest TEDA desorption rate charcoal, bed depths were varied 1.4-5.6 cm at an airflow rate of 200 cm^3/min. Desorption rates were again measured at 70°C, 90°C, and 110°C. Figure 3 shows an apparently linear decrease in the logarithms of the TEDA desorption rates (per gram charcoal) with bed depth. Within experimental uncertainties, which are greater for lower temperatures, the slopes of the semilog plots for the three temperatures are identical. The average slope for results normalized to 90°C was -0.32 (std dev = 0.04); i.e., D = exp [2.83-0.32d], with bed depth d in cm.

The decrease in desorption rates (per gram charcoal) with increasing bed depth is likely due to readsorption of TEDA desorbed nearer the front (inlet) of the bed. This is the reverse of the process of adsorption of a vapor from air onto activated charcoal.

IV. Conclusions

Calculated TEDA Losses from an Adsorber

Significant loss of TEDA from an air cleaning adsorber filled with TEDA impregnated charcoal could result in degradation of efficiency for organic radioiodide removal. A standard (IES CS-8) Type II tray adsorber cell will be assumed for this calculation. It is designed with 5.08 cm (2 inch) deep beds containing approximately 22.7 kg (50 lbs) of charcoal. It is rated for a bed contact time of 0.25 s at 9.4 m^3/min airflow (333 cfm), which corresponds to an airflow velocity of 20.3 cm/s. Initial desorption rates calculated at 1 atm are given in Table II. Values at temperatures higher than 50°C can be estimated by doubling for each 5°C (9°F) rise. After significant TEDA loss, the absolute desorption rates (μg/g-min) will decrease with time, but the relative rates (%/month) may remain the same.

Table II. TEDA from an Adsorber

Temperature (°C)	Temperature (°F)	Initial Desorption Rate (μg/g min)	Initial Desorption Rate (%/month)	TEDA Concentrations (mg/m^3)	TEDA Concentrations (ppm)
25	77	0.007	0.6	0.018	0.004
30	86	0.015	1.3	0.036	0.008
35	95	0.029	2.6	0.070	0.016
40	104	0.056	4.9	0.135	0.031
50	122	0.193	16.9	0.465	0.110

The desorption rates in Table II near normal ambient temperatures (25-35°C) may be significant for bed performance deterioration over 12-24 month use lifetimes of adsorber beds. However, other weathering and poisoning processes are likely to be more significant. At higher temperatures, such as may result from high loading of radioactive nuclides, TEDA desorption becomes quite significant. This can result in rapid deterioration of efficiency for removal and retention of organic iodides. It may also contribute to ignition by providing TEDA vapor as fuel, which may explain why charcoal ignition temperatures are lowered by TEDA impregnation.

The data chosen for these calculations was that for the "worst case" (highest desorbing rate) 5% TEDA charcoal. Use of one of the others should reduce TEDA loss below the significance level at normal ambient temperatures. And it should reduce the problem of TEDA loss and charcoal ignition in accident situations.

Calculated TEDA Concentrations from an Adsorber

Concentrations of TEDA in effluent air passing through the same adsorber are also given in Table II. There are no toxicological data available for TEDA; however, TEDA belongs to the class of organic aliphatic amines, some of which have established toxicity. Threshold Limit Values (1979) for similar amines are:

	mg/m^3	ppm
Ethylamine	18	10
Diethylamine	75	25
Triethylamine	100	25
Ethylenediamine	25	10
Diethylenetriamine	4	1

The obvious conclusion is that if TEDA toxicity is similar to the toxicity of these other amines, the TEDA releases from such adsorbers are well below the level of concern.

DISCUSSION

WOOD: I would like to add one comment. Although we are nearing the completion of this program, we might be willing to look at some additional materials under limited conditions if someone has a particular material they would like us to investigate.

BELLAMY: I just want to be sure that I understood the last chart you showed. My interpretation is that at a temperature of 50°C I could lose all of the TEDA in three months under the worst conditions.

WOOD: No, that is not entirely true. That is the initial rate. It is like compound interest, it is 35% per month initially. You will lose TEDA that fast at first, but every succeeding day, you will lose fractionally less.

BELLAMY: So, there is a concentration effect.

WOOD: The percentage per month should be the same, as it is a first order process.

BELLAMY: I just wanted to make sure everyone understood that.

EVANS: I would like to comment that when we were doing experimental impregnations with TEDA, and on occasion encountered runaway dry over-temperatures, we found that we could lose all of the TEDA within four hours at 120°C.

FIRST: Would you kindly interpret the remark you made on the first slide that this was the worst of the data that you had.

WOOD: By "worst," I meant that this was the fastest TEDA loss.

FIRST: Does this suggest that you had other results which were significantly better in terms of experiencing less loss?

WOOD: Yes. In the first slide, I showed a range of 10. I selected the highest desorbing one for further study. So, we were expecting the best one, i.e., the lowest desorbing carbon, would be a factor of 10 lower.

NUCLEAR POWER PLANT
AIR FILTER MAINTENANCE PROGRAM AND RECORDS

James F. Fish
Nuclear Environmental Systems
American Air Filter Co., Inc.
Louisville, Kentucky

Air filter maintenance can be and often is a casual requirement for commercial and industrial buildings, fossil power plants and similar installations. This, often off-hand approach is not good enough for Nuclear Power Plants where air filtration systems must be in good operating condition at all times to protect plant workers and the general public from emissions in case of accident.

This process is not complicated but to be effective, it must be introduced and followed up as a standard procedure. Simple records (see attached) will suffice to indicate condition of all filtration systems to 1) Company supervisory personnel, or 2) government inspectors at any time. Responsibility for periodic checks must be assigned to specific personnel to make the system work. Procedures must be specifically drawn up and responsibility specifically assigned.

All systems include initial tests, air flow measurements, HEPA and charcoal leak tests, etc. This is the first reference to be noted on the log sheets.

In the case of a new installation, pressure drop checks will initially be made and recorded every 30-60 days. This is because of original system "built in" dirt which will be collected in the filters. As further experience warrants, the rate of pressure drop increase should stabilize and hold for the remainder of plant life, assuming no special conditions occur to interrupt the normal cycle. This is basically applicable to non-safety systems operating continuously.

ESF systems require operation of 10 hours per month with heaters (if available) operating. The log should show that this has been done. With so little operation, filter maintenance should be very limited. The log will, however, show what was done and why.

There are seldom so many filter systems in a plant as to make this procedure unduly burdensome. Use of this sytem permits accurate identification of maintenance requirements weeks or months before the critical date, thus permitting supplies to be ordered and received prior to need. A sample sheet plus blank forms are attached.

If anyone has specific questions, I will be happy to discuss all ramifications of instituting and implementing such a system in your plant.

FILTER MAINTENANCE RECORD

PLANT _____

SYSTEM NO. _____ SHEET _____ LOCATION _____ DESIGN CFM _____ ACTUAL CFM _____ OPERATION CONTINUOUS OR ESF

TECH. SPEC REQUIREMENTS (1) PER REG. GUIDE 1.52 (2) PER REG. GUIDE 1.140 OR OTHER

SYSTEM COMPONENTS			OBSERVED ΔP - INCHES WATER GAUGE								
Date	Hours	Observer	Rough Filter	Water Separ.	Heater	Prefilter	HEPA	Charcoal Tray or Rechar.	HEPA	Total	COMMENTS

*HEPA leak test - Following cell change or per 1.52 or 1.140 (5.c) or plant tech. spec - See ANSI/ASME N510, Section 10

**Charcoal leak test - Following charcoal change or per 1.52 or 1.140 (5.d) or plant tech. spec - See ANSI/ASME N510, Section 12

***Charcoal performance test per 1.52 or 1.140 (Table 2, note c) or per plant tech. spec - See ANSI/ASME N510, Section 13

*, **, *** test results on file.

19 Feb 80
J.F. Fish

FORM NO. 3898

EXPLANATION OF FILTER MAINTENANCE RECORD FORM

PLANT	Name of plant
SYSTEM NO.	Self-explanatory
LOCATION	Aux. Bldg, Fuel Bldg, Containment, etc.
DESIGN CFM	That CFM specified originally which determines size of filter system
ACTUAL CFM	After balancing, actual airflow is often not exactly as originally designed. Actual airflow will determine pressure drops to be expected in service.
OPERATION	Some systems operate continuously. Some ESF systems operate only under incident conditions except for a few hours a month to insure they are in good condition. Cross out the designation not applicable to the subject system.
TECH SPEC REQUIREMENTS	Circle either (1) or (2) as applicable or note other requirements from Plant Tech Specs for subject system.
SYSTEM COMPONENTS	
Date:	Day reading taken
Hours:	System operating time to this point
Observer:	Initials of observer who took readings
OBSERVED Δ P	This is the actual reading from gauges on the date noted previously. Under this heading are listed the most common components. Some systems may not have all components, for example, water separators. If so, "X" out the non-applicable headings for the subject system. Cross out either "trays" or "rech", whichever is non-applicable. If beds are other than normal 2" depth in subject system, note charcoal depth adjacent to this heading as, for example, (6) or whatever it may be.
COMMENTS	All general comments or observation at time readings were taken. For example, if filter pressure drop is close to required change point, note that cells require change (routine maintenance) by or before next scheduled reading.
ASTERISKED ITEMS	When first HEPA is changed, it requires a leak test. When this is successfully made, report is filed and an asterisk is noted beside the new HEPA filter pressure drop notation and test is noted in "comments". When charcoal is changed, a leak test is also required. When this report is completed satisfactorily, file report and add double asterisk beside the charcoal pressure drop reading. Record under "comments". After 720 hours operation for an ESF system or every 18 months, a charcoal performance test is required on a charcoal sample. If test is successful, file report and note with a triple asterisk by recorded pressure drop. If charcoal requires change out, note under "comments".

7 Feb 80
J.F. Fish

FILTER MAINTENANCE RECORD

PLANT NUKE 1

SYSTEM NO. X 84 | SHEET 1 | LOCATION AUX BLDG | DESIGN CFM 12,000 | ACTUAL CFM 11,300 | OPERATION CONTINUOUS ~~OR ESF~~

TECH. SPEC REQUIREMENTS (1) PER REG. GUIDE 1.52 (2) PER REG. GUIDE 1.140 OR OTHER

SYSTEM COMPONENTS			OBSERVED ΔP - INCHES WATER GAUGE							
Date	Hours	Observer	~~Rough~~ Filter	~~Water~~ Separ.	Heater	Prefilter	HEPA	Charcoal Tray or ~~Recher.~~	HEPA	Total	COMMENTS
3/20/79	12	JR			.1	.3	1.0*	1.1**	1.0*	3.5	TESTED OK 3/20 SEE REPORT
4/10/79	492	JR			.1	.4	1.0	1.1	1.0	3.6	OK
5/15/79	1320	JR			.1	.55	1.1	1.1	1.0	3.85	OK
↓											
8/20/79	~				.1	.9	1.25	1.1	1.0	4.35	CH. PREF. BEFORE NEXT CHECK
9/15/79	~				.1	.3	1.3	1.1	1.0	3.8	OK
3/2/80	8590	JR			.1	.85	2.75	1.1	1.0	5.8	CH. PREF & HEPA BEFORE NEXT CHECK
4/5/80					.1	.3	1.0*	1.1	1.0	3.5	OK
					.1	.6	1.2	1.1***	1.0	3.9	OK CHAR. TESTED - SEE REPORT

*HEPA leak test - Following cell change or per 1.52 or 1.140 (5.c) or plant tech. spec - See ANSI/ASME N510, Section 10

**Charcoal leak test - Following charcoal change or per 1.52 or 1.140 (5.d) or plant tech. spec - See ANSI/ASME N510, Section 12

***Charcoal performance test per 1.52 or 1.140 (Table 2, note c) or per plant tech. spec - See ANSI/ASME N510, Section 13

*, **, *** test results on file.

FORM NO. 3898

19 Feb 80
J.F. Fish

FILTER MAINTENANCE RECORD

PLANT _____

SYSTEM NO. _____ SHEET _____ LOCATION _____ DESIGN CFM _____ ACTUAL CFM _____ OPERATION CONTINUOUS OR ESF

TECH. SPEC REQUIREMENTS (1) PER REG. GUIDE 1.52 (2) PER REG. GUIDE 1.140 OR OTHER

SYSTEM COMPONENTS			OBSERVED ΔP - INCHES WATER GAUGE								
Date	Hours	Observer	Rough Filter	Water Separ.	Heater	Prefilter	HEPA	Charcoal Tray or Rechar.	HEPA	Total	COMMENTS

*HEPA leak test - Following cell change or per 1.52 or 1.140 (5.c) or plant tech. spec - See ANSI/ASME N510, Section 10

**Charcoal leak test - Following charcoal change or per 1.52 or 1.140 (5.d) or plant tech. spec - See ANSI/ASME N510, Section 12

***Charcoal performance test per 1.52 or 1.140 (Table 2, note c) or per plant tech. spec - See ANSI/ASME N510, Section 13

*, **, *** test results on file.

19 Feb 80
L.E. Fish

1413

FILTER MAINTENANCE RECORD

PLANT NUKE 1

SYSTEM NO. X 84 | SHEET 1 | LOCATION AUX BLDG | DESIGN CFM 12,000 | ACTUAL CFM 11,300 | OPERATION CONTINUOUS ~~OR ESF~~

TECH. SPEC REQUIREMENTS (1) PER REG. GUIDE 1.52 (2) PER REG. GUIDE 1.140 OR OTHER

SYSTEM COMPONENTS			OBSERVED ΔP - INCHES WATER GAUGE							
Date	Hours	Observer	~~Rough Filter~~	~~Water Separ.~~	Heater	Prefilter	HEPA	Charcoal Tray or ~~Recher.~~	HEPA	Total	COMMENTS
3/20/79	12	JR			.1	.3	1.0*	1.1**	1.0*	3.5	TESTED OK 3/20 SEE REPORT
4/10/79	492	JR			.1	.4	1.0	1.1	1.0	3.6	OK
5/15/79	1320	JR			.1	.55	1.1	1.1	1.0	3.85	OK
↓											
8/20/79	~				.1	.9	1.25	1.1	1.0	4.35	CH. PRE. BEFORE NEXT CHECK
9/15/79	~				.1	.3	1.3	1.1	1.0	3.8	OK
3/2/80	8590	JR			.1	.85	2.75	1.1	1.0	5.8	CH. PRE & HEPA BEFORE NEXT CHECK
4/5/80					.1	.3	1.0*	1.1	1.0	3.5	OK
					.1	.6	1.2	1.1***	1.0	3.9	OK CHAR. TESTED - SEE REPORT

*HEPA leak test - Following cell change or per 1.52 or 1.140 (5.c) or plant tech. spec - See ANSI/ASME N510, Section 10

**Charcoal leak test - Following charcoal change or per 1.52 or 1.140 (5.d) or plant tech. spec - See ANSI/ASME N510, Section 12

***Charcoal performance test per 1.52 or 1.140 (Table 2, note c) or per plant tech. spec - See ANSI/ASME N510, Section 13

*, **, *** test results on file.

1419

FORM NO. 3898

19 Feb 80
J.F. Fish

REVIEW OF WORK CARRIED OUT 1978-80 ON HEPA FILTERS AND VENTILATION SYSTEMS AT THE DOUNREAY SITE OF THE UKAEA

E. Lillyman
UKAEA
Dounreay Nuclear Establishment
Thurso
Caithness, Scotland

Abstract

1. This review covers work in the past 2 years on ventilation system design on new active plants and buildings, improved HEPA filter housings and HEPA filter modifications to assist in disposal. Further work has commenced on leak rates through building materials.

Introduction

2. This review is essentially a follow up to a paper presented to the 15th DOE Conference on UKAEA work in the nuclear air cleaning field. Major changes have taken place at the Dounreay site following the start of operation of the plutonium fuelled 600 MW(T) Prototype Fast Reactor. Thus the site has changed over from an enriched uranium fuel cycle to reactor grade plutonium and its associated actinides. This has had considerable influence on containment and ventilation standards and particularly in demands upon HEPA filters.

New Ventilation System, Fast Reactor Fuel Reprocessing Plant, Dounreay

3. A new active ventilation system has been installed and commissioned on the FFR Reprocessing Plant at Dounreay. It has now been in active operation for a year, and after some initial teething troubles is now functioning to its design specification.

The new system consists of four separate components namely, active cells, breakdown caves, active vessel ventilation and glove boxes all coupled to a common HEPA filtration system and discharging into the building space extract system.

The unique features of the system are

(a) The use of fluidic devices - Vortex amplifiers - to maintain constant depressions in the system under all operational conditions. It also allows the use of a single fan to deal with all the active extract.

(b) It operates on a minimum flow basis, approx 1/10 of the flow of the system it replaced, this reducing the HEPA filtration requirements to a minimum. At the same time aerosol generation is also minimised.

(c) The use of a new HEPA filter housing, fully shielded and remotely operated. HEPA changing is carried out by a programmed robot and is mainly automatic. Designed flow is 3000 cfm, although it is

normally half this figure.

The four primary filters have now been changed after nearly 1 year service. These filters were gamma active to the extent of 130 R/hr at contact, essentially Cs_{137}.

After 10 months operation the Δp was about 4" wg. This rapidly built up to 8" wg during a period when considerable amounts of smoke were employed for leak detection purposes, prior to putting large amounts of plutonium fuel into the plant.

After changing the primary filters, DOP tests indicated efficiencies of 99.3 to 99.8%. This is considered satisfactory for a remote high $\alpha/\beta\gamma$ situation and is within the safety requirements.

Ventilation flow rates are within predicted tolerances and the depressions also are satisfactory. Some tuning has been necessary on the VXA's, the glovebox depression controller requiring some flow restriction to avoid instability.

Ventilation Control Systems

4. The use of Vortex Amplifiers for depression control has been extended to other active facilities such as caves, cells and in particular gloveboxes where it is a standard fitment for all Pu gloveboxes which are air filled. These have proved to be very stable and absolutely trouble free during over 2 years active use.

In this period there has been several incidents when box containments have been impaired. In all cases system response was virtually instantaneous and no activity escape was detected. Smoke tests were also carried out on boxes to confirm that the predicted operational response was being achieved.

Current practice is to fit suites of gloveboxes, typical 4 or 6, but up to 14 to a single VXA controller of adequate capacity. Further developments are in hand for use of VXA's on inert gas boxes. There are no real problems, other than siting and flow rate, on once through inert gas systems. Systems have been developed which can operate in a re-cycle mode.

Other developments include the use of VXA's to control inlet flows to boxes.

Improved Filter Housing and Changing Systems

5. This work has continued and a new laboratory filter bank containing 24 x 1700 m^3 filters has been constructed. This system was briefly described in 1978 and uses double door technology to achieve a clean change without the need to use PVC bags. The system was devised to comply with site policy to (a) eliminate use of PVC bags which creates Pu active waste, and (b) improve safety by adopting a fully engineered system.

The production units on this system have been manufactured from aluminium castings. A feature of the design of this system is that the HEPA efficiency is independent of sealing efficiency. Two seals are used and the housing is ventilated to atmosphere so that any seal fault results in an in-leakage.

In association with these housings a special glovebox is required which will also deal with the breakdown and disposal of the dirty HEPA's. This is under construction.

HEPA Dismantling and Disposal

6. Trials with the active HEPA coiling machine described in the 1978 paper were not very successful on filters which had been in use for a few months or more. Attempts were made to coil the paper from HEPA's used on laboratory fume cupboard extracts systems. Considerable chemical attack had taken place and the paper tended to disintegrate when coiling was attempted. Whilst the method of dealing with HEPA's proved to be not very practicable, detailed examination of used HEPA provided information on effects of various atmospheres on filters. Aluminium spacers had in some cases disintegrated or largely corroded away.

Much more successful has been the use of quick release steel cases developed in conjunction with VOKES Ltd to facilitate size reduction and disposal of HEPA filters. A trial batch of filters has been in active use at DNE. All were pretested and found to be better than 99.95% and a similar figure when installed in Vokes housings. Removal of the steel case has proved very rapid and crushing of the filter module accomplished with very simple equipment. The intention is to use this type of filter in Pu and high gamma installations so that remote dismantling is greatly facilitated.

Trials are in hand of wooden case HEPA filters which have been subject to fire retardant treatment. The object of this exercise is to enable a wooden case HEPA to satisfactorily resist a high temperature excursion but will ultimately be capable of disposal by incineration. These filters are unusual in that the filter element is sealed into the wooden case with a high temperature medium - glass fibre "wool" ie. similar to the typical fire retardant filter. Filters and housings are being subject to high temperature tests, which have already confirmed that the glass fibre 'wool' used for the seal forms an excellent heat barrier. The test also confirmed the heat resistance of silicone rubber seals.

Containment Standards of Buildings

7. Considerable attention has been paid to standards of building construction, particularly porosity of some building materials. Some types of cement building blocks proved to be 60-70% penetrated by DOP smoke with diffusion rates of 1 cfm per ft^2 at about 0.8" WG. Interest in this work was indicated by the need to eliminate unfiltered air ingress into active buildings which would interfere with α in air monitoring in an area with a considerable background of radon/thoron activity. Further, in an area subject to high winds (not tornadoes) buildings are frequently

subject to pressures and depressions from 2" WG +ve to 1.8" -ve. A test facility is being constructed to follow up this work and provide information for building designers.

Improvements in leak testing methods for gloveboxes and Similar containments

8. A quick and very acurate method of leak rate measurement on gloveboxes, ventilation ducting, etc has been developed. Initially, it was used for acceptance testing of glove boxes at makers works. Subsequently it has been extended to leak testing of new ductwork.

A more recent development has been the adaption of the method for use on active boxes. The main advantage of the method is its speed and simplicity and its total independence of temperature and the barometric pressure changes.

Future Work

9. When describing briefly the ventilation system for the Fast Reactor Reprocessing Plant, I made no mention of removal of Kr_{85}, H_3, C_{14} or I_{129} from the offgases. Worst case calculations indicate that the maximum dose received from these species is less than 1 mrem per year.

Consequently, there is no justification for any special treatment systems at present. Further, the necessity for treatment systems for the above species based on a doses liable to be received by the public are probably several decades away.

However, the fact that Dounreay is handling, examining and reprocessing very high burn up mixed Pu/U oxide fuels will enable realistic information to be obtained for some of the more critical species present. A comprehensive programme of fuel examination coupled with samplers on various off-gas streams will allow full characterisation particularly of I_2 and H_3. Until the physical and chemical forms of such species are investigated, I consider much of the work on head end off gases, which is going on in many countries of the world to be somewhat premature.

Further, I think the possibility should be borne in mind of these species appearing in off-gas streams other than the dissolver.

DISCUSSION

MILLER: Would you quote some leakage figures for infiltration through building blocks? Are these concrete building blocks?

LILLYMAN: The building blocks were sand and cement. I could not tell you the exact composition, but it was some typical mixture.

FISH: I believe that some number of conferences ago, there was a paper given on an investigation of the filtering capacity of cracks in the containment structure (CONF 700816, Vol. 2, p. 817, 11th AEC Conf., Sept. 1970). Do you remember that?

LILLYMAN: Yes. We have seen these papers, which is why we were so amazed, in fact, when we tested this. I didn't believe them when they told me that it penetrated and I went and tested it myself. Visually, you can see the DOP coming through the brick. So, it does happen--most amazingly, I might add.

FIRST: I can only make a further comment perhaps, that there may be cement bricks and cement bricks. That does seem to be an extraordinarily high leakage rate. I assume these are unpainted. I might refresh Mr. Fish's memory a bit by recalling that the crack filtration experiments he referred to were conducted with freshly generated sodium oxide aerosols.

CLOSING REMARKS OF SESSION CHAIRMAN:

We have come to the end of individuals who have asked to be on this program. I would like to comment that this has been a most interesting part of the Air Cleaning Conference; I think it has been one of the best we have had with respect to the variety of topics. The information that was presented was certainly superb.